Interactions, Entanglement, and Anomalies in Topological Semimetals

by

Lei Gioia Yang

A thesis
presented to the University of Waterloo
in fulfillment of the
thesis requirement for the degree of
Doctor of Philosophy
in
Physics

Waterloo, Ontario, Canada, 2023

Examining Committee Membership

The following served on the Examining Committee for this thesis. The decision of the Examining Committee is by majority vote.

External Examiner:	John McGreevy Professor, Dept. of Physics, University of California San Diego
Supervisor(s):	Anton A. Burkov Professor, Dept. of Physics and Astronomy, University of Waterloo
	Chong Wang Adjunct Faculty, Dept. of Physics and Astronomy, University of Waterloo
Internal Member:	Roger Melko Professor, Dept. of Physics and Astronomy, University of Waterloo
Internal-External Member:	Adam Wei Tsen Assistant Professor, Dept. of Chemistry, University of Waterloo
Other Member(s):	David Hawthorn Professor, Dept. of Physics and Astronomy, University of Waterloo

Author's Declaration

I hereby declare that I am the sole author of this thesis. This is a true copy of the thesis, including any required final revisions, as accepted by my examiners.

I understand that my thesis may be made electronically available to the public.

Abstract

Topology and symmetry have become one of the backbones of modern condensed matter physics. These concepts play a large role in determining the possible effects of interactions and entanglement in both gapped and gapless systems. Gapped systems possess a well-developed description via topological quantum field theory (TQFT) that has given rise to many exciting concepts such as topological orders. However gapless systems are far less well-understood in the context of topology as they cannot be described by a simple TQFT due to the presence of local degrees of freedom at low energy. In this thesis I will explore these concepts in the framework of topological response in gapless systems with a focus on 3+1d Weyl and Dirac semimetallic systems. I develop a theory of unquantized topological response, as opposed to the usual quantized response of gapped systems, and explore the effects of strong interaction in the presence of these terms. I show that the associated unquantized topological quantities arise from crystalline symmetries such as discrete translations and rotations. Inspired by the topological crystalline quantity of momentum, I also develop a general theorem involving just discrete translation symmetry that can distinguish long-range entangled states from short-range entangled states. Such a statement can be seen as a generalisation of the well-known Lieb-Schultz-Mattis theorems and many are shown to be consequences from the pure translation theorem that I develop here.

Acknowledgements

I thank my wonderful and supportive supervisors Anton Burkov and Chong Wang without whom this degree would have been impossible. There have been many who have supported my journey both academically and personally throughout my Ph.D. such as my mentors Lauren Hayward and Liujun Zou, my collaborator and mentor Taylor Hughes, and my previous supervisors Ulrich Zuelicke and Michele Governale.

Also I am grateful to my cohort of graduating students, especially Ruochen Ma and Weicheng Ye who suffered alongside me in the job market hunt. I also thank my collaborators Julian May-Mann and Mark Hirsbrunner for physics and life.

I thank my human-embodiment of sunshine Ryan Thorngren, and my family Petrik, mum, dad, Ocean, Victor, Eve, Oma, Opa, Nai Nai, Ye Ye, Lao Lao, Lao Ye, Monique, Heike, and Walfried. Of course I also thank my dear friends who have supported me along the way such as Finnian Gray, Kasia Budzik, Maxence Corman, Suzanne Bintanja, Joseph Bennett, Mereana Latimer and many more!

Dedication

Interactions, Entanglement, and Anomalies in Topological Semimetals (I EATS) is dedicated to all food lovers around the world. Also to tardigrades.

Finally, this work is also dedicated to women and other historically marginalised groups in science and those who help them overcome systemic barriers.

Table of Contents

Examining Committee Membership ii

Author's Declaration iii

Abstract iv

Acknowledgements v

Dedication vi

List of Figures x

1 Introduction 1

1.1 Phases of matter . . . 1

1.1.1 Landau symmetry-breaking . . . 2

1.1.2 Quantum phases of matter . . . 3

1.1.3 Gapless phases of matter . . . 6

1.2 3+1d semimetals . . . 8

1.2.1 Weyl semimetal . . . 8

1.2.2 Dirac semimetal . . . 12

1.3 Topological response . . . 13

1.3.1 SPT and 't Hooft anomalies . . . 15

1.3.2 Gauging crystalline symmetries . . . 16
1.3.3 Quantum anomalies in gapless systems . . . 19

2 Fractional quantum Hall effect in Weyl semimetals 23
2.1 Introduction . . . 23
2.2 Construction . . . 25
2.3 Symmetric gapped state . . . 29

3 Unquantized anomalies in topological semimetals 32
3.1 Introduction . . . 32
3.2 Preliminaries . . . 35
3.2.1 Topological response and "unquantized quantum anomalies" . . . 36
3.2.2 Review of lattice symmetry gauge fields . . . 38
3.3 Chiral anomaly in (1+1)d lattice systems . . . 41
3.3.1 $U(1) \times \mathbb{Z}$ chiral anomaly . . . 41
3.3.2 $\mathbb{Z} \times \mathbb{Z}_2$ anomaly . . . 45
3.3.3 $\mathbb{Z} \times \mathbb{Z}$ anomaly . . . 49
3.4 Three-dimensional topological semimetals . . . 54
3.4.1 TR-broken Weyl semimetal . . . 54
3.4.2 Type-I Dirac semimetal . . . 57
3.4.3 TR-invariant Weyl semimetal . . . 62
3.5 Discussion and conclusion . . . 65

4 Non-zero momentum requires long-range entanglement 67
4.1 Introduction . . . 67
4.2 Proof . . . 69
4.2.1 Proof in 1d . . . 69
4.2.2 Higher-dimensional extension . . . 75

4.2.3 Fermion systems . . . 75
4.3 Consequences . . . 76
4.3.1 LSMOH constraints . . . 77
4.3.2 Topological orders: weak CDW . . . 79
4.3.3 Crystalline symmetry-protected topological phases . . . 81
4.4 Discussions . . . 82

5 Outlook **84**

References **86**

APPENDICES **121**

A Band inversion mechanism motivated **122**

B Quantum anomalies in high-energy physics **124**

C Another formulation of the chiral anomaly **126**

D Fermi arcs in the FFLO Weyl superconductor **128**
D.1 Helical Majorana fermions in a vertical vortex line . . . 130

E Some formal details on vortex condensation in (3+1) dimensions **133**

F The $\mathbb{Z}_2\times\mathbb{Z}$ anomaly in $(1+1)d$: exceptional points and emergent anomalies **135**

G Stability analysis of the $\mathbb{Z}\times\mathbb{Z}$ anomaly **138**

H Lowest Landau Levels for type-I DSM **141**

I Higher dimensional FD quantum circuit **142**

J Proof for fermion systems **145**

K Weak CDW example - Toric code **148**

List of Figures

1.1 (Color online) Finite-depth quantum circuit with a depth of four that connects two states $|\Psi(0)\rangle$ and $|\Psi(1)\rangle$. 4

1.2 (Color online) The lightcone construction shows us that there is only correlation between operators where there exist some local Hilbert space states that fall under the same lightcone. We see that the correlation length $\xi \sim \mathcal{O}(D)$ where D is the depth of the circuit. 7

1.3 (Color online) Positive (left) and negative (right) chirality around Weyl nodes. We see that the nodes form a sink or source of the Berry curvature. 9

1.4 (Color online) Schematic of a possible transition between a Dirac semimetal (right) to a Weyl semimetal with broken time-reversal symmetry (middle) or parity symmetry (left). The charges are annotated and indicated by the colouring of the spheres overlaid on the nodes. In (left), note that in general the nodes are not necessarily positioned with this exact symmetry. 11

1.5 (Color online) The mechanism underlying the creation of a pair of Dirac nodes in type I Dirac semimetals. (left) The non-inverted/normal regime where there is no crossing point. (middle) The inverted regime with hybridization of the crossing point, which gaps the spectrum. (right) Hybridisation is prevented since the rotation symmetry prevents mixing terms from occurring along the symmetry axis k. This protection results in a pair of Dirac nodes along k and a type I DSM is obtained. Figure is adapted from Ref. [12]. 13

1.6 (Color online) (a) A perfect defect-free lattice with translation symmetry in $\hat{z}$. (b) A lattice with an edge dislocation where the Burgers vector is $\mathbf{b} = \hat{z}$. 18

1.7 (Color online) (a) A perfect lattice with C_4 symmetry. (b) A disclinated lattice where we fold over the shaded region in (a). 19

2.1 (Color online) (a) A vortex loop linked with a dislocation with the Burgers vector $\mathbf{B} = \hat{z}$. Fractional quantum numbers and nontrivial braiding statistics can emerge in such a configuration. (b) A pair of vortex loops linked with a dislocation with the Burgers vector $\mathbf{B} = \hat{z}$. Braiding the two loops may be accomplished by adiabatically shrinking the left loop, then moving it to the right by crossing the disc, enclosed by the right loop, then expanding and moving it back to the original place without crossing the disc, enclosed by the second loop. 27

2.2 (Color online) Hall conductivity as a function of the magnetization with a fractional plateau corresponding to $\sigma_{xy} = 1/4\pi$ 3D FQHE. 30

3.1 (Color online) Spatial symmetry point defects in 2D. (a) A defect-free 2D lattice with highlighted (blue) point possessing both translational and $\pi/2$ rotational symmetry. (b) A translational symmetry defect, known as a dislocation, is obtained by inserting an extra (red) half-plane and represented by the red dot. A Wilson loop around the defect gives $\int_C \mathcal{X}_i = 1$. (c) Gluing together the yellow lines in (a) produces a $\pi/2$ rotational defect known as a disclination. (d) Here we depict a periodic 2D lattice in the xz-plane with linear size in the z-direction $\int_{z=0}^{L_z} z = L_z$ (red line) and a shear strain in z given by $\int_{x=0}^{L_x} z = 1$ (green line). The four blue dots are equivalent to each other due to the periodic boundary conditions. 40

3.2 (Color online) Illustration of the $(1+1)$d chiral anomaly: (a) A one band fermionic dispersion at fractional filling $\nu = 2Q/2\pi$. (b) Once we thread a flux $\int dz A_z = 2\pi$, which gives rise to an electric field $\vec{E}$, all filled states gain a unit of momentum resulting in a change of $2\pi\nu$ in chiral charge (i.e. crystal momentum). 43

3.3 (Color online) Band dispersion corresponding to the Hamiltonian in Eq. (3.20). The filled red and blue states correspond to different C_2 eigenvalue states. The sum of the individual filled charges gives the total C_2 charge which may be non-trivial, leading to a $\mathbb{Z} \times \mathbb{Z}_2$ chiral anomaly. 47

3.4 (Color online) The blue (red) band in Fig. 3.3 is shifted to the right (left) by δQ. C_2 symmetry is not necessary for the protection of the states anymore as indicated by the colour hybridisation. Instead, the filled states now possess a non-trivial total momentum, leading to a $\mathbb{Z} \times \mathbb{Z}$ chiral anomaly. 50

3.5 (Color online) A C_4 disclination with the Frank vector along $\hat{z}$ is depicted by gluing two lattice faces, rotated by $\pi/2$ with respect to each other, together (shown as yellow surface) to create a defect line shown as a bold yellow line. Close to this defect the lattice appears distorted, however far away the regular square lattice shape is retained. 60

3.6 (Color online) Cartoon of a screw dislocation, represented by a lattice shear strain along the green surface. The defect line is shown in bold green with a Burgers vector $\mathbf{b} = \hat{z}$. 63

4.1 (Color online) Depiction of finite-depth quantum circuits applied on $|\Psi_P\rangle$. Here qudits are depicted as solid circles while unitaries are depicted as rectangles. (a) A SRE state $|\Psi_P\rangle$ is always connected to the $|\mathbf{0}\rangle$ trivial state via a FD quantum circuit U. From U a lightcone-like 'adiabatic cut' $\tilde{U}$ can be created (framed in blue). (b) $\tilde{U}$ connects $|\Psi_P\rangle$ to a state that is completely decoupled across the cut. 71

4.2 (Color online) Illustration of the adiabatic cutting procedure on a periodic length $L = mn$ chain. Here we take $m = 4$ example to demonstrate how four identical cuts, applied by $\tilde{U}$ (blue rectangle) at every nth link, on a length $L = 4n$ state $|\Psi_{P(L)}\rangle$ (purple circle) produces four decoupled length n SRE states. 72

4.3 (Color online) Illustration of splitting $TV_L^\dagger T^\dagger V_L = \tilde{V}_{L,1}\tilde{V}_{L,2}$ with $\tilde{V}_{L,1}\tilde{V}_{L,2}|\mathbf{0}\rangle = e^{-iP(L)}|\mathbf{0}\rangle$. Here we have taken a snapshot of the circuit to focus on $\tilde{V}_{L,1}$ (framed in blue), however the support of $\tilde{V}_{L,1}$ (in the depicted example 16 qudits) is actually much smaller than the system length. Recall that the circuit is periodic such that the orange arrows, corresponding to components of $\tilde{V}_{L,2}$ (framed in orange), eventually connect on the far side of the ring. . 74

D.1 (Color online) Energy eigenstates for $k_y = 0$ slice along k_z corresponding to Nambu Hamiltonians given by Eq. D.3 (a) and D.8 (b). (a) The zero mode spans the entire Brillouin zone due to doubling of degrees of freedom in the Nambu picture. (b) Intranodal interaction gaps out the bulk Weyl nodes but leaves the surface states unaltered. For both figures $m = 1.1$, $N_x = 50$ and for (b) $\Delta = 0.5$. 132

I.1 (Color online) A sample 2d FD quantum circuit U decomposed along $\hat{x}$ into 'extended lightcone' unitaries $\{V_i\}$ (shaded red) and 'extended reverse lightcone' unitaries $\{W_i\}$ (shaded blue). The exact position to begin the lightcone cut is variable, although here we have done so symmetrically. . . 143

K.1 (Color online) The Toric code system on a periodic lattice with $L_y = 1$. There are two spin degrees of freedom (d.o.f) per unit cell in $\hat{x}$. 149

Chapter 1

Introduction

In this chapter I will introduce most of the ideas that are necessary for the comprehension of this thesis. First I will touch upon the concepts of phases of matter in Sec. 1.1, which gives an overview into the area of topological quantum phases of matter and entanglement. Then, in Sec. 1.2, I will explain some of the physics of semimetallic systems which are a central topic of this thesis. Finally, in Sec. 1.3, I will review topological responses and quantum anomalies for both gapped and gapless systems and motivate some unsolved questions that we will tackle in this thesis.

1.1 Phases of matter

One of the central questions in condensed matter physics is the classification and comprehension of different phases of matter. Originally, distinct phases were thought to arise exclusively due to the presence or absence of symmetries [175]. This idea became known as the Landau symmetry-breaking paradigm, which ascribed a local order parameter to each symmetry. Phase transitions between symmetry-preserving and symmetry-breaking phases such as those between paramagnetic states and ferromagnetic states, where the local order parameter is the local magnetisation, were accounted for by this description. However with the discovery of high-T_c superconductivity and quantum Hall states there were obvious gaps to this description. For example, in the quantum Hall phases there were observations of different Hall conductivity plateaus, which all possessed the same symmetry group, yet still required a gap closure, i.e. phase transition, to deform to one another. This revelation led to the development of quantum phases of matter, i.e. phases at zero temperature, such as topological orders and symmetry-protected topological orders [294, 366]. Additionally,

the concept of phases of matter for gapless systems such as Fermi surfaces transcended the Landau symmetry-breaking description. In the following section I will start by giving an overview of the Landau symmetry-breaking formalism in Sec. 1.1.1. Then I will describe the issues with Landau's original formulation, and introduce quantum phases of matter in Sec. 1.1.2. Following this, in Sec. 1.1.3 I will also touch upon gapless phases of matter and how we may potentially understand them.

1.1.1 Landau symmetry-breaking

In the Landau symmetry-breaking formalism, we assume the physics of a phase transition may be described by a local order parameter[1] σ. This order parameter transforms non-trivially, i.e. is charged, under the symmetry of the system and thus indicates the presence of spontaneous symmetry-breaking when the order parameter acquires a non-zero ground state expectation value, i.e. $\langle\sigma\rangle \neq 0$.

The canonical example of such a phase transition is the transverse quantum Ising chain [218], described by Hamiltonian

$$H = -J\sum_{\langle i,j\rangle}\sigma_i^z\sigma_{i+1}^z - h\sum_i \sigma_i^x \quad , \tag{1.1}$$

where $\boldsymbol{\sigma}$ are the Pauli matrices and $\langle i,j\rangle$ denotes the nearest-neighbours. This Hamiltonian has a $\mathbb{Z}_2$ symmetry, enacted by operator $U = \prod_i \sigma_i^x$, and an associated second-order $\mathbb{Z}_2$ phase transition at $J = h$. The local order parameter is given by σ_i^z which has a non-trivial charge under the symmetry operator $U\sigma_i^z U^\dagger = -\sigma_i^z$.

The two phases correspond to the limits where (i) $J = 0$, $h > 0$ and (ii) $J > 0$, $h = 0$. In (i) the ground state is $|\Psi_+\rangle = |+\rangle^{\otimes L}$ (where L is the length of the system) so $\langle\sigma_i^z\rangle = 0$. This corresponds to the symmetric disordered state where we have a unique ground state. In (ii) the ground state manifold is spanned by states $|\Psi_\uparrow\rangle = |\uparrow\rangle^{\otimes L}$ and $|\Psi_\downarrow\rangle = |\downarrow\rangle^{\otimes L}$. These states give $\langle\sigma_i^z\rangle \neq 0$ and correspond to the spontaneous $\mathbb{Z}_2$ symmetry-broken phase. It is also important to note that we could have chosen the ground state to be a macroscopic superposition (i.e. a cat state) $|\Psi_\uparrow\rangle \pm |\Psi_\downarrow\rangle$ which is symmetric under $\mathbb{Z}_2$. However this state is unphysical as it fails to satisfy the cluster decomposition: the connected Green's function does not decay with distance $\lim_{r\to\infty}\langle\sigma_i^z\sigma_{i+r}^z\rangle_c \neq 0$. Physically this means that the state is

[1] Here we follow the initial definition of an order parameter that is *local*. For simplicity we will gloss over the existence of non-local order parameters and higher-form symmetries that may be used to also used to understand topological orders and other equilibrium phases of matter [220].

'non-local' and may easily decohere into either the $|\Psi_\uparrow\rangle$ or $|\Psi_\downarrow\rangle$ state, i.e. spontaneously breaks $\mathbb{Z}_2$ symmetry.

One of the properties of these ground states is that they have no (or little) entanglement. All entanglement arises locally and is not connected to any global feature. However it turns out that there exist states such as the fractional quantum Hall states which have a ground state degeneracy that depends on the topology of the underlying manifold, i.e. they must possess some entanglement knowledge that is global. Such states do not fall under the scope of Landau symmetry-breaking, and indicate that there is a notion of entanglement beyond that of product states and the like. To understand the notion of entanglement beyond the Landau symmetry-breaking picture, we must first review the notion of quantum phases of matter, i.e. phases of matter at $T = 0K$.

1.1.2 Quantum phases of matter

Quantum phases of matter usually involves the study of zero temperature gapped phases of matter. The idea of quantum phases can be understood by looking at the continuity of local operators $\mathcal{O}$: if we alter a parameter of the Hamiltonian, the ground state undergoes a phase transition only when a local operator experiences a singularity, i.e. some discontinuity or discontinuity in a derivative of the ground state expectation value of the local operator.

Such a definition of a quantum phase transition is equivalent to a gap closure of Hamiltonian spectrum [61]. Ground states $|\Psi(g)\rangle$ are in the same phase if there exists a gapped Hamiltonian that may be adiabatically deformed as a function of g such that there is no gap closure. In this case one can show that the local operators experience no singularities as a function of g.

In particular, one may show that two states are in the same phase if and only if they can be related to each other via a local unitary (LU)

$$U_{LU} = \mathcal{T}\left[e^{-i\int_0^1 dg\tilde{H}(g)}\right] \quad , \tag{1.2}$$

where $\mathcal{T}$ indicates time-ordering, and $\tilde{H}(g)$ is some local Hamiltonian[2], potentially with terms that possess exponential tails [133].

Local unitaries can be equivalently formulated in terms of finite-depth quantum circuits. Finite depth quantum circuits (FDQC) $U_{FD} = \prod_{l=1}^{D}(\prod_i U_{li})$ are made out of D finite layer

[2] $\tilde{H}(g)$ is not to be confused with the Hamiltonian $H(g)$ for which the state is a ground state. Generally these will be distinct and not the same.

of self-commuting local unitary matrices U_{li} such that $[U_{li}, U_{lj}] = 0$ [3]. See Fig. 1.1 for an illustration of a FDQC with a depth of four. Such FDQCs can faithfully represent local unitaries up to an operator norm error ϵ with depth $\mathcal{O}(\text{polylog}(L/\epsilon))$ which scales polylogarithmically with the length of the system L [123]. In the thesis we will generally use LU and FDQC interchangeably.

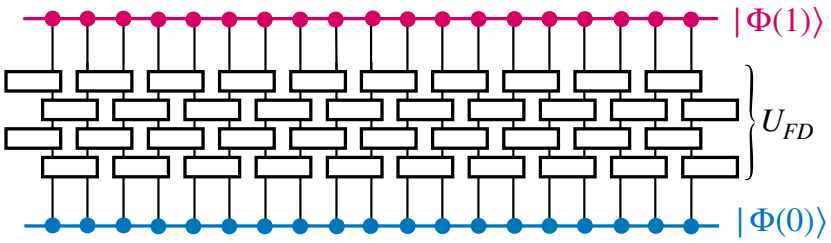

Figure 1.1: (Color online) Finite-depth quantum circuit with a depth of four that connects two states $|\Psi(0)\rangle$ and $|\Psi(1)\rangle$.

With this definition in hand we may proceed to evaluate the different possible quantum phases of matter, such as short-range entangled and long-range entangled phases.

Short-range entanglement

Definition 1. *A short-range entangled state, and phase of matter, is one that can adiabatically evolved to a product state in real space, i.e. a state of the form* $|\alpha_1\rangle \otimes |\alpha_2\rangle \otimes ... \otimes |\alpha_L\rangle$ *which has zero entanglement.*

Such states can be thought of possessing 'low' amounts of entanglement since they are similar to a product state and only possess entanglement locally.

Although these states possess low entanglement, they form distinct phases of matter when we allow for symmetries to play a role. We may define symmetric LUs (and symmetric FDQC) such that the $\tilde{H}(g)$ in Eq. 1.2 (or the FDQC) commutes with the symmetry. Note that the symmetric LU is immediately connected to the identity transformation, however this is not automatically the case for symmetric FDQC. In this case we require that the FDQC must be continuously tunable to the identity transformation while being symmetric.

[3] Here for simplicity we assume that these U_{li} do not have exponential tails. To represent local unitaries that possess exponential tails we would also have to allow for U_{li} with exponential tails.

Definition 2. *Classes of symmetric states that cannot be connected via a symmetric LU to each other are defined as possessing different symmetry-protected topological orders (SPTs).*

Examples of such SPT SRE states include the Su–Schrieffer–Heeger (SSH) chain which is protected by particle number $U(1)_q$ and particle-hole symmetry, quantum spin Hall states which are protected via particle number $U(1)_q$ and spin S_z symmetry, Haldane chain which is protected via the spin $\mathbb{Z}_2 \times \mathbb{Z}_2$ symmetry, and $3+1$d topological insulators (TIs) which are protected via particle number $U(1)_q$ and time-reversal symmetry.

Another class of SRE states are those that come from the spontaneous symmetry-broken phases such as $|\Psi_\uparrow\rangle$ and $|\Psi_\downarrow\rangle$ in the ferromagnetic phase. This does not encapsulate all symmetry-broken states since some of these may not be purely SRE, as we will discuss in the next section.

Long-range entanglement

Definition 3. *A state is long-range entangled (LRE) if it is not connected to a product state via a local unitary.*

Gapped LRE phases possess a type of global entanglement that may be classified into two cases. In the first case, such an entanglement structure may allow for features of such phases to depend on topology of the underlying manifold, thus explaining the features in the fractional quantum Hall states. In general, such phases are known as topological orders (TOs) [4], which include both invertible and non-invertible TOs [171]. Invertible TOs can be stacked such that they can be trivialised to a product state via a local unitary, while non-invertible TOs cannot. The hallmarks of invertible TOs include the presence of a gravitational anomaly, examples include the integer quantum Hall phases and the Kitaev chain. On the other hand, non-invertible TOs possess topology dependent ground state degeneracy and fractionalized excitation, as well as non-trivial braiding statistics [164]. Examples include the fractional quantum Hall states, the Toric code, and gapped quantum spin liquids. Similarly to the SRE states, these states may also be symmetry-enriched and can be (at least partially) classified such as in Ref. [225].

The second class of gapped (and gapless) LRE phase are those that have a GHZ-type entanglement structure (i.e. those that are related via local unnitary to $|\mathrm{GHZ}\rangle \equiv (|00...0\rangle + |11...1\rangle)/\sqrt{2}$ [399]), i.e. cat states that are the symmetric superpositions of spontaneous symmetry-broken states. As previously discussed, these phases disobey the

[4] Note that there also exist gapless topological orders, but here we will focus on gapped TOs.

cluster decomposition, are highly non-local, and are a sign of spontaneous symmetry-breaking in the thermodynamic limit. Examples of such states include the translation-symmetric superposition of charge-density waves, and the $U(1)$ symmetric superposition of Bogoliubov-deGennes ground states.

In addition to the gapped phases that are generally covered under the umbrella of quantum phases, there also exist gapless phases of matter at zero temperature. Now we turn our attention to LRE gapless phases of matter in the next section.

1.1.3 Gapless phases of matter

We begin by clarifying that the gapless phases of matter that are considered in this section are those that exhibit algebraic decaying connected correlation functions, i.e. $\langle \mathcal{O}_i \mathcal{O}_j \rangle_c \sim \frac{1}{|i-j|^n}$ for some $n > 0$. This requirement for example excludes fine-tuned gapless states (imagine fully filled bands at a quadratic touching point in 1d [344]), and disordered gapless states such as from Anderson localization [8].

It is straightforward to see that gapless states, defined in the manner above, must be LRE: their correlation length ξ is infinite, meaning that in the quantum circuit picture one can see that one needs at least circuit depth L to create such a correlation length (recall that circuit depth is approximately the correlation length, as can be seen via lightcone constructions - see Fig. 1.2). Examples of such LRE gapless phases include conformal field theories (CFTs), Fermi gasses and liquids, non-Fermi liquids, intrinsically gapless SPTs, certain high-T_c superconductors, and semimetal systems. Some of the most exciting topics with yet-to-be unlocked physics appears in these gapless materials.

The classification of gapped quantum phases is relatively well-understood and usually involves either group cohomology [275, 59, 63, 60, 122, 159, 160] or tensor category theory [164, 171, 17, 81], and can often be summarised in terms of quantized topological invariants. Examples of such quantized topological invariants includes the ten-fold way for non-interacting systems [165, 292], pure crystalline topological invariants [336, 323, 310], and more. These invariants often have implications on transport and other interesting topological phenomena in a variety of systems [28, 106, 104], and we will explore them in the context of topological responses in Sec. 1.3.

However this picture becomes complicated for gapless systems where we are often not able to naively generalise the gapped formulation. In fact, the very notion of what is meant by 'topological' is complicated! The type of topological features for gapless systems that we are interested in for this thesis are those that are generally non-quantized and can be

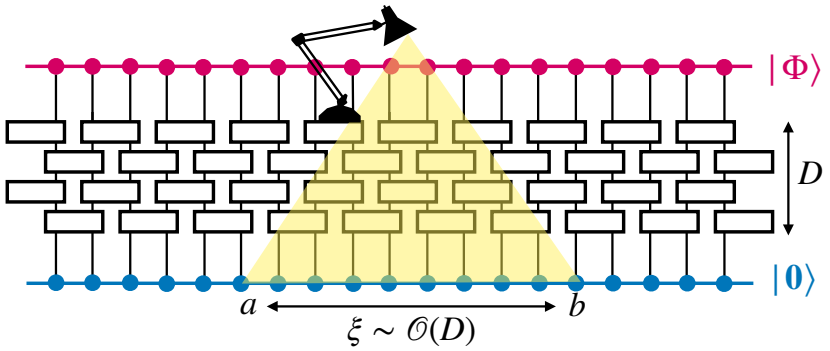

Figure 1.2: (Color online) The lightcone construction shows us that there is only correlation between operators where there exist some local Hilbert space states that fall under the same lightcone. We see that the correlation length $\xi \sim \mathcal{O}(D)$ where D is the depth of the circuit.

sometimes be associated with submanifolds of the underlying manifold (e.g. momentum space or real space). Here we give a few examples of possible topological invariants:

1. A metal with a Fermi surface has a topological invariant associated with translation and $U(1)$ symmetry: counting the filled energy levels inside and outside the Fermi surface stabilises the Fermi surface.

2. Graphene is a 2d semimetal where each Dirac cone possesses a Berry phase (also known as Zak phase) of π. This topological invariant stabilizes the existence of the Dirac nodes in the presence of $U(1)$ and time-reversal symmetry.

In general we see that for these gapless phases one may associate a quantized topological invariant with a $p-1$ dimensional surface, where p is the codimension of the Fermi surface [334]. In the above examples, 1. $p = 1$, so there is a $p-1 = 0$ dimensional surface invariant (i.e. the counting of the filled states); 2. $p = 2$, $p - 1 = 1$, so there is a 1d surface with a topological invariant, i.e. the Berry phase. In the next section we will see that Weyl and Dirac semimetals possess similar topological invariants related to 2d surfaces in momentum space. Finally note that other distinct notions of topology in gapless systems exist, such as those that are similar to topological orders, but with gapless excitations, such as the $\nu = 1/2$ Fermi liquid, but this viewpoint will generally not be the focus of this thesis.

1.2 3+1d semimetals

Three-dimensional (3+1d) semimetal states have garnered increasing interest in the last years due to their physical realisability [12, 383, 47], and topological properties associated with their stable point- and line-like Fermi surfaces [45, 385]. Semimetals come in a large variety such as a Weyl semimetal (WSM), with two-fold nodal degeneracy at the Fermi energy, Dirac semimetal (DSM), with four-fold degeneracy, and nodalline semimetal with linelike Fermi surfaces. When the relevant symmetries are taken into account, these gapless states possess a topologically-mandated gaplessness, meaning that their gaplessness is symmetry-protected or enforced such that any perturbation respecting such symmetries can not open a gap.

There exist two complimentary views of their topological-mandated gaplessness: one from the aspect of symmetry, and another from the aspect of quantum anomalies. The well-studied symmetry aspect is often presented in a free fermion context, involving arguments that rely on the separation of Weyl nodes and Berry curvature conservation arguments. The quantum anomalies viewpoint on the other hand relies on the idea that anomalies prevent systems from gapping to a symmetric trivial state, even in the interacting theory [374]. The by-product of this statement is that such a system has to naturally be gapless in the free fermion picture, and when gapped symmetrically must possess some topological order to compensate for the anomaly. In effect, one may argue that the anomaly viewpoint allows for a deeper understanding of gapless states since these statements hold in both the free fermion and interacting pictures. In this section we will first explore the free-fermion viewpoint, and in Sec. 1.3 we will explore its connection to quantum anomalies and topological response theory.

1.2.1 Weyl semimetal

Weyl semimetals are three dimensional (3D) materials that possess non-degenerate energy bands that cross at points, known as Weyl nodes, creating a two-fold degeneracy at specific momenta. Initially, one could assume that these crossing points are rare since degeneracies can often be lifted by perturbations. However this neglects the possibility of *accidental degeneracies* that may occur specifically in 3D solids due to the coincidence that there are three Pauli matrices and three spatial dimensions.

An expansion of the Hamiltonian close to a linearly-dispersing Weyl node, positioned at crystal momentum $\mathbf{k}_0$ and energy ϵ_0, can be written as

$$H(\mathbf{k}) = \epsilon_0\sigma_0 \pm \hbar v_F(\mathbf{k}-\mathbf{k}_0)\cdot\boldsymbol{\sigma} \quad , \tag{1.3}$$

where σ_0 is the 2×2 identity matrix, $\boldsymbol{\sigma} = (\sigma^x, \sigma^y, \sigma^z)$ is a vector of the Pauli matrices, $\mathbf{k}$ is the crystal momentum vector and v_F is the Fermi velocity. If $\epsilon_0 = 0$ in Eq. (1.3), we recover the exact Weyl Hamiltonian for right-handed (+ sign) and left-handed (− sign) relativistic massless particles [390]. Naturally, all perturbations in this 2-band model can be written in terms of the identity and Pauli matrices. In 3D these perturbations will only result in a shift of the position of the Weyl node since the perturbation terms can all be absorbed into the $\mathbf{k}_0$ or ϵ_0 terms. Thus the Weyl node cannot be perturbatively destroyed in the presence of $U(1)$ and translation symmetry, which makes its occurrence in 3D materials much more feasible. These nodes result as accidental degeneracies since their occurrence requires three parameters to be tuned to zero which in three-dimensions occurs naturally in momentum space, i.e. k_x, k_y, k_z. Of course, although these band crossing points occur naturally in many materials, only Weyl nodes close to the Fermi energy will have a substantial effect on the transport properties of these materials. Therein lies the true difficulty of finding a Weyl *semimetal*.

Weyl nodes exhibit non-trivial topological features resulting from a topological invariant associated to their chirality. The topological invariant may be defined via the Berry curvature $\boldsymbol{\Omega}(\mathbf{k})$ generated by a node through an enclosing two-dimensional surface [41]. The Berry curvature may be thought of as a momentum space analogy to the real space magnetic field. This topological feature is rooted in the fact that the chirality of the fermion determines the direction of the Berry curvature which forms an outwards or inwards pointing ball around the Weyl node. These degeneracies act as monopoles of the Berry curvature in the Brillouin zone (BZ).

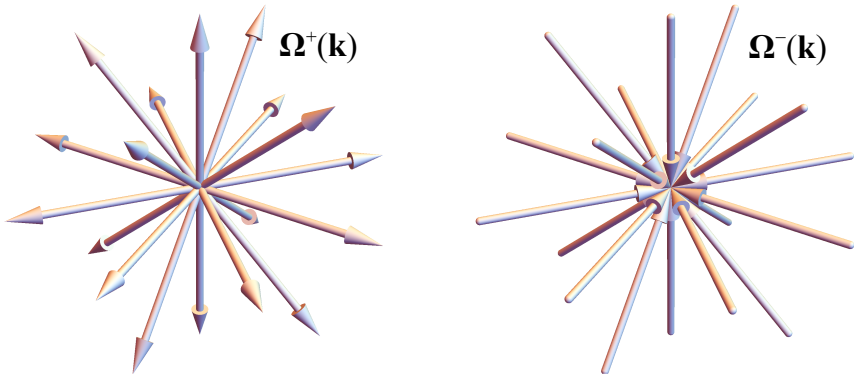

Figure 1.3: (Color online) Positive (left) and negative (right) chirality around Weyl nodes. We see that the nodes form a sink or source of the Berry curvature.

The expression of the Berry curvature for a linearly-dispersing Weyl node $\boldsymbol{\Omega}^{\pm}(\mathbf{k})$ situ-

ated at $\mathbf{k} = \mathbf{0}$ takes the form [377]

$$\mathbf{\Omega}^{\pm}(\mathbf{k}) = \pm\frac{\mathbf{k}}{2|\mathbf{k}|^3} \quad , \tag{1.4}$$

from which we can calculate the Chern number C via

$$C = \frac{1}{2\pi}\oint \mathbf{\Omega}^{\pm}(\mathbf{k}) \cdot d\mathbf{S} = \pm 1 \quad , \tag{1.5}$$

where we are integrating over a surface enclosing the Weyl node. The Chern number characterises the topological charge of the Weyl node. Naturally we see that the negative (positive) charge corresponds to a sink (source) of Berry curvature that is enabled by the crossing of two bands. A visualisation of this feature can be seen in Fig. 1.3. Generally, the charge corresponds directly to the chirality of the node which can be calculated via

$$C = \text{sign}[\mathbf{v}_x \cdot (\mathbf{v}_y \times \mathbf{v}_z)] \quad , \tag{1.6}$$

where $\mathbf{v}_i$ are the effective velocities that classify the Weyl nodes

$$H(\mathbf{k}) = \epsilon_0\sigma_0 + \sum_{\alpha=x,y,z} \mathbf{v}_\alpha \cdot \mathbf{k}\, \sigma^\alpha \quad . \tag{1.7}$$

Eq. (1.7) is a generalisation of Eq. (1.3) for different velocities in the k_x, k_y and k_z directions. So far we have only concentrated on scenarios where the topological charge is ± 1 as demonstrated by Eqs. (1.4) and (1.5). However, we may also have materials that possess Weyl nodes with larger topological charges, such as ± 2, which are commonly known as double Weyl nodes [148]. WSs that harbour these higher charged nodes are generally referred to as multi-Weyl semimetals [83, 152]. A double Weyl node is characterised by a quadratic dispersion in two directions around the node, e.g. $\partial E/\partial k_{x/y} = 0$. In general, the low energy approximation around multi-Weyl nodes possess only higher order momenta terms in at least two k directions. Their existence has been shown to be stabilised by point group symmetries [83]. In particular, point groups C_4 and C_6 contribute to the existence of quadratically dispersing Weyl nodes (charge magnitude 2) and cubically dispersing Weyl nodes (charge magnitude 3).

As mentioned before, Weyl semimetals also have non-degenerate bands, the requirements for which we have so far skipped over. Non-degenerate bands require a breaking of parity P or time-reversal T, as well as the breaking of PT. Thus we are restricted to non-centrosymmetric (broken P symmetry) or magnetic materials (broken T symmetry). It becomes of importance to note that the Berry curvature, $\mathbf{\Omega}(\mathbf{k})$ is odd under time-reversal,

i.e. $\mathbf{\Omega}(-\mathbf{k}) = -\mathbf{\Omega}(\mathbf{k})$, and even under parity, i.e. $\mathbf{\Omega}(-\mathbf{k}) = \mathbf{\Omega}(\mathbf{k})$ [390, 35]. In the case of broken time-reversal symmetry with preserved parity symmetry, if a Weyl point exists at $\mathbf{k}$ then another node of opposite chirality must be present at $-\mathbf{k}$ (see Fig. 1.4). Here the minimum amount of Weyl nodes is two. Alternatively, in the case of broken parity symmetry and preserved time-reversal symmetry, a Weyl point at $\mathbf{k}$ requires the existence of a node with the same chirality at $-\mathbf{k}$. Here since the total charge of the BZ must come to zero, i.e. all Berry curvature lines must start and end somewhere in the BZ, we require the existence of two extra Weyl nodes of opposite charge (see Fig. 1.4) such that the minimum model possesses at least four Weyl nodes.

One of the appealing features on Weyl semimetals is that they are physically realisable in a variety of materials [383, 389, 211, 201, 192]. The first experimental discovery of these materials was in 2015 where the inversion symmetry-breaking Weyl semimetal TaAs was observed to possess the predicted topological Fermi arcs associated to the surface projection of the bulk Weyl nodes [383]. Since then a variety of other materials has been experimentally confirmed including magnetic, i.e. time-reversal breaking, Weyl semimetal $Co_3Sn_2S_2$ [194, 192, 356] and nodalline semimetal Co_2MnGa [52, 23]. Additionally, an external magnetic field is also known to induce Weyl semimetallic states in $EuCd_2Sb_2$ [328] and $EuCd_2As_2$ [314].

One way of obtaining a Weyl semimetal is to modify a *Dirac semimetal* by adding, for example, a magnetic field (i.e. breaking T symmetry). Dirac semimetals possess both time-reversal and parity invariance, thus doubly degenerate bands, with quadruply degenerate nodes around the Fermi energy. Thus when we break either the time-reversal or parity symmetry, we may obtain a WS. In the next section, we introduce some important features of Dirac semimetals.

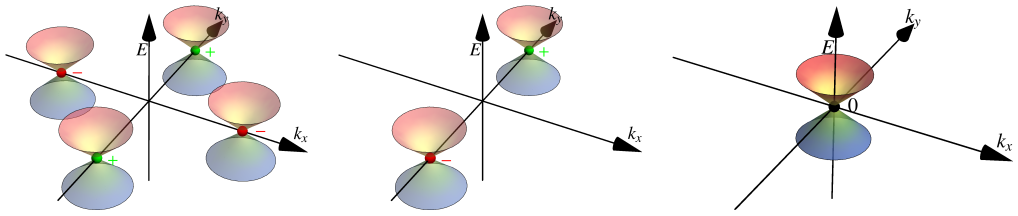

Figure 1.4: (Color online) Schematic of a possible transition between a Dirac semimetal (right) to a Weyl semimetal with broken time-reversal symmetry (middle) or parity symmetry (left). The charges are annotated and indicated by the colouring of the spheres overlaid on the nodes. In (left), note that in general the nodes are not necessarily positioned with this exact symmetry.

1.2.2 Dirac semimetal

As emphasised before, Weyl semimetals require the breaking of at least one of the two following symmetries: time-reversal or inversion symmetry. When both time-reversal and inversion symmetry are present (or the combination PT), each band becomes locally doubly degenerate at all momenta. Additionally, since in this case $\mathbf{\Omega}(\mathbf{k}) = -\mathbf{\Omega}(\mathbf{k})$, i.e. $\mathbf{\Omega}(\mathbf{k}) = 0$ for all $\mathbf{k}$, all Weyl nodes are required to annihilate or, alternatively, merge to uncharged nodes. The latter mentioned merging phenomenon may allow for the existence of quadruple degeneracies at specific crystal momenta. Generally, these degeneracies are unstable since they are no longer topologically protected, i.e. there is no Berry curvature, and there are many extra perturbations that may lift the quadruple degeneracy of the bands. However, when we are able to stabilise a quadruple degeneracy at a given crystal momentum, otherwise known as a Dirac node, we form what is called a *Dirac semimetal* (DSM).

There exist two distinct types of Dirac semimetals: Type I DSMs are facilitated by a band-inversion mechanism whereby the crossing points are protected, i.e. hybridisation is prevented, by a rotational symmetry [12]. Type II DSMs have symmetry-enforced Dirac nodes that may naturally occur at time-reversal invariant momentum (TRIM) points [397]. In this thesis we will primarily deal with type I DSMs, but for the sake of completeness, we will give a brief overview of both type I and II.

In type I DSMs, a *pair* of Dirac crossing points must exist along the symmetry axis due to the nature of the band inversion mechanism. This type of semimetal is achievable since hybridization, i.e. mixing between different band eigenstates, of separate bands may be prevented along a symmetry axis where the mixing terms disappear [12, 387]. A motivation for how this protection may occur is presented in Appendix A and a figure demonstrating this mechanism can be seen in Fig. 1.5. These points are stable within a range of physical parameters, but can be eliminated by tuning the material from a band-inverted phase into a normal phase, which causes the two Dirac points to merge and annihilate. Some examples of experimentally realised type I Dirac semimetals are Na_3Bi and Cd_3As_2 [197, 359, 360], where the Dirac semimetal phase is stable for a wide range of system parameters.

In the case of type II DSMs, we may get rid of the necessity of tuning due to the presence of symmetry-enforced Dirac points which are required and unremovable [397]. Generally, although not necessarily, these Dirac points occur at TRIM points. Due to our focus, we refrain from giving a more expansive overview of this topic[5]. Some experimentally realisable type II DSMs are zirconium pentatelluride ($ZrTe_5$) [186, 56] and thallium-based ternary chalcogenide alloy ($TlBi(S_{1-x}Se_x)_2$) [297].

[5] A comprehensive review on this topic may be found in Ref. [12].

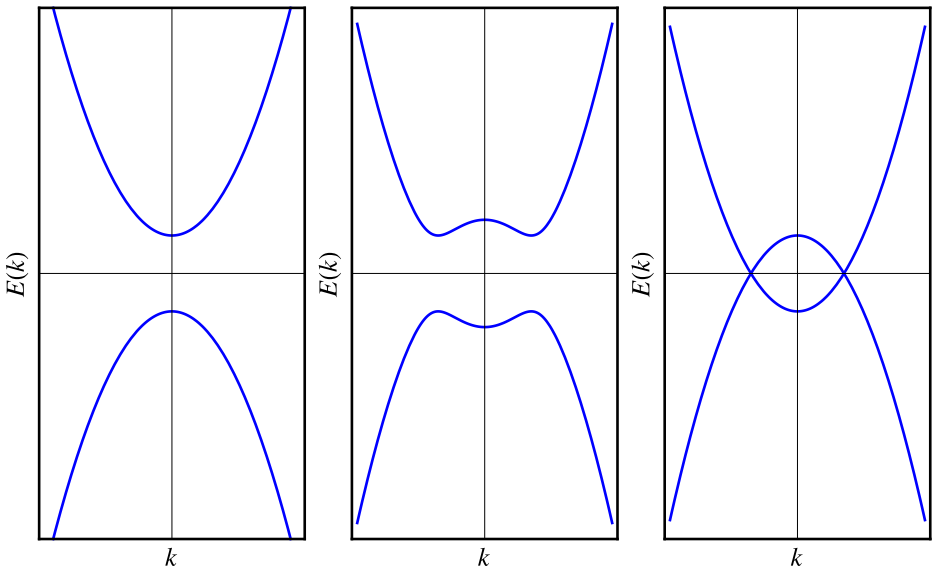

Figure 1.5: (Color online) The mechanism underlying the creation of a pair of Dirac nodes in type I Dirac semimetals. (left) The non-inverted/normal regime where there is no crossing point. (middle) The inverted regime with hybridization of the crossing point, which gaps the spectrum. (right) Hybridisation is prevented since the rotation symmetry prevents mixing terms from occurring along the symmetry axis k. This protection results in a pair of Dirac nodes along k and a type I DSM is obtained. Figure is adapted from Ref. [12].

Now that we have reviewed different types of semimetals, we move on to providing the reader with an introduction on the topic of topological response and quantum anomalies in the context of condensed matter physics. However, a (very) brief refresher regarding quantum anomalies in a more general context can also be found in Appendix B.

1.3 Topological response

Topological response of materials is an incredibly broad subject that spans both gapped and gapless systems. The basis of topological response lies in the effective action formalism [364, 219] in the presence of external 'probe' gauge fields: imagine for example setting up a laboratory and applying some electric field to your system and measuring the response of electric charges. If we assume that the dynamical effects of this laboratory electric field is small, then we can effectively treat it as a probe to our system. Response to these sort of probes are encapsulated in the effective action S_{eff} that arises from integrating out the

dynamical degrees of freedom, such as the charged particles, in the partition function. In the example of charged particles in some electric field we have

$$Z_{\text{eff}}[A_\mu] = e^{iS_{\text{eff}}[A_\mu]} = \int D[\Psi, \bar{\Psi}] e^{iS[A_\mu, \Psi, \bar{\Psi}]} \quad , \tag{1.8}$$

where Z_{eff} is the partition function, A_μ is the $U(1)$ probe gauge field, and Ψ denotes the charged degree of freedom. The probe gauge field couples to the conserved charge current of the system j_μ, such that $S[A, \Psi, \bar{\Psi}] = S_\Psi[\Psi, \bar{\Psi}] - iqA_\mu j^\mu + \mathcal{O}(A^2)$ (up to first order in A_μ). Recall that there exists a gauge redundancy in the $U(1)$ gauge field formalism such that $S[A, \Psi, \bar{\Psi}]$ must satisfy gauge invariance under the gauge transformations $A_\mu \to A_\mu + \partial_\mu \theta(x)$ and $\Psi \to e^{iq\theta(x)}\Psi$. Once we have the correct effective action, there are many things we can compute such as the expectation value of the current

$$\langle j_\mu \rangle = \frac{\delta S_{\text{eff}}[A_\mu]}{\delta A_\mu} = \frac{1}{Z_{\text{eff}}[A_\mu]} \int D[\Psi, \bar{\Psi}] j_\mu e^{iS[A_\mu, \Psi, \bar{\Psi}]} \quad , \tag{1.9}$$

as well as many linear response quantities such as conductivity and magnetic susceptibility [89]. The effective action formalism allows for a convenient characterization of the response of condensed matter systems.

So far there has been no mention of what makes a response *topological*. Generally we refer to a response as topological if it only depends on the topology of the underlying manifold or, more precisely, fiber bundle. These effective action terms appear in such a way that local deformations have no effect, i.e. the metric does not appear[6], and can be associated to a topological invariant of the fiber bundle. An example of such a term is the integer Hall conductivity which can be written as

$$S_{\text{eff}}[A_\mu] = \frac{n}{4\pi} \int d^2x dt \, \epsilon^{\mu\nu\lambda} A_\mu \partial_\nu A_\lambda \quad , \tag{1.10}$$

where $n \in \mathbb{Z}$. Note that there is no appearance of the metric in such a term. The topological aspects of SPT and invertible topological order responses can be summarised in this effective action formalism. The presence of such a topological response usually indicates the presence of a boundary 't Hooft or gauge anomaly which implies the existence of a non-trivial gapless edge theory [365]. We will now explore this aspect of the story in the context of 't Hooft anomalies.

[6]Here we note exceptions such as the gravitational topological responses that describe the thermal Hall effect. These do inherently involve the metric, and more precisely the frame bundle of the tangent bundle of the manifold.

1.3.1 SPT and 't Hooft anomalies

A canonical example of an SPT with a 't Hooft anomaly at the edge is the quantum spin Hall (QSH) state. Let us take the system with a charge $U(1)_q$ and spin S_z $U(1)_z$ symmetry, with external gauge fields A_μ and C_μ, respectively. The effective action for a QSH insulator is

$$S_{\text{eff}}[A_\mu, C_\mu] = \frac{n}{2\pi}\int d^2x dt\, \epsilon^{\mu\nu\lambda} C_\mu \partial_\nu A_\lambda \quad , \tag{1.11}$$

where $n \in \mathbb{Z}$ determines the spin-Hall conductance, as can be seen if we vary with respect to C_μ. This expression is fully gauge-invariant for $n \in \mathbb{Z}$ in the absence of a boundary. However in the presence of a boundary to a trivial insulator (or more generally an insulator with another spin-Hall coefficient), the gauge transformation of $C_\mu \to C_\mu + \partial_\mu \alpha(x)$ is not gauge invariant at the boundary (let the boundary be at $y = 0$ with the upper plane being the trivial insulator and lower plane being the QSH insulator with $\sigma_{xy}^{\text{spin}} = n/2\pi$) via the term

$$\delta S_{\text{eff}}[A_\mu, C_\mu] = -\frac{n}{2\pi}\int dx dt\, \epsilon^{\mu\nu} \alpha(x) \partial_\mu A_\nu \quad , \tag{1.12}$$

which at first sight is quite concerning! We of course require our theory to be fully gauge invariant, so what is going on here? Before we embark on resolving this conundrum, let us note one other odd feature: $U(1)_z$ charge conservation is in fact also violated at the boundary as can be seen if we vary Eq. 1.11 with respect to C_μ and contract the indices with ∂_μ we get

$$\partial_\mu j_z^\mu = -\delta(y)\frac{n}{2\pi}\epsilon^{\mu\nu}\partial_\mu A_\nu \quad . \tag{1.13}$$

Where does this non-conservation arise from and how do we maintain $U(1)_z$ symmetry?

The resolution to both these conundrums is to note that there is some missing low-energy physics at the interface that both compensates both the gauge non-invariance issues and also fixes the $U(1)_z$ charge non-conservation. In fact, this low-energy physics is exactly what leads to the $U(1)_q \times U(1)_z$ symmetric n pairs of gapless counterpropagating spin modes with a right-mover with S_z eigenvalue $\frac{1}{2}$ and left mover with S_z eigenvalue $-\frac{1}{2}$. Back-scattering is prevented as long as the $U(1)_q \times U(1)_z$ symmetries are preserved. Such a 1d system is known to possess the $1+1$d chiral anomaly which leads to non-conservation of 'chiral' charge, i.e. in this case $U(1)_z$ charge with spin current j_z^μ, in the presence of a $U(1)_q$ electric field. The non-conservation is given by

$$\partial_\mu j_z^\mu = \frac{n}{2\pi}\epsilon^{\mu\nu}\partial_\mu A_\nu \quad . \tag{1.14}$$

This non-conservation indicates that either $U(1)_z$ is only an emergent symmetry at low energies and is in fact broken in the UV (such as in a Luttinger liquid [105]), or one or more of these symmetries acts in a non on-site manner (which was recently realized in [67, 337]) or, alternatively, $U(1)_z$ is an exact on-site symmetry but the non-conserved charge must flow to or from somewhere, i.e. into a higher-dimensional bulk. The latter is exactly how the non-conservation of the QSH system is preserved: there is $U(1)_z$ charge flow between the bulk (Eq. 1.13) and the gapless surface modes (Eq. 1.14). More generally, this phenomenon is also known as *anomaly inflow*.

Now, as to resolving the apparent gauge non-conservation of the bulk at the boundary: a chiral gauge transformation of the $1+1$d $U(1)_q \times U(1)_z$ gapless modes can be shown via the Fujikawa method [246] to result in a change in the action of

$$\delta S_{1\mathrm{d}}[A_\mu, C_\mu] = \frac{n}{2\pi} \int dx dt\, \epsilon^{\mu\nu} \alpha(x) \partial_\mu A_\nu \quad , \tag{1.15}$$

which can be seen to be equal and opposite to the term from the bulk in Eq. 1.12. Now putting the $1+1$d gapless contribution together with the bulk contribution, we see that the theory is in fact fully gauge invariant.

The example of QSH demonstrates the power of the effective action: we can differentiate different states via their effective actions, and also observe the effects of 't Hooft anomalies that govern the physics of their gapless edge states. In general all SPT states may be described by different effective action terms with quantized coefficients [159, 160] (in the QSH term n is quantized!). These quantized effective actions can be connected to their band-theory topological quantities (e.g. $\mathbb{Z}_2$ index of a topological insulator [158]), but also go beyond this description since they are even valid in the interacting regime. Recently there has also been a shift towards understanding the interplay of crystalline symmetries, as opposed to the usual on-site symmetries, with SPT phases, resulting in the physics of crystalline SPT (cSPT) states. In the next section we will explore some general ideas of effective actions involving crystalline symmetries.

1.3.2 Gauging crystalline symmetries

In order to use the effective action formalism for crystalline phases of matter we need a method to gauge crystalline symmetries such that we can write responses in terms of topological defects of these symmetries. We are used to the gauging procedure for on-site symmetries such as particle number $U(1)$ or spin $SO(3)$ symmetries. However things are more complicated in the case of crystalline symmetries, which are non on-site symmetries,

i.e. they take states from local Hilbert spaces to other local Hilbert spaces. To understand how to gauge such symmetries we need to recognise that for on-site symmetries one may choose to view the flux Φ threading non-contractible loops as being the result of a non-trivial Wilson loop, or alternatively a non-trivial transition functions of the associated principle bundle[7]. Such transition functions apply a group element $e^{iq\Phi}$ whenever a charge-q particle winds around the non-contractible loop, i.e. the physics of the Aharanov-Bohm effect. Similarly, when applied to crystalline symmetries, which are all discrete groups[8], we may consider the physics of non-contractible loops as acting upon the 'particle' (charged under crystalline symmetry) by some crystalline group element, classified by the Wilson loops (or alternatively the transition functions).

Let us take the example of the discrete translation symmetry group, which is isomorphic to $\mathbb{Z}$. The unit translation $\hat{T}_a$ acts as a single translation of unit cell size a upon a charged state, i.e. a state with crystalline momentum k, by the phase factor e^{ika}. Now imagine a perfect crystalline lattice with discrete translation in $\hat{z}$ and taking the state with momentum k along a contractible loop as shown in Fig 1.6(a). The phase factor gained upon completion of this loop is $1 = e^{ikna-ikna}$ since we traversed an equal amounts in the positive and negative $\hat{z}$ directions. However if we took the loop to be along the whole lattice in the $\hat{z}$ direction, i.e. along a non-contractible loop, then we would gain a phase factor of e^{ikL} where L is the length of the lattice in $\hat{z}$ direction. Since momentum is quantized via periodic boundary conditions we have $e^{ikL} = 1$ for a perfect lattice. Now consider inserting a dislocation, see Fig. 1.6(b), with Burgers vector $\mathbf{b}$ and evaluating the Wilson loop around such a configuration to get a phase factor $e^{ik\mathbf{b}\cdot\hat{z}} = e^{ik\int_C \tilde{z}}$ where $\tilde{z}$ is the translation gauge field. So we see that fluxes $\int \tilde{z} = \mathbf{b}\cdot\hat{z}$ for discrete translation symmetries are determined by the Burgers vector and thus the dislocations of the lattice, which is very cute! Having these tools in our arsenal will allow us to explore topological phases protected by translation symmetry.

We may also consider another relevant crystalline symmetry that will feature in the later chapters of this thesis: discrete n-fold rotations of angles $\frac{2\pi}{n}$ (where n is an integer) which forms a group that is isomorphic to $\mathbb{Z}_n$. States charged under rotation symmetry possess a definite angular momentum j such that these states transform as $e^{ij\frac{2\pi}{n}}$ under the

[7]Note that in 1d all $U(1)$ bundles are trivial, meaning that we can always set the transition functions to triviality and globally define our connection 1-form. In higher dimensions we may have obstructions to such a description due to non-removable transition function (i.e. non-trivial $U(1)$ bundle) with non-trivial Chern numbers. Conveniently, all such higher-dimensional bundles can be fully classified by the Wilson loops by restricting the bundle to a 1d loop upon which you can define a global 1-form connection again and evaluate the Wilson loop.

[8]Note that for discrete groups, the connection is fully determined by the principle bundle, i.e. the transition functions. The connection itself is flat.

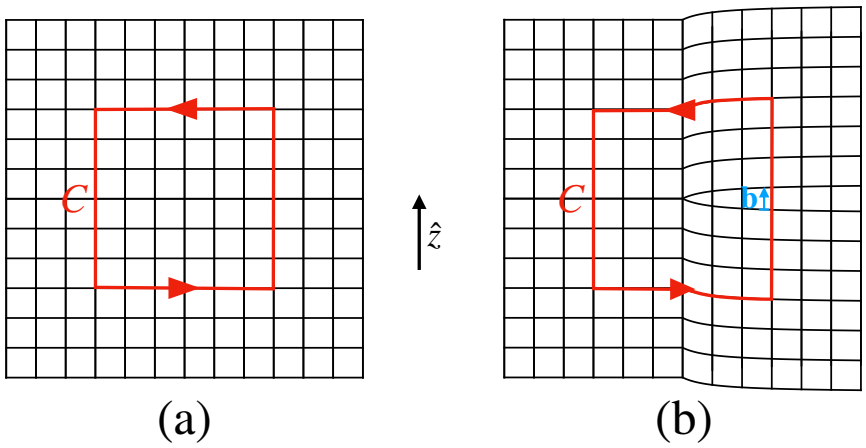

Figure 1.6: (Color online) (a) A perfect defect-free lattice with translation symmetry in $\hat{z}$. (b) A lattice with an edge dislocation where the Burgers vector is $\mathbf{b} = \hat{z}$.

action of the unit rotation. Here the fluxes of the rotation gauge field c are determined by the Frank angle $\mathbf{f}$ which details the disclination type in the lattice, see Fig. 1.7, i.e. $\int_C c = \mathbf{f} \cdot \hat{z} \mod n$ for rotations in the xy plane.

This analogy with gauge fluxes has inspired the study of crystalline phases by topological response [336], and led to the *crystalline equivalence principle* conjecture. This conjecture specifically proposes that cSPT phases are classified identically to regular SPT by treating all crystalline symmetry groups as though they are on-site symmetry groups, and has been successful in understanding a variety of different materials. Let us consider one simple example: a 3+1d weak topological insulator, made out of a stack of 2+1d QSH states. Such a system is a cSPT but not a strong TI since it requires the presence of translation symmetry to be a well-defined phase. The topological response is

$$S_{\text{eff}}[A_\mu, C_\mu, \tilde{z}_\mu] = \frac{n}{2\pi} \int d^3x dt \, \epsilon^{\mu\nu\lambda\delta} \tilde{z}_\mu C_\nu \partial_\lambda A_\delta \quad , \tag{1.16}$$

where if we vary by $\tilde{z}_z$ we see that each layer is a QSH insulator. Such a term predicts the existence of surface edge states (the counterpropagating gapless states as discussed in Sec. 1.3.1) per layer in the stacking direction of the material. If we were to break the translation symmetry in this direction, then we could hybridise neighbouring gapless modes and trivially gap out the edge thereby obtaining a trivial insulator with no topologically-protected features. Additionally, when we insert a dislocation, this becomes equivalent to inserting a half-layer of QSH. The effective action immediately predicts the existence of a pair of topologically-protected counterpropagating gapless modes along the dislocation

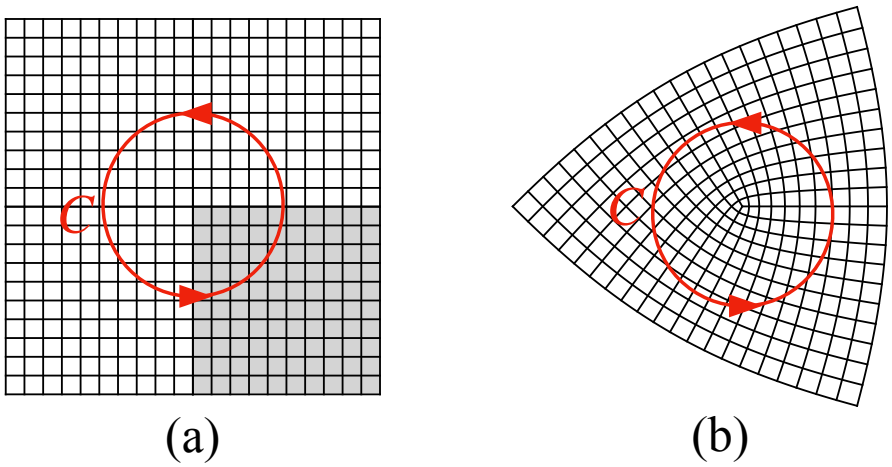

Figure 1.7: (Color online) (a) A perfect lattice with C_4 symmetry. (b) A disclinated lattice where we fold over the shaded region in (a).

line. This can be seen through the Wilson loop of Eq. 1.16 by moving the ∂_λ onto the $\tilde{z}$ gauge field and integrating out $\int_{xz} d\tilde{z} = 1$ to get a 1+1d theory in $\hat{y}$ of the form $\int C \wedge A$ that is now gauge non-invariant and requires 1+1d $U(1)_q \times U(1)_z$ gapless modes to fix the gauge non-invariance, as discussed in Sec. 1.3.1. This physics is essentially that of the weak TI $\mathbb{Z}_2$ index (where we use time-reversal symmetry as opposed to spin $U(1)_z$) that may be calculated in the band theory. Such a term even holds when we add perturbative symmetry-preserving interaction terms, i.e. it is a stable 3+1d cSPT state.

Now that we have explored 't Hooft anomalies, SPT and cSPT phases of matter, and have seen the usefulness of crystalline gauge fields, we are now ready to discuss topological response and quantum anomalies in the context gapless systems.

1.3.3 Quantum anomalies in gapless systems

So far we have only discussed gapped systems and their quantized topological responses. For gapless systems we have seen that the topological invariants are associated to submanifolds, as discussed in Sec. 1.1.3. We will connect these quantized submanifold topological invariants to unquantized topological responses.

The simplest gapless topological response is that of fractional particle number filling in Fermi liquids. We saw previously that this was associated with a 0d topological invariant that counted the difference in the electron filling at two momentum points. To define such

a particle filling we need both $U(1)_q$ and translation symmetry. Let us take a 1+1d Fermi liquid as an example: here the topological invariant can in fact be summarised as the following topological response

$$S_{\text{eff}}[A_\mu, \tilde{z}_\mu] = \nu \int dz dt \epsilon^{\mu\nu} \tilde{z}_\mu A_\nu \quad , \tag{1.17}$$

where ν is the filling fraction per unit cell. We can see that ν represents this filling fraction by varying with respect to A_t (time component of the current) which gives the charge filling as

$$\rho_q = \nu \tilde{z}_z \implies Q_q = \nu L \quad ,$$

which tells us that the ν is the filling fraction of system size L (up to a $\mathcal{O}(1/L)$ correction required to have an integer total number of charges). The filling fraction is defined in the thermodynamic limit as $\nu = \lim_{L\to\infty} Q_q(L)/L$. In fact, this term implies the existence of gapless modes at low energy due to the gauge non-invariance under gauge transformation of A_μ. Similar to the story with 't Hooft anomalies, we see here that low energy gapless modes are required to maintain gauge invariance. In fact this term also encodes the chiral anomaly of adiabatic flux threading, but we will see this in Chapter 3. Such a term can also be generalised to a general $n+1$ dimensional system since we may simply write $\nu \int \tilde{x}_1 \wedge \tilde{x}_2 \wedge ... \wedge \tilde{x}_n \wedge A$ where $\tilde{x}_i$ is the translation gauge field in the $\hat{i}$th orthonormal direction.

We see that the topological response of this Fermi liquid in Eq. 1.17 is unquantized and 'less' protected compared to the quantized cases as one can symmetrically (keeping $U(1)_q$ and translation symmetry) change the coefficient of such a term by adding, for example, a chemical potential term to the Hamiltonian. However if we were to play the game of fixing the microscopic filling, e.g. via experimental measurements or a constraint on the Hilbert space, then we can have many exciting things to say about the system! This specific particle number filling example is known under the principle of the $U(1)_q \times \mathbb{Z}_{\text{transl}}$ Lieb-Schultz-Mattis (LSM) theorem which states that ground states with translation and $U(1)_q$ symmetry at non-integral filling must be long-range entangled. This immediately implies that the ground state must be gapless, topologically-ordered, or spontaneously symmetry-breaking. Similarly, Eq. 1.17 also predicts that there must be some non-trivial IR behaviour; we see that these two formalisms are two sides of the same beautiful coin.

Topological response has also been well-studied in the context of magnetic Weyl semimetals [408, 349, 105]. The gaplessness of these systems is protected by a crystal translation and $U(1)_q$ charge symmetry, which in turn gives rise to a chiral anomaly response term whose coefficient depends on the separation of the Weyl nodes in momentum space. This

feature can also be understood as a consequence of the Weyl nodes being sinks and sources of the Berry curvature in momentum space, as was discussed in Sec. 1.2.1. The Berry curvature causes the existence of a Dirac string that connects the two nodes (say, separated in momentum space by a magnitude $2Q$) such that every momentum slice that is pierced by the string contributes a non-trivial Chern number of one that leads to a Hall conductivity of

$$\sigma_H = \frac{1}{2\pi}\frac{2Q}{2\pi} \quad .$$

This Hall conductivity effect, as well as the well-known chiral magnetic effect [408], can be summarised in the term

$$S = -\frac{Q}{4\pi^2}\int dt\, d^3r\, \tilde{z}_\mu \epsilon^{\mu\nu\alpha\beta} A_\nu \partial_\alpha A_\beta, \tag{1.18}$$

where we assume the Weyl nodes to be separated along the $\hat{z}$ momentum axis. Importantly this chiral anomaly does not microscopically involve the usual $U(1)_q \times U(1)_a$ (charge and axial) symmetry, but instead arises from a $U(1)_q \times \mathbb{Z}_{\text{transl}}$ symmetry, where the $\mathbb{Z}$ symmetry is attributable to the translation symmetry along the axis of Weyl node separation. In particular, the non on-site nature of the $\mathbb{Z}$ translation symmetry allows us to forego the low-energy emergent $U(1)_q \times U(1)_a$ 't Hooft chiral anomaly, and associated no-go theorem, thereby realising such a system in 3+1d, instead of on the boundary of some higher dimensional object. This situation can be contrasted to that of the 2+1d time-reversal and $U(1)$ symmetric massless Dirac fermion which suffers the parity anomaly and, due to the on-site nature of the symmetries involved, can only be realised on the surface of a 3+1d topological insulator [374]. The situation of the $U(1)_q \times \mathbb{Z}_{\text{transl}}$ chiral anomaly can be viewed as a 3+1d analogue of the 1+1d Lieb-Schultz-Mattis (LSM) statement which implies that 1+1d states with $U(1)_q \times \mathbb{Z}_{\text{transl}}$ at non-integral filling must be gapless due to the 1+1d chiral anomaly which may be tuned by adjusting the filling fraction [189, 70, 80]. In the case of Weyl semimetals, where the filling factor is integral, the gaplessness once again arises due to the chiral anomaly but is now tuned by the separation of the Weyl nodes in momentum space.

Some similar studies have been performed on Dirac and other semimetal systems [70, 43, 44], and the filling constraints on gappable 3+1d lattice states have been explored [362], but a general study of the realisability of quantum anomalies via lattice symmetries has not yet been accomplished, especially in the context of semimetals. In this thesis we will explore the effects of strong interactions on the magnetic WSM anomaly term in Chapter 2, where we will discover an intrinsically 3+1d fractional quantum Hall state with loop excitations and three-loop braiding. In Chapter 3 we will generalise the magnetic WSM anomaly term to type-I DSM and time-reversal invariant WSM systems, where we will see that the lowest

Landau level physics contains non-trivial filling of both rotation and momentum charges, respectively. In Chapter 4 we will explore this momentum charge in detail and prove an LSM-type theorem involving pure translation symmetry that can be viewed as the root of all LSM theories. Finally, in Chapter 5 current work in progress as well as potential generalisations will be explored.

Chapter 2

Fractional quantum Hall effect in Weyl semimetals

In this chapter we will explore the effects of strong interactions in magnetic Weyl semimetals when we fix the Hall conductivity per layer to be half of a conductivity quanta. We arrive at the 3+1d fractional quantum Hall state and show that the resultant $\mathbb{Z}_4$ topologically ordered state possesses interesting qualities such as three-loop braiding. This chapter is lifted from the published work in Ref. [349][1].

2.1 Introduction

Weyl semimetal is the first example of a bulk gapless topological phase [12, 45, 385, 131]. The gaplessness of the bulk electronic structure in Weyl semimetals is mandated by topology: there exist closed surfaces in momentum space, which carry nonzero Chern numbers (flux of Berry curvature through the surface), which makes the presence of a band-touching point inside the Brillouin zone (BZ) volume, enclosed by the surface, inevitable. This picture, however, relies on separation between the individual Weyl nodes in momentum space, which involves symmetry considerations. In particular, either inversion or time reversal (TR) symmetry need to be violated in order for the Weyl nodes to be separated. In addition, crystal translational symmetry needs to be present, since otherwise even separated Weyl nodes may be hybridized and gapped out.

A very useful viewpoint on topology-mandated gaplessness is provided by the concept of quantum anomalies. The best known example of this is the gapless surface states of three dimensional (3D) TR-invariant topological insulator (TI). The relevant anomaly in this case is the parity anomaly: the θ-term topological response of the bulk 3D TI [280] violates TR (and parity) when evaluated in a sample with a boundary. This anomaly of the bulk response must be cancelled by the corresponding anomaly of the gapless surface state [406], which is simply the parity anomaly of the massless 2D Dirac fermion [305, 288, 374].

Analogously, the gaplessness of the bulk spectrum in Weyl semimetals may be related to the chiral anomaly [3, 22]. Suppose we have a magnetic Weyl semimetal with two band-touching nodes, located at $\mathbf{k}_\pm = \pm\mathbf{Q} = \pm Q\hat{z}$. Crystal translations in the z-direction act on the low-energy modes near the Weyl points as chiral rotations

$$T_z^\dagger c_{\pm\mathbf{Q}}^\dagger T_z = e^{\mp iQ} c_{\pm\mathbf{Q}}^\dagger, \tag{2.1}$$

where we have taken the lattice constant to be equal to unity (we will also use $\hbar = c = e = 1$ units throughout the paper). However, the chiral symmetry of Eq. (2.1) is anomalous: an attempt to gauge this symmetry fails and produces a topological term [408]

$$S = -\frac{1}{4\pi^2}\int dt\, d^3r\, Q_\mu \epsilon^{\mu\nu\alpha\beta} A_\nu \partial_\alpha A_\beta, \tag{2.2}$$

which expresses the impossibility to conserve the chiral charge and underlies all of the interesting observable properties of Weyl semimetals. In particular, variation of Eq. (2.2) with respect to the electromagnetic gauge potential gives the anomalous Hall conductivity of the Weyl semimetal

$$\sigma_{xy} = \frac{1}{2\pi}\frac{2Q}{2\pi}, \tag{2.3}$$

which depends only on the separation $2Q$ between the Weyl nodes in momentum space. By Wiedemann-Franz law, Eq. (2.3) also implies a thermal Hall conductivity

$$\kappa_{xy} = \sigma_{xy}\left(\frac{\pi^2 k_B^2 T}{3}\right) = \frac{Q}{2\pi^2}\left(\frac{\pi^2 k_B^2 T}{3}\right), \tag{2.4}$$

which, alternatively, may also be viewed as a manifestation of the chiral-gravitational mixed anomaly [205, 110]. In the Appendix C we discuss a more formal, but physically equivalent, way to describe the chiral anomaly in a Weyl semimetal.

Tuning the node separation $2Q$ between 0 and 2π realizes the transition between a trivial and an integer quantum Hall insulator in 3D [128, 329], which has to proceed through the intermediate Weyl semimetal phase [47], unlike in 2D, where there is a critical

point (plateau transition). The chiral anomaly also leads to the appearance of Fermi arc surface states, since the action in Eq. (2.2) fails to be gauge invariant in the presence of a boundary, which makes the existence of a boundary-localized state necessary [116].

Apart from giving rise to topological response and protected surface states, anomalies can also place strong restrictions on the possible effect of electron-electron interactions. In particular, anomalies prohibit opening a gap without either breaking the protecting symmetry or creating an exotic state with topological order, as was recently discussed extensively in the context of strongly-interacting 2D surface states of 3D symmetry-protected topological orders [59, 63] in bosonic [340] and fermionic [84, 351, 227, 58, 32, 353, 226, 278] systems. In this Letter, we aim to answer analogous questions in the case of a 3D Weyl semimetal: can one open a gap in a Weyl semimetal without breaking translational or charge conservation symmetries while preserving the chiral and the gravitational anomalies, which lead to the electrical and thermal Hall conductivities of Eqs. (2.3) and (2.4)? What would be the universal properties of such gapped phases? We note here that effects of strong correlations in topological semimetals have been addressed before in Refs. [224, 239, 295, 223, 286], but from different viewpoints.

To answer these questions we will adopt the strategy known as "vortex condensation", which has been successful in the context of 2D surface states of 3D bulk TI [351, 227]. We will start by inducing a phase-coherent superconducting state in a magnetic Weyl semimetal (with only a single pair of nodes for simplicity, although the results readily generalize to any odd number of node pairs), which violates the charge conservation. We then attempt to produce a gapped insulator by proliferating vortices and restoring the charge conservation symmetry, while keeping the pairing gap intact. In order to make this procedure well-defined, we will assume the superconducting pairing to be weak, i.e. the induced gap is taken to be much smaller than $v_F Q$, where v_F is the Fermi velocity of the Weyl cones. In this case it is impossible to gap out the Weyl nodes by simply pushing them to the edge or the center of the BZ, where they can mutually annihilate without breaking translational symmetry. In the language of the anomaly, we are demanding that the coefficient of the anomaly Q, which takes continuous values and is thus not strictly protected, is fixed throughout the procedure.

2.2 Construction

It is easy to see that, in this situation, a BCS-type pairing of time-reversed states can not produce a gapped superconductor [222, 69, 19, 187]. It is, however, possible to open a gap by inducing a Fulde-Ferrell-Larkin-Ovchinnikov (FFLO)-type superconducting state

instead, where states on each side of the two Weyl nodes are paired [69, 19]. Since pairing in the FFLO state may (approximately) be taken to occur independently in each Weyl cone, let us consider a single (right-handed) Weyl fermion with singlet pairing

$$H = v_F \sum_{\mathbf{k}} c^\dagger_{\mathbf{k}} \boldsymbol{\sigma} \cdot \mathbf{k}\, c_{\mathbf{k}} + \Delta \sum_{\mathbf{k}} (c^\dagger_{\mathbf{k}\uparrow} c^\dagger_{-\mathbf{k}\downarrow} + c_{-\mathbf{k}\downarrow} c_{\mathbf{k}\uparrow}), \tag{2.5}$$

Introducing Nambu spinor $\psi_{\mathbf{k}} = (c_{\mathbf{k}\uparrow}, c_{\mathbf{k}\downarrow}, c^\dagger_{-\mathbf{k}\downarrow}, -c^\dagger_{-\mathbf{k}\uparrow})$, this may be written as

$$H = \frac{1}{2} \sum_{\mathbf{k}} \psi^\dagger_{\mathbf{k}} (v_F \tau^z \boldsymbol{\sigma} \cdot \mathbf{k} + \Delta \tau^x) \psi_{\mathbf{k}}, \tag{2.6}$$

which is simply the Hamiltonian of a Dirac fermion of mass Δ. This, however, leads to a density modulation and thus broken translational symmetry. Since $\Delta(\mathbf{Q}) \sim \sum_{\mathbf{k}} \langle c^\dagger_{\mathbf{Q}+\mathbf{k}} c^\dagger_{\mathbf{Q}-\mathbf{k}} \rangle$ carries momentum $2\mathbf{Q}$, a gauge-invariant density modulation $\varrho(\mathbf{Q}) \sim \Delta^*(-\mathbf{Q})\Delta(\mathbf{Q})$ will carry momentum $4\mathbf{Q}$. In general, this breaks translational symmetry, which may not be restored even when the superconductivity is destroyed by proliferating vortices. This is true, except when $\mathbf{Q} = \mathbf{G}/4$, where $\mathbf{G}$ is the smallest nonzero reciprocal lattice vector. In this case a gapped FFLO state does not break translational symmetry. We will thus concentrate on the $\mathbf{Q} = \mathbf{G}/4$ case henceforth.

An important question is what happens to the Fermi arc surface modes of the Weyl semimetal in the FFLO state. The Fermi arc is in principle unaffected by pairing since it is spin-polarized. However, due to the effective doubling of degrees of freedom, induced by pairing, which is corrected by the factor of $1/2$ in Eq. (2.6), the Fermi arc get copied to the part of the BZ outside of the Weyl points, and occupies the range of $4\mathbf{Q}$, which always coincides with the size of the new BZ, reduced by the translational symmetry breaking in the FFLO state [129]. When $\mathbf{Q} = \mathbf{G}/4$, however, this range is identical to the size of the original BZ, which is another way to see why the FFLO state does not break translational symmetry when and only when the Weyl node separation is exactly half the size of the BZ [2]. This implies that, while the electrical Hall conductivity in the FFLO state is no longer the same as in the non-superconducting Weyl semimetal due to the breaking of the charge conservation symmetry, the thermal Hall conductivity remains unaffected and is determined by the length of the Fermi (Majorana) line

$$\kappa_{xy} = \frac{Q}{2\pi^2} \left(\frac{\pi^2 k_B^2 T}{3} \right) = \frac{1}{4\pi} \left(\frac{\pi^2 k_B^2 T}{3} \right). \tag{2.7}$$

[2] See Supplemental Material for an alternative chiral anomaly formulation, the calculation of the Fermi surface state in the FFLO superconductor, the derivation of the straight-line vortex Majorana modes, and some formal details on vortex condensation

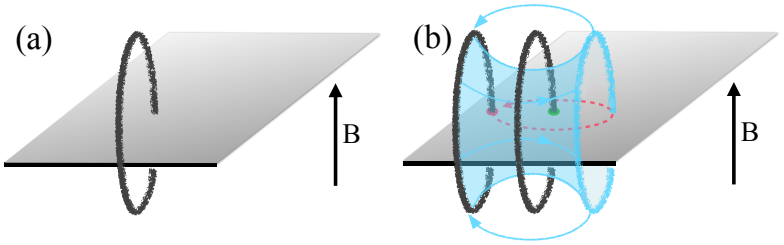

Figure 2.1: (Color online) (a) A vortex loop linked with a dislocation with the Burgers vector $\mathbf{B} = \hat{z}$. Fractional quantum numbers and nontrivial braiding statistics can emerge in such a configuration. (b) A pair of vortex loops linked with a dislocation with the Burgers vector $\mathbf{B} = \hat{z}$. Braiding the two loops may be accomplished by adiabatically shrinking the left loop, then moving it to the right by crossing the disc, enclosed by the right loop, then expanding and moving it back to the original place without crossing the disc, enclosed by the second loop.

In other words, the chiral-gravitational mixed anomaly is unaffected by the formation of the FFLO state.

We now try to restore the charge conservation symmetry by proliferating vortices in the superconducting order parameter while keeping the pairing gap for the Weyl fermions. If the vortices can be condensed without breaking the translational symmetry, we will obtain a gapped state that is fully symmetric. This state must have $\sigma_{xy} = 1/4\pi$ to match the chiral anomaly. To accomplish this, we need to understand carefully what does it mean to condense vortices, which form loops in 3D, without breaking the translational symmetry. In the simpler case of condensing particles, we would want the particle to carry zero momentum (up to a gauge choice). Now we want to achieve the same goal for vortex loops, which means that we want to condense vortex loops that transform trivially under translation. A good way to probe the properties of a loop under translation is to link the loop to a lattice dislocation with the Burgers vector $\mathbf{B} = \hat{z}$, which inserts a half xy-plane, ending on a dislocation line, as shown in Fig. 2.1(a). If a vortex is truly trivial under translation, such a link should not create any nontrivial effect.

Consider first a vortex loop with an odd vorticity, trapping a magnetic flux $\Phi = (2n + 1)\pi$. A straightforward calculation shows that each time the vortex penetrates an atomic xy-plane, a Majorana zero mode is trapped at the intersection (see Appendix D). An ordinary closed loop contains an even number of such zero modes since the xy-plane is penetrated an even number of times. However when linked with a dislocation with $\mathbf{B} = \hat{z}$, the total number of such penetrations becomes odd and the vortex now carries an unpaired

Majorana zero mode.

The effect becomes more drastic when two vortices with an odd vorticity are simultaneously linked to a $\mathbf{B} = \hat{z}$ dislocation. In this configuration we can consider braiding between the two vortices, as illustrated in Fig. 2.1(b). This process was first discussed in Ref. [348] and is known as three-loop braiding – the only difference in our case is that the "base" loop is a static dislocation rather than a dynamical excitation. Because of the Majorana zero modes, carried by the vortices when linked with the dislocation, the loop braiding process is non-abelian.

The above reasoning shows that odd vortices should be considered nontrivial under translation symmetry and cannot be condensed without breaking the symmetry. Yet another way to see this is that if we were to condense such vortices, inserting a dislocation into the system would require the inserted half-plane to be out of the bulk ground state to cancel the nontrivial braiding statistics of the linked vortices (only then a condensate is possible). This implies an energy cost $\sim O(L^2)$ instead of $\sim O(L)$ for an ordinary dislocation, where L is the system size. This simply means that the translation symmetry has actually been broken in the process.

Now what about vortices with even vorticity? There is no unpaired Majorana zero mode in this case, even when linked with a dislocation (see Appendix E). But the braiding statistics between two such vortices, linked with the same dislocation, can still be nontrivial (though must be abelian). Since to match the chiral anomaly we need the Hall conductivity of $\sigma_{xy} = 1/4\pi$ per layer, a two-fold vortex (with flux $\Phi = 2\pi$) will induce a semionic particle with the self-statistical phase $\theta = \pi\sigma_{xy}/(1/2\pi) = \pi/2$ each time it penetrates the xy-plane. As before, an ordinary two-fold vortex loop will not possess nontrivial self-statistics since the xy-plane is penetrated twice. But when linked with a $\mathbf{B} = \hat{z}$ dislocation, each vortex traps an unpaired semion, which leads to semion braiding statistics for the two-loop braiding process in Fig. 2.1(b). This nontrivial abelian braiding of 2π vortices, linked to dislocations, is the fingerprint of the chiral anomaly when the $U(1)$ symmetry is broken. We thus come to the conclusion that two-fold vortices are also nontrivial under translations and cannot be condensed.

Analogous considerations imply that four-fold ($\Phi = 4\pi$) vortex loops have bosonic statistics even when linked with dislocations and thus may be condensed. This produces an insulating state, which does not break either the charge conservation or the translational symmetry and has an electrical Hall conductivity $\sigma_{xy} = 1/4\pi$ and a thermal Hall conductivity $\kappa_{xy} = (1/4\pi)(\pi^2 k_B^2 T/3)$ per layer. This is an insulating state that preserves all the symmetries and both the chiral and the gravitational anomaly of a Weyl semimetal with $2Q = \pi$.

2.3 Symmetric gapped state

The insulator thus obtained is not a trivial one – it possesses a $\mathbb{Z}_4$ topological order [16, 306]. The uncondensed one-, two- and three-fold vortices survive as nontrivial gapped loop excitations in the topological order, with inherited nontrivial braiding statistics when linked with dislocations. There are also nontrivial particle excitations. The Bogoliubov fermion in the paired state survives as a neutral fermion excitation. The condensation of 4π vortices also leads to the emergence of a charge-1/2 boson as a gapped excitation – this can be understood as a point defect which, when taken around the condensed 4π vortex loop, acquires a Berry phase of 2π. Furthermore, due to a nontrivial mutual braiding statistical phase of π between a π vortex and a 4π vortex, when linked with a dislocation, the condensation of 4π vortices will also bind a 1/4-charge on a π vortex.

In fact, all of the above properties are closely related to the 2D topological order obtained on the surface of an electronic TI through vortex condensation [351, 227]. This topological order can be viewed as a Moore-Read Pfaffian state plus a neutral antisemion (with the self-statistics angle $-\pi/2$). The only difference in our case is that some of the "vortex-like" particles in the topological order show up as links between loop excitations and a dislocation with $\mathbf{B} = \hat{z}$.

This motivates the following parton construction of the anomalous topological order [303, 278]. We decompose the electron operator as

$$c = b^2 f, \tag{2.8}$$

where b is a charge-1/2 boson, while f is a neutral fermion. The neutral fermion experiences the same electronic structure as the original Weyl semimetal with $2Q = \pi$ and the FFLO pairing gap, that does not violate translational symmetry. The neutral Fermi surface state then leads to the thermal Hall conductivity $\kappa_{xy} = (1/4\pi)(\pi^2 k_B^2 T/3)$, which is equivalent to a layered $p + ip$ superconductor [287]. The charge-1/2 bosons form a layered bosonic integer quantum Hall state [204, 307]. This state has even integer Hall conductance and zero thermal Hall conductance (more details can be found in Refs. [204, 307, 375]). In our case the bosonic integer quantum Hall state contributes a Hall conductivity $\sigma_{xy} = 2(1/2)^2/2\pi = 1/4\pi$ per layer. This gapped insulating state thus reproduces exactly the chiral and the gravitational anomalies of the Weyl semimetal, while preserving its translational and charge conservation symmetries.

The parton decomposition of Eq. (2.8) and the mean field states of b and f are invariant under a $\mathbb{Z}_4$ gauge transform $b \to i^n b,\ f \to (-1)^n f,\ n \in \mathbb{Z}_4$, which is consistent with the $\mathbb{Z}_4$ topological order. One can check explicitly that the $\mathbb{Z}_4$ gauge flux loops have the same

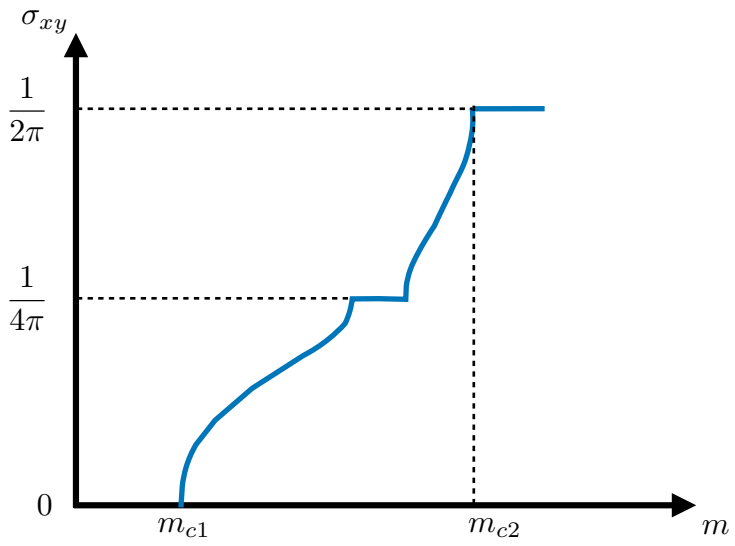

Figure 2.2: (Color online) Hall conductivity as a function of the magnetization with a fractional plateau corresponding to $\sigma_{xy} = 1/4\pi$ 3D FQHE.

properties with the remnants of the uncondensed vortex loops from the vortex-condensation construction. For example, a fundamental ($\Phi = \pi$) vortex is seen by the fermion f as a π vortex, and therefore leads to a Majorana zero mode whenever the vortex penetrates the xy-plane. The fundamental vortex is also seen by the boson b as a $\pi/2$ vortex, which leads to a fractional charge $q = (\pi/2)\sigma_{xy}/(1/2) = 1/4$ whenever the vortex penetrates the xy-plane. The bosonic integer quantum Hall state also leads to a semion whenever a two-fold vortex penetrates the xy-plane. Again all these properties are sharply manifested when the vortices are linked with dislocations.

In addition to realizing the chiral and the gravitational anomalies of the Weyl semimetal, the above state also provides a realization of the fractional quantum Hall effect (FQHE) in 3D, which may not be regarded as simple layering of weakly-coupled 2D FQHE systems. As discussed above, a magnetic Weyl semimetal with two Weyl nodes is an intermediate phase between an ordinary 3D insulator with $\sigma_{xy} = 0$ and an integer quantum Hall insulator with $\sigma_{xy} = 1/2\pi$. We may tune between the two phases by varying a TR-breaking parameter, i.e. magnetization m. One may view this as an analog of tuning the filling factor by an applied

magnetic field in the case of the 2D quantum Hall effect. There are two critical values of the magnetization, m_{c1} and m_{c2}, which correspond to transitions from the ordinary insulator to the Weyl semimetal and from the Weyl semimetal to the integer quantum Hall insulator correspondingly. The function $Q(m)$, which determines the separation between the pair of Weyl points and the Hall conductivity $\sigma_{xy}(m) = Q(m)/2\pi^2$ as a function of the magnetization, is model-dependent, but becomes universal near each critical point. For noninteracting electrons, we have [47] $Q(m) \sim A_1(m - m_{c1})^{1/2},\ \pi - A_2(m_{c2} - m)^{1/2}$, where $A_{1,2}$ are nonuniversal coefficients. We then claim that, in the presence of strong electron-electron interactions, a fractional plateau may exist in $\sigma_{xy}(m)$, at which the Hall conductivity is quantized to half the value of the integer plateau, $\sigma_{xy} = 1/4\pi$, as shown in Fig. 2.2.

It is important to note that the constraint on the possible plateau comes mainly from the thermal Hall response. For a topological order that is genuinely three dimensional, in the sense that all excitations can move in all three directions, the particle excitations can only be bosonic or fermionic. This constrains the thermal Hall conductance per layer to be quantized to $\kappa_{xy} = (n/2)(\pi k_B^2 T/6)$, where n is odd only if the fermion excitations form layered topological ($p + ip$ - like) superconductors. Plateaus at other values of σ_{xy} are certainly possible, but these states will be unrelated to Weyl semimetals.

A general feature of 3D FQHE liquids (with intrinsic 3D topological orders) is that there will be loop excitations with nontrivial braiding statistics when linked with lattice dislocations. In particular, there will be a loop excitation that can be induced by a 2π magnetic flux loop, with an abelian braiding statistical phase of $4\pi^2\sigma_{xy}$, when linked with a dislocation with $\mathbf{B} = \hat{z}$. This is in parallel with the 2D FQHE, where there always exists an anyon (known as "fluxon") with abelian statistics, determined by the fractional Hall conductance.

Chapter 3

Unquantized anomalies in topological semimetals

In this chapter we will elucidate the topological responses of type-I DSMs and time-reversal invariant WSMs, which were previously unclear. The content of this chapter is lifted from published work in Ref. [105][1].

3.1 Introduction

While the concepts of nontrivial electronic structure topology have traditionally been associated with insulators [130, 282], recent work has lead to the realization that gapless metallic states may also be topological [345, 343, 12]. According to the standard band theory of crystalline solids, whether a given material is a metal or an insulator is determined by the electron filling per unit cell. When the filling is an odd integer, we necessarily get a metal with a Fermi surface, whose volume is directly determined by the filling and is not renormalized by the electron-electron interactions [209, 264, 132]. When the filling is an even integer, on the other hand, the net Fermi surface volume must be zero, which corresponds to either an insulator or a compensated semimetal, with electron and hole Fermi surfaces enclosing equal volume. The compensated semimetal arises due to fact that the bands may overlap in energy and is accidental, in the sense that the overlap may be removed without altering the crystal symmetry, whether it exists or not is a matter of microscopic detail.

[1]

Recently discovered topological semimetals are different from compensated semimetals in that their existence is not accidental, they arise inevitably under certain conditions, either as intermediate phases between topologically distinct insulators or in crystals with certain symmetry groups. In particular, Weyl semimetal (WSM) arises as either an intermediate phase between a quantum anomalous Hall insulator and an ordinary three-dimensional (3D) insulator [47]; or as an intermediate phase between a time reversal (TR) invariant 3D topological insulator and an ordinary 3D insulator, when inversion symmetry is violated [242].

When TR and inversion symmetry are present and all bands are thus doubly degenerate, pairs of opposite-chirality Weyl nodes must occur at the same momenta in the Brillouin zone (BZ), which generally means that a gap is opened. However, certain point group crystal symmetries may protect four-fold degenerate band-touching points. Such materials are called Dirac semimetals (DSM). These come in two classes, type-I and type-II [387]. In type-I Dirac semimetals, such as Na_3Bi and Cd_3As_2 [359, 360], Dirac points occur in pairs at generic BZ momenta on an axis of rotation, and are protected by a symmetry of rotations about this axis. This type of Dirac semimetal arises as an intermediate phase between an ordinary insulator and a weak topological insulator, in which the direction of the weak index (a reciprocal lattice vector) coincides with the rotation axis. In type-II Dirac semimetals, in contrast, there is a single Dirac node at a time reversal invariant momentum (TRIM) at the edge of the BZ, terminating an axis of nonsymmorphic rotation [397, 325] (the minimum total number of such Dirac points in the BZ is still two, unless TR is explicitly broken). Such a Dirac semimetal is not an intermediate phase between two insulators, but exists in crystals with certain nonsymmorphic symmetry groups, which inevitably have four-fold band degeneracies at TRIM at the edge of the BZ [387, 270, 268].

The band-touching points in both Weyl and Dirac semimetals are stable as long as the protecting symmetries are present or as long as the points are not pairwise annihilated by bringing them to the same position in the BZ (this applies to Weyl and type-I Dirac semimetals). This stability may be connected with the existence of a momentum-space topological invariant, associated with the band-touching point. In the case of Weyl semimetals, this topological invariant is a nonzero Chern number (± 1) of any closed surface in momentum space, enclosing the node. In the Dirac semimetal case, the invariant is more subtle and involves counting rotation eigenvalues of occupied and empty states on the rotation axis on the opposite sides of the Dirac point [386].

An important limitation of this picture is that it is based on noninteracting band eigenstates. A question then arises to what extent topological semimetals are stable with respect to the electron-electron interactions. By stability here we do not mean perturbative stability with respect to gap opening: all 3D point-node semimetals are stable in this sense

thanks to the vanishing density of states at the Fermi energy. Rather, we are interested in the question to what extent their topologically nontrivial nature is still manifest when the interactions are not weak. We have recently addressed this issue in the simplest case of a magnetic Weyl semimetal [349, 335, 301] (see Refs. [224, 239, 295, 223, 286] for related work). In this paper we generalize this earlier work to TR-invariant Weyl and type-I Dirac semimetals. As explained above, what unifies these three classes of topological semimetals is that they arise as intermediate phases between topologically-distinct insulators. Type-II Dirac semimetals are not of this type, leading to a significantly different physics, which we will address in a separate publication.

A way to formulate this question precisely in the case of a magnetic Weyl semimetal is as follows. In addition to topological invariants, formulated in terms of band eigenstates, magnetic Weyl semimetals are also characterized by topological response, which, in particular, takes the form of an anomalous Hall effect [47]. Specializing to the simplest case of a Weyl semimetal with a single pair of opposite-chirality nodes, the anomalous Hall conductivity is proportional to the distance between the nodes in momentum space

$$\sigma_{xy} = \frac{1}{2\pi}\frac{2Q}{2\pi} \quad , \tag{3.1}$$

where we are using $\hbar = e = c = 1$ units here and throughout this paper and the nodes are taken to be located at $k_z = \pm Q$. This Hall conductivity, which is a fraction of a conductivity quantum $1/2\pi$ per atomic layer, is a characteristic property of magnetic Weyl semimetals, which is well-defined even when the band eigenstates are not. We may then ask whether a trivial gapped insulator at the same electron filling per unit cell as the Weyl semimetal may have the Hall conductivity given by Eq. (3.1). The answer to this is no since Eq. (3.1) implies a $\frac{\sigma_{xy}}{2} AdA$ term in the Lagrangian for the electromagnetic field, which is not invariant with respect to large gauge transformations. Gapless modes are needed to restore gauge invariance, which, in the absence of a Fermi surface, makes the Weyl nodes necessary. However, a fractionalized insulator with a particular type of topological order is consistent with Eq. (3.1) when $2Q = \pi$, taking the lattice constant in the z-direction to be unity [349].

Here we ask whether this line of reasoning may be generalised to other point-node topological semimetals, in particular TR-invariant Weyl and type-I Dirac semimetals. It is not at all obvious that this is possible since, unlike the magnetic Weyl semimetal, these do not possess any topological electromagnetic responses. This makes one wonder if the nontrivial topology of TR-invariant Weyl and type-I Dirac semimetals only exists in the weakly interacting limit. In this paper we demonstrate that this is not the case. We show that both TR-invariant Weyl and type-I Dirac semimetals possess "unquantized" topological

responses, similar to the magnetic Weyl semimetal, except involving crystalline symmetry, rather than purely electromagnetic, gauge fields. These manifest as fractional electric charge density induced on crystalline symmetry defect (i.e. dislocations and disclinations) configurations.

Alternatively, the Hall conductivity of a magnetic Weyl semimetal Eq. (3.1) may be viewed as being a consequence of a nonzero charge density, induced in the ground state of the Weyl semimetal by an applied magnetic field, given by the Streda formula

$$\sigma_{xy} = \left(\frac{\partial n}{\partial B}\right)_{\mu} \quad . \tag{3.2}$$

Similarly, we demonstrate that topological responses of TR-invariant Weyl and type-I Dirac semimetals may be expressed in terms of nontrivial ground state symmetry charges, induced by the applied magnetic field. These symmetry charges are the crystal momentum (translational symmetry charge) in the case of the TR-invariant Weyl semimetal and the angular momentum (rotational symmetry charge) in the case of the type-I Dirac semimetal.

The rest of the paper is organized as follows. In Section 3.2 we introduce and review the concepts of unquantized anomalies and of symmetry gauge fields, which may be unfamiliar to some readers. In Section 3.3 we discuss a series of one-dimensional lattice models, which introduce the mixed crystalline symmetry-electromagnetic anomalies in the simplest possible setting. We show that these anomalies may be viewed as a generalization of the familiar notion of fractional $U(1)$ charge density, which is formally related to the $(1+1)d$ chiral anomaly, to discrete symmetry gauge fields. In Section 3.4 we generalize the results of Section 3.3 to 3D topological semimetals. As familiar from the standard discussions of the chiral anomaly, when the semimetals are placed in an external magnetic field, the resulting lowest Landau levels encode the anomaly physics and connect the anomalies in $3+1$ dimensions to their $1+1$-dimensional counterparts. Finally, we generalize the vortex condensation analysis of Ref. [349] to the cases of TR-invariant Weyl and type-I Dirac semimetal, which provides yet another viewpoint on their topological nontriviality in the presence of strong interactions. We conclude in Section 3.5 with a brief summary and discussion of the main results of the paper.

3.2 Preliminaries

Since we will be using a number of concepts, such as anomalies and symmetry gauge fields, that may be unfamiliar to some readers, in this section we will briefly review these concepts.

3.2.1 Topological response and "unquantized quantum anomalies"

We will start by reviewing how certain types of unquantized topological response can constrain the low energy phases in a way that is similar to the usual quantum anomalies.

We illustrate the idea using a familiar example. Consider a $(2+1)d$ fermion system with charge $U(1)$ symmetry. If the Hall conductance $\sigma_{xy} = -\sigma_{yx}$ is not an integer (in units of $e^2/h = 1/2\pi$), then it is well known that the ground state cannot be short-range entangled: if the ground state is gapped, it should realize a non-trivial topological order, as in fractional quantum Hall effects; the ground state can also be gapless, for example by having a Fermi surface that encloses a Berry phase $\Phi = 4\pi^2\sigma_{xy}$ [126]. One way to see this is to notice that if the ground state is short-range entangled, the theory of response to a probe $U(1)$ gauge field should be expressed as the integral of a local term. The Hall conductance corresponds to the familiar Chern-Simons (CS) term:

$$\int d^3x \frac{k}{4\pi} AdA \quad , \tag{3.3}$$

where $\sigma_{xy} = k/2\pi$. It is well known that if $k \notin \mathbb{Z}$, the CS term is not consistent as it is not invariant under certain large gauge transforms. The inconsistency should be cured once the low energy (IR) degrees of freedom are properly included, namely the full theory

$$\mathcal{S}_{IR}[A] + \int d^3x \frac{k}{4\pi} AdA \quad , \tag{3.4}$$

should be fully gauge invariant. A familiar situation is when $k = 1/2$, where the IR theory can be a gapless Dirac fermion. The Dirac fermion can be represented in the (Euclidean time) path integral formulation as

$$\begin{aligned} Z_{IR} &= \int D\bar{\psi} D\psi \exp\left(\int d^3x \bar{\psi} i \not{D}_A \psi\right) \\ &= |\det(\not{D}_A)| \exp\left(\frac{i\pi}{2}\eta[A] - \int d^3x \frac{i}{8\pi} AdA\right), \end{aligned} \tag{3.5}$$

where $\eta[A]$ is the η-invariant. We refer to Ref. [374] for a detailed review of the η-invariant. Here we only emphasize that the η-invariant is classically similar to the $k = 1/2$ CS term in terms of equation of motion (and hence Hall conductivity), but is fully gauge-invariant unlike the $k = 1/2$ CS term. The IR theory of the Dirac fermion thus fulfills two important

requirements: it carries the opposite gauge non-invariance with the $k = 1/2$ CS term, with a vanishing contribution to the net Hall conductance.

From a field theoretic point of view, it is somewhat arbitrary to separate the theory into a CS term and $\mathcal{S}_{IR}$. In fact the Dirac fermion can be defined in a gauge-invariant way with just the η-invariant [374], for example using the Pauli-Villars regulator. However, it will be useful to clearly separate the two contributions since it allows interesting generalizations that will be discussed later in this paper: the CS term can be interpreted as a "UV" contribution that comes from integrating out high-energy degrees of freedom and should therefore be analytic (but not necessarily fully consistent); Eq. (3.5) is interpreted as an "IR" contribution. The IR contribution does not have to be analytic since it comes from gapless degrees of freedom (in this case the η-invariant is not analytic), and should restore gauge invariance while keeping the UV response (in this case Hall conductance) unchanged.

The above story is similar to quantum anomalies, in the sense that the IR theory should be nontrivial and match certain gauge non-invariance condition. However it is also different from the standard quantum anomalies, since the gauge non-invariance is imposed by fine-tuning the Hall conductance to a fixed fractional value. This "unquantized quantum anomaly" is therefore not protected like the standard anomalies, in the sense that a general perturbation can in principle change the Hall conductance. However we can adopt a rule of game in which the Hall conductance is fixed, which is justified if it is measured directly from the experiments or numerics. Then gauge invariance will impose strong constraints on the IR phases in a way similar to the standard quantum anomalies. In particular, the constraints can be applied to strongly correlated system — in this case it leads to the familiar result that a system with a fractional quantum Hall conductance, even with strong interactions, must necessarily be long-range entangled.

Our "unquantized anomaly" can be viewed as a type of gauge non-invariant counter terms. The most familiar example of such counter term in condensed matter physics is perhaps the diamagnetic term in metals: $(n/2m)|\mathbf{A}|^2$, where n is the electron density, m is the fermion mass and $\mathbf{A}$ is the electromagnetic vector potential. The analogue of the fractional Hall conductance discussed above would be the optical conductivity $\sigma(\omega) \sim 1/i\omega$ due to this counter term. This term is obviously gauge non-invariant and in the case of metals it demands a nontrivial Fermi surface to restore gauge invariance. The difference between the diamagnetic term and the fractional CS term is that the former is non-invariant under general (small and large) gauge transforms while the latter is non-invariant only under large gauge transforms, and is therefore more "topological". In the rest of this work we will focus on such "topological" counter terms.

The rest of this paper is devoted to generalizing the above story to a variety of topo-

logical semimetals. The theory of such topological semimetals can be written, in a similar fashion to Eq. (3.4), as

$$S_{IR}[\psi, \mathcal{A}] + S_{UV}[\mathcal{A}] \quad , \tag{3.6}$$

where $S_{IR}[\psi, \mathcal{A}]$ represents the low energy degrees of freedom such as the gapless fermions, S_{UV} is a topological response term, which is a generalization of the Hall conductance, and $\mathcal{A}$ represents the probe gauge fields of the relevant symmetries, such as $U(1)$ and lattice symmetries. The inconsistency of S_{UV} implies that the topological semimetal phase must remain long-range entangled even with strong interactions, as long as the topological response from S_{UV} is fixed.

The relation between the standard and unquantized anomalies can be made more precise through the notion of *emergent anomalies*. The IR theory often enjoys a symmetry larger than that of the microscopic system. This emergent IR symmetry, which we denote as G_{IR}, can have some nontrivial t'Hooft anomalies, in the sense that if we formally couple the IR theory to a probe G_{IR} gauge field, the theory is only sensible when viewed as the boundary of a bulk (denoted as M), with a nontrivial bulk response action $i\int_M w[G_{IR}]$ where $w[G_{IR}]$ is the corresponding topological term. We then re-insist that the true microscopic symmetry G_{UV} is smaller, and is implemented in the IR theory as a subset of G_{IR} through a map (a homomorphism)

$$\varphi : G_{UV} \to G_{IR} \quad , \tag{3.7}$$

which gives a map (a pullback) φ^* from the IR anomaly $w[G_{IR}]$ to the anomaly of the UV symmetry

$$w[G_{UV}] = \varphi^* w[G_{IR}] \quad . \tag{3.8}$$

The unquantized anomaly we discuss here corresponds to the situation where the above $w[G_{UV}]$ is a total derivative as a bulk term: $w[G_{UV}] = d\Omega[G_{UV}]$, so that the UV anomaly is trivial at the cohomology level. However, it still reduces to a nontrivial counter term on the boundary $\Omega[G_{UV}]$. Ω is the analogue of the unquantized CS term AdA, where the corresponding bulk term is just the theta term $w = dAdA$.

Before entering the detailed discussions, we shall first review the notion of gauge fields for lattice symmetries.

3.2.2 Review of lattice symmetry gauge fields

For an ordinary on-site discrete symmetry G (such as the Ising $\mathbb{Z}_2$), what the probe gauge field $\mathcal{A}$ measures is essentially the twisted boundary conditions around each space-time

1-cycle C. Specifically, a nontrivial Wilson loop $\int_C \mathcal{A} = g \in G$ means that adiabatically travelling along C for a full cycle is equivalent to acting on the system by g. Here C could also be a small cycle around a gauge defect (a vortex), in which case $\int_C \mathcal{A}$ measures the flux trapped in the defect. If we view vortices (with nontrivial gauge flux) as defects in the continuum space-time, the discrete gauge field becomes locally flat in the continuum $d\mathcal{A} = 0$. Mathematically this means that $\mathcal{A} \in H^1(M, G)$, the first cohomology group of G, where M is the space-time manifold.

The above definition can be generalized to lattice symmetries [336]. We start with lattice translation symmetries in d space dimensions, where the symmetry forms the group $\mathbb{Z}^{\otimes d}$. For each translation symmetry T_{x_i} in the i'th direction ($1 \le i \le d$), we introduce a $\mathbb{Z}$-gauge field $\mathcal{X}_i$. Just like the Wilson loops in ordinary gauge theories, the integer $\int_C \mathcal{X}_i$ measures the number of $\hat{x}_i$-translations one has to go through to travel across the 1-cycle C. To be more concrete consider a path integral description, with dynamical degrees of freedom ψ (bosonic or fermionic) defined in continuous time $t \in [0, T)$ and on discrete lattice sites s in space:

$$e^{-iS_{eff}[A,x_i]} = \int D[\psi(s,t)] \exp\left(-i \sum_s \int dt \mathcal{L}_s[\psi, A]\right), \tag{3.9}$$

where we have used locality and translation symmetries to write the Lagrangian as a sum of local terms of identical form, $\mathcal{L}_s[\psi, A]$, which involves only fields near site s. We take periodic boundary conditions in space and time (so M is a torus). The translation gauge fields enter the partition function by specifying exactly how the periodic boundary conditions are taken:

$$\begin{aligned} \psi(s,t) &= \psi\left(s + \hat{x}_j \int_i \mathcal{X}_j, t\right); \\ \psi(s,t) &= \psi\left(s + \hat{x}_j \int_t \mathcal{X}_j, t + T\right). \end{aligned} \tag{3.10}$$

We now explain these equations in more detail. The Wilson loop of $\mathcal{X}_i$ in the $\hat{x}_i$ direction gives the lattice size $\int_i \mathcal{X}_i = L_i$. For $j \neq i$ the number $\int_i \mathcal{X}_j$ measures how much the slice of the lattice at $x_i = L_i$ is displaced along the $\hat{x}_j$ direction before it is identified with the slice at $x_i = 0$. Similarly the time component $\int_t \mathcal{X}_i$ measures the displacement of the entire lattice at $t = T$ before identified with $t = 0$. In other words, while the "longitudinal" parts of the translation gauge fields measure the lattice size, the "transverse" parts measure the quantized shear strains of the lattice in both space and time. We can also consider a $(d-2)$ dimensional defect in space, around which $\int \mathcal{X}_i = n \neq 0$: this is simply a lattice dislocation

with Burgers vector $\vec{B} = n\hat{x}_i$. This relation can also be written as $\int_S d\mathcal{X}_i = N$ where N is the total charge of dislocations penetrating through the 2-surface S. This is illustrated in Fig. 3.1.

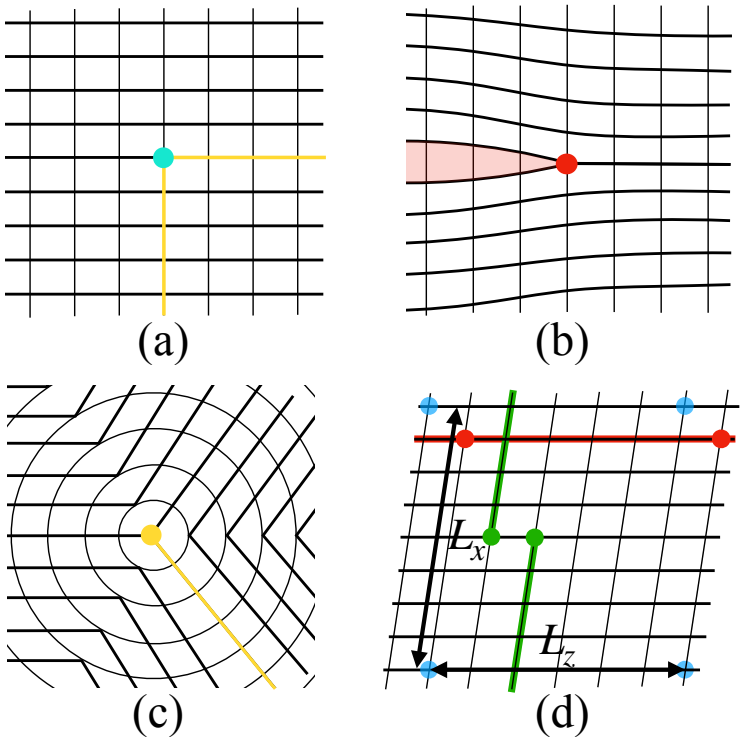

Figure 3.1: (Color online) Spatial symmetry point defects in 2D. (a) A defect-free 2D lattice with highlighted (blue) point possessing both translational and $\pi/2$ rotational symmetry. (b) A translational symmetry defect, known as a dislocation, is obtained by inserting an extra (red) half-plane and represented by the red dot. A Wilson loop around the defect gives $\int_C \mathcal{X}_i = 1$. (c) Gluing together the yellow lines in (a) produces a $\pi/2$ rotational defect known as a disclination. (d) Here we depict a periodic 2D lattice in the xz-plane with linear size in the z-direction $\int_{z=0}^{L_z} z = L_z$ (red line) and a shear strain in z given by $\int_{x=0}^{L_x} z = 1$ (green line). The four blue dots are equivalent to each other due to the periodic boundary conditions.

In the above discussion the lattice is viewed as a set of discrete points, which could exist without referring to any microscopic continuum geometry. However it is often convenient to embed the lattice into a continuous space, so that each site s can be assigned a continuous coordinate $\vec{u}(s)$. Following usual practice in elasticity, the lattice coordinate can be treated

as a field in the continuous space-time by assigning to each point $\vec{r}$ the value of $\vec{u}(s(\vec{r}))$, where $s(\vec{r})$ is the lattice point closest to $\vec{r}$. In this case the translation gauge field $\mathcal{X}_i$ can be interpreted as the elasticity tetrad $\mathcal{X}_i = \vec{\nabla} u_i$ [76], since the tetrad also satisfies Eq. (3.10). Different continuum embeddings of the lattice lead to different tetrad representations of the $\mathcal{X}_i$ gauge fields, but the Wilson loops $\int_C \mathcal{X}_i$ do not depend on the details of the embedding. In this work we focus on universal properties, such as the Wilson loops, that do not depend on how the lattice is embedded into a continuum space. For example, we do not discuss the couplings between local elastic deformations (such as phonons or local strains) and the electrons [272, 221]. This allows us to treat $\mathcal{X}_i$ purely as a $\mathbb{Z}$-valued gauge field, and view the tetrad representation as a "gauge choice" of the translation gauge fields.

We note that the concept of translation gauge fields and elasticity tetrad have been used in recent literature in various contexts, including three dimensional integer quantum Hall effect [9, 254, 255], Weyl semimetals [151, 349, 176], chiral anomaly [256], electric polarizations [322, 252] and crystalline symmetry-enriched topological orders [214].

We can similarly introduce probe gauge fields for lattice rotation symmetries. For example for a lattice C_n rotations ($n = 2, 3, 4, 6$), we can introduce a $\mathbb{Z}_n$ gauge field c. A defect around which $\int c = m \neq 0 \pmod{n}$ is simply a lattice disclination. This lattice rotation gauge field has been used recently to characterize certain crystalline topological phases [195].

3.3 Chiral anomaly in (1+1)d lattice systems

3.3.1 $U(1) \times \mathbb{Z}$ chiral anomaly

We begin by reviewing the well known chiral (or filling) anomaly in (1+1)-dimensional lattice systems, with the aim to generalize these concepts to more complex situations. This $(1+1)$d chiral anomaly may be viewed as the fundamental anomaly, from which the higher dimensional anomalies in topological semimetals, that we will be concerned with in this paper, follow.

Let us consider a $(1+1)$d ring of length L_z with a single spinless fermionic band at a fractional filling ν. This system possesses the discrete lattice translational symmetry $\mathbb{Z}$ and the $U(1)$ charge conservation symmetry. The band dispersion is shown in Fig. 3.2(a). Luttinger [209, 264] or, more generally, Lieb-Schultz-Mattis [189, 263, 132]), theorems tell us that this system is necessarily gapless in the presence of the $U(1)$ and translational symmetries. Alternatively, we may view this gaplessness as being mandated by a $U(1) \times \mathbb{Z}$

chiral anomaly that requires the existence of low-energy gapless modes in order to maintain gauge invariance [101, 68, 70, 228, 156].

This $U(1) \times \mathbb{Z}$ anomaly is a lattice descendant of the continuum $U(1) \times U(1)_a$ $(1+1)$d chiral anomaly, where $U(1)_a$ corresponds to the chiral (or axial) symmetry group. In the presence of a $U(1)$ flux there follows a non-conservation of the chiral charge, despite the presence of the chiral symmetry (hence *anomaly*). In the lattice system this continuous chiral symmetry is replaced by the $\mathbb{Z}$ translational symmetry and as such leads to a non-conservation of the $\mathbb{Z}$ translational charge (which is simply the crystal momentum) when treated as an on-site symmetry. This is most easily demonstrated if we adiabatically thread a magnetic flux $\Phi = \oint dz A_z$ through the center of the ring, which causes a change in $\Phi = 0$ momentum given by

$$\partial_t P_{tot} = \nu \int dz \, \partial_t A_z \quad , \tag{3.11}$$

where $\nu = 2Q/2\pi$ with $2Q$ being the momentum separation between the chiral modes. For notational simplicity we will set the lattice constant a to unity henceforth. Upon an insertion of $\Phi = 2\pi$ we have

$$\frac{\Delta P_{tot}}{2\pi} = \nu \ (\mathrm{mod}\, \mathbb{Z}) \quad , \tag{3.12}$$

where $\mathrm{mod}\, \mathbb{Z}$ arises due to the crystal momentum being only defined modulo a reciprocal lattice vector. This demonstrates non-conservation of the chiral charge, i.e. momentum, when $\nu \neq 0 \, (\mathrm{mod}\, \mathbb{Z})$ and is illustrated in Fig. 3.2.

Another facet of the chiral anomaly has to do with the overall $U(1)$ charge of the ground state, which is given by

$$Q_{U(1)} = \sum_{k_z=-Q}^{Q} 1 = \nu L_z \quad , \tag{3.13}$$

where L_z is the length of the system, which means that the charge per unit cell is ν. Any noninteger value of ν is incompatible with a trivial gapped insulator state. An intuitive way to see this is to notice that the total $U(1)$ charge in Eq. (3.13) is not properly quantized for some L_z if $\nu \notin \mathbb{Z}$. This means that some additional charge $\delta Q \sim O(1)$ has to supplement Eq. (3.13) to make the charge quantized, no matter how large L_z becomes. Furthermore, this $\sim O(1)$ additional charge cannot come from a trivially gapped state, since it is non-analytic with respect to $1/L_z$ – for example, an acceptable example will be $\delta Q = \lfloor \nu L_z \rfloor - \nu L_z$, which is badly non-analytic in $1/L_z$. The correction δQ then has to come from some long-range entanglement – in our case the gapless fermions. Although the relation

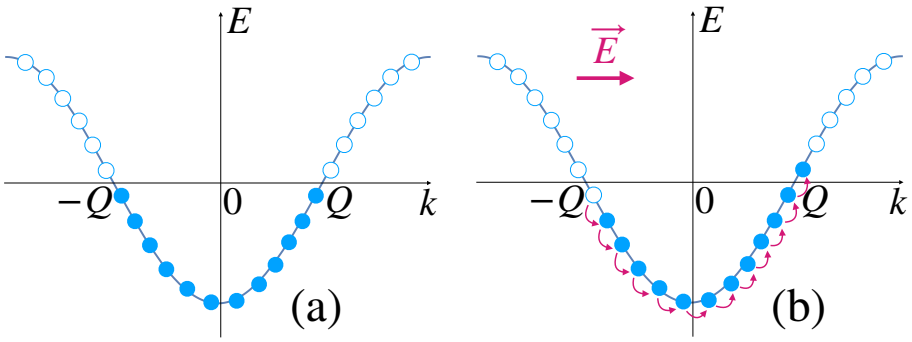

Figure 3.2: (Color online) Illustration of the $(1+1)$d chiral anomaly: (a) A one band fermionic dispersion at fractional filling $\nu = 2Q/2\pi$. (b) Once we thread a flux $\int dz A_z = 2\pi$, which gives rise to an electric field $\vec{E}$, all filled states gain a unit of momentum resulting in a change of $2\pi\nu$ in chiral charge (i.e. crystal momentum).

Eq. (3.13) is rather trivial, its generalizations, which will be discussed extensively later, are not.

Both of the above manifestations of the $(1+1)$d chiral anomaly may be compactly expressed in terms of the following action, involving the translation (chiral) and the electromagnetic gauge fields

$$S = \nu \int z \wedge A = \nu \int dt dz \, \epsilon^{\mu\nu} z_\mu A_\nu \quad , \tag{3.14}$$

where A is the usual $U(1)$ gauge field, $z \in H^1(\mathcal{M}, \mathbb{Z})$ is the $\mathbb{Z}$ translational gauge field, and $\epsilon^{\mu\nu}$ is the Levi-Civita tensor in $(1+1)$d. All discrete gauge fields should be locally flat in the continuum limit since discrete fluxes lead to singular points in space. For the z gauge field this means that $\int_{\mathcal{C}_2} dz = 0$ when integrated over any closed 2-cycle $\mathcal{C}_2$. Around a 1-cycle $\mathcal{C}$, $\oint_{\mathcal{C}} z$ counts the number of z translations traversed by the cycle, which is generally zero unless the loop is non-contractible, i.e. encloses omitted points in space. For example if we choose the cycle $\mathcal{C}_z$ to be along the length of the system then we obtain $\oint_{\mathcal{C}_z} z = L_z$. In general $\int_i z_j$, where $i \neq j$ measures the number of z lattice slice displacements that are traversed along a cycle from $x_i = 0$ and $x = L_{x_i}$. Physically the flatness requirement $dz = 0$ corresponds to disallowing insertions of defects, i.e. layers which carry $U(1)$ charge, such that total number of charges stays fixed over time. Let us now show how this action term reproduces the previously discussed physics of the chiral anomaly.

Recall that the minimal coupling between the current j^μ and gauge field A_μ is given by $-j^\mu A_\mu$. This means that when we vary Eq. (3.14) with respect to the time component

of the gauge field, A_t, we arrive at the expression for the total $U(1)$ charge as shown in Eq. (3.13). When we vary with respect to the time component of the translation gauge field, z_t, we get the total ground state momentum

$$P_{tot}(\Phi) = -\oint_{\mathcal{C}_z} \frac{\delta S}{\delta z_t} = -\nu\Phi \quad . \tag{3.15}$$

The momentum difference between the $\Phi = 0$ and 2π ground states is then given by

$$\frac{P_{tot}(2\pi) - P_{tot}(0)}{2\pi} = -\nu \ (\mathrm{mod}\,\mathbb{Z}) \quad . \tag{3.16}$$

We note that the apparent sign difference between Eq. (3.16) and (3.12) is in fact consistent. Eq. (3.16) describes the change of *ground state momentum* in the presence of a 2π-flux, while Eq. (3.12) is the momentum carried by the low energy (particle-hole) excitation induced by an adiabatic 2π-flux insertion. The two should sum to zero since the process of adiabatic flux-insertion commutes with lattice translation and should not induce an actual momentum change. In our language (discussed in Sec. 3.2) Eq. (3.16) can be interpreted as a "UV" response since it is fixed by the lattice-scale information (the charge filling), and Eq. (3.12) can be interpreted as the "IR" contribution since it originates from gapless particle-hole excitations of the IR theory.

The incompatibility of the anomaly action Eq. (3.14) with a trivial insulator ground state may be clearly seen by examining how the action transforms under large gauge transformations. For example, if A_t is taken to be spatially constant and wind by $2\pi n$ around the temporal cycle, the corresponding contribution to the action is given by

$$S = -2\pi\nu n L_z \quad , \tag{3.17}$$

which is generally nontrivial. This contradicts the fact that such a $2\pi n$ winding of A_t may be generated by a gauge transformation, i.e. Eq. (3.14) is not gauge invariant. This means that there must exist gapless modes, which compensate for this gauge non-invariance.

We now comment on the relation between the "unquantized anomaly" Eq. (3.14) and the standard t'Hooft anomaly. Although physically the only exact symmetry we impose here is $U(1) \times \mathbb{Z}$, at low energy the emergent Dirac fermion possesses an emergent $U(1)_c \times U(1)_a$ symmetry (the charge and axial charge conservation). If this $U(1)_c \times U(1)_a$ symmetry is exact and on-site, the system can only be defined on the edge of a $(2+1)d$ "quantum spin Hall insulator" bulk. This means that when coupled to a $U(1)_c$ gauge field A and a $U(1)_a$ gauge field B, the Dirac fermion must be defined together with a mutual Chern-Simons (CS) term in one higher dimension:

$$\frac{1}{\pi}\int_{X_3} d^3x B dA \quad , \tag{3.18}$$

where the Dirac fermion lives on the boundary ∂X_3. For our example, A is the electromagnetic gauge field. The axial charge is nothing but the crystal momentum, so we should set $B = -k_F z$ – here we temporarily treat the gauge field z as continuous (defined in $\mathbb{R}$ instead of $\mathbb{Z}$), and recall that the charges under z are nothing but the momenta of the fermion modes $\pm k_F$. Using the Luttinger theorem $2k_F = 2\pi\nu$ and the fact that $dz = 0$ for $z \in H^1(X_3, \mathbb{Z})$ (the z gauge field is discrete at the end of the day), the total anomaly becomes

$$-\nu \int_{X_3} z dA = \nu \int_{\partial X_3} z \wedge A \quad , \tag{3.19}$$

which is just Eq. (3.14). Importantly, the BdA anomaly becomes trivial as a bulk term, but on the boundary it produces a nontrivial counter term which forces the IR theory to be nontrivial.

Now we will demonstrate how this basic $(1+1)$d chiral anomaly may be generalized to more complex situations, involving other crystalline symmetries, such as rotations.

3.3.2 $\mathbb{Z} \times \mathbb{Z}_2$ anomaly

Discrete symmetries, such as discrete lattice rotations and translations, do not admit local charge densities (in contrast to $U(1)$). Nevertheless the charges of these discrete symmetries are globally defined and much of the discussion from the previous example can be generalized accordingly. We now discuss the simplest example with lattice $\mathbb{Z}$ translation in $\hat{z}$ direction and an on-site $\mathbb{Z}_2$ symmetry. For later use we interpret this $\mathbb{Z}_2$ as a C_2 rotation around the $\hat{z}$ axis.

Consider a $(1+1)$d spinful fermionic square lattice model with translational symmetry in z, and C_2 symmetry, described by the following Hamiltonian

$$\begin{aligned} H &= \frac{1}{2} \sum_i \left(c_i^\dagger \sigma^z c_{i+1} - m\, c_i^\dagger \sigma^z c_i + h.c. \right) \quad , \\ &= \sum_k \left(\cos k - m \right) c_k^\dagger \sigma^z c_k \quad , \end{aligned} \tag{3.20}$$

where σ corresponds to the spin-degree of freedom, and we have two zero energy nodes at momentum $k = \pm Q$, with $Q = \cos^{-1}(m)$. The dispersion is shown in Fig. 3.3. The gaplessness of the band dispersion is protected by the combination of $C_2 = \sigma^z$ symmetry and translational symmetry. The total C_2 charge Q_{C_2}, defined through the C_2 eigenvalue

$e^{iQ_{C_2}}$ for the many-body ground state, is determined by the filling fraction $\nu = 2Q/2\pi$ of the band with C_2 eigenvalue -1:

$$Q_{C_2} = \pi\nu L_z + O(1) \quad , \tag{3.21}$$

where $\nu = 2Q/2\pi$ describes the separation between the band-touching nodes. A trivial symmetric gapped ground state with C_2 may only be a product state in C_2 charges of either 0, or π at every sites. Thus the total C_2 charge of a trivial symmetric system can correspond to 0 or πL_z respectively. We see that a trivial state is unable to capture the total charge of the system for a fixed general nodal separation of $2Q/2\pi \notin \mathbb{Z}$. One can also heuristically understand the "anomaly" of Eq. (3.21) in a similar way as the previous example: the C_2 charge in Eq. (3.21) is not properly quantized for certain L_z when $\nu \notin \mathbb{Z}$, so an additional $\delta Q_{C_2} \sim O(1)$ has to be added. In general δQ_{C_2} will be non-analytic in $1/L_z$ and therefore should come from some nontrivial IR modes, like the gapless fermions in our example.

Parallel to the $U(1) \times \mathbb{Z}$ anomaly case, this inability to form a trivial state at certain nodal separations is the result of a $\mathbb{Z} \times \mathbb{Z}_2$ chiral filling anomaly associated with the z translation and C_2 symmetries. Analogous to the $U(1) \times \mathbb{Z}$ anomaly, the effect of the C_2 charge is encoded in the following topological term

$$S = \pi\nu \int z \wedge c \quad , \tag{3.22}$$

where $c \in H^1(\mathcal{M}, \mathbb{Z}_2)$ is the C_2 gauge field which is the on-site spin rotation gauge field.[2] The general trivial states correspond to $\nu \in \mathbb{Z}$.

By construction, when we vary the action in Eq. (3.22) with respect to the time component of the C_2 gauge field, c_t, we arrive at the Q_{C_2} in agreement with Eq. (3.21). In addition, varying with respect to z_t, we obtain

$$P_{tot}(\Phi_c) = \oint_{\mathcal{C}_z} \frac{\delta S}{\delta z_t} = -\pi\nu\Phi_c \quad , \tag{3.23}$$

where $\Phi_c = \oint_{\mathcal{C}_z} c_z$ is the C_2 flux. This means that a nontrivial C_2 flux (a periodic boundary condition twisted by C_2) induces a nontrivial momentum. What appears inconsistent is that even a trivial flux $\Phi_c = 2$ also induces a nontrivial momentum:

$$\frac{P_{tot}(2) - P_{tot}(0)}{2\pi} = -\nu \ (\mathrm{mod}\, \mathbb{Z}) \quad . \tag{3.24}$$

[2]Strictly speaking we should be using the cup product $\cup$ for discrete gauge fields. But for most purposes in this paper it suffices to consider the standard wedge product $\wedge$.

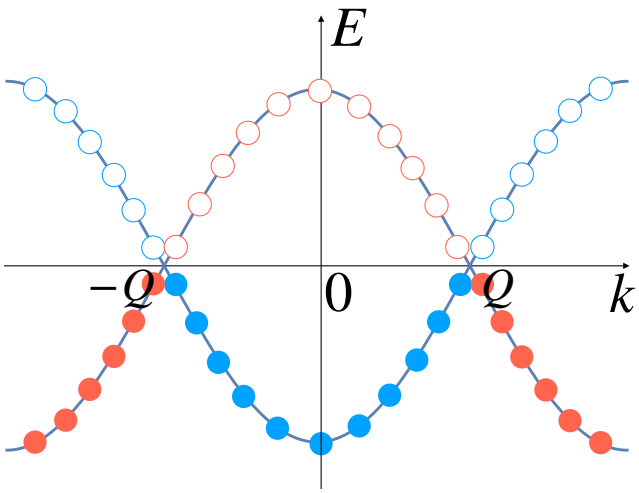

Figure 3.3: (Color online) Band dispersion corresponding to the Hamiltonian in Eq. (3.20). The filled red and blue states correspond to different C_2 eigenvalue states. The sum of the individual filled charges gives the total C_2 charge which may be non-trivial, leading to a $\mathbb{Z} \times \mathbb{Z}_2$ chiral anomaly.

The resolution is that the trivial $\Phi_c = 2$ flux induces a gapless excitation with momentum $-2\pi\nu = -2Q$ – this is nothing but a particle-hole excitation near the Fermi points. This provides another physical reason for the existence of nontrivial IR modes.

Here we comment on the exact meaning of Eq. (3.23). We consider the low energy spectra of the system with and without the C_2 flux – by "low energy spectrum" we mean the ground state and excitations with energy $\sim O(1/L)$ (i.e. states that are degenerate with the ground state in the thermodynamic limit). Of particular interest are two quantum numbers of these states: the crystal momentum P and the total $U(1)$ charge $q \in \mathbb{Z}$ (let us define the charge so that $q = 0$ for the ground state in the absence of the C_2 flux). In the absence of the C_2 flux the low energy states satisfy the relation $P = qQ \pmod{2Q}$. With the C_2 flux, one can check that the relation is modified to $P = qQ + Q \pmod{2Q}$. The difference between these two relations is the true meaning of Eq. (3.23) (recall that $\pi\nu = Q$). This also shows that although $U(1)$ symmetry is not explicitly involved in the response function Eq. (3.22), it is required to make the response sharply defined – otherwise the charge q is no longer defined in the above relations and Eq. (3.23) loses its sharp meaning. The necessity of the $U(1)$ symmetry can also be seen directly: if the $U(1)$ is broken, we could gap out the system by simply adding a pairing term, without breaking either the translation or the C_2 symmetry. This phenomenon is similar, though

perhaps not completely identical, to SPT phases in certain systems – for example, certain anomalies (SPTs) in charged fermion systems only involve time-reversal symmetry, but the anomalies become trivial once the $U(1)$ symmetry on the fermions is broken [353].

The formal way to express the above anomaly, just as in the case of the $U(1) \times \mathbb{Z}$ anomaly, is to notice that the topological term in Eq. (3.22) is not gauge invariant under large gauge transformations $c \to c + 2\alpha$ where α is an integer 1-form, which mandates gapless low-energy modes to restore gauge invariance. As we will see later, this anomaly has a $(3+1)$d extension, which corresponds to rotation symmetry protected (type-I) Dirac semimetals.

The $\mathbb{Z}_2 \times \mathbb{Z}$ anomaly Eq. (3.22) does have a subtle aspect not present in the $U(1) \times \mathbb{Z}$ case. We are always free to redefine the $\mathbb{Z}_2$ gauge field $c \to (2n+1)c$ for any $n \in \mathbb{Z}$. Therefore different values of ν should give identical response (or anomaly) if they differ by a factor of $2n+1$, which means the following equivalence relation

$$\nu \sim (2n+1)\nu, \quad n \in \mathbb{Z}. \tag{3.25}$$

This equivalence relation can be understood physically from either Eq. (3.21) or Eq. (3.23). In Eq. (3.21) we can multiply the total charge by any odd integer without changing the physical meaning, since the total charge Q_{C_2}/π is only defined in $\mathbb{Z}_2$. Likewise in Eq. (3.23), we can multiply the flux Φ_c by any odd integer without changing the physics since Φ_c is defined in $\mathbb{Z}_2$.

An immediate consequence of the equivalence relation Eq. (3.25) is that the anomaly is in fact trivial if

$$\nu = \frac{n}{2m+1} \sim n, \quad n, m \in \mathbb{Z}. \tag{3.26}$$

These *exceptional values* form a measure zero but dense subset within the interval $[0, 1]$. We can also demonstrate the triviality of these values of ν more explicitly by constructing a trivial phase starting from the metallic state: we can first gap out all the fermions by introducing a charge-density-wave (CDW) order that breaks the $\mathbb{Z}$ translation symmetry but keeps the $\mathbb{Z}_2$. For the values in Eq. (3.26) the CDW order parameter lives in $\mathbb{Z}_{2m+1}$. We can recover the $\mathbb{Z}$ translation symmetry by proliferating (condensing) domain walls of the $\mathbb{Z}_{2m+1}$ CDW order parameter. A standard calculation (see Appendix F) shows that the domain wall (denoted as σ) formally carries $\mathbb{Z}_2$ charge $\pi/(2m+1)$, namely $\mathbb{Z}_2 : \sigma \to e^{i\pi/(2m+1)}\sigma$. We can combine this with a $\mathbb{Z}_{2m+1}$ gauge transform for the domain wall $\sigma \to e^{i2m\pi/(2m+1)}\sigma$ and realize that the domain wall in fact carries only an integer charge[3]

[3]Mathematically this is the familiar statement that $\mathbb{Z}_2$ symmetry cannot be fractionalized on a $\mathbb{Z}_{2m+1}$ gauge-charged particle, or $H^2(\mathbb{Z}_2, \mathbb{Z}_{2m+1}) = 0$.

of π under Z_2. We can therefore neutralize this $\mathbb{Z}_2$ charge by attaching to the domain wall a local operator that is odd under $\mathbb{Z}_2$. This way we obtain a domain wall operator σ' which can now be condensed without breaking any other symmetry, and the resulting state is fully symmetric and gapped. Notice that if we had $\nu = 1/2^n$ instead, the domain wall will carry $\mathbb{Z}_2$ charge $\pi/2^n$ which is now truly fractional, i.e. it cannot be eliminated through gauge transforms and attaching local operators. In this case the domain walls cannot be proliferated without breaking $\mathbb{Z}_2$ symmetry, and a gapped symmetric phase is impossible.

The anomaly and exceptional points can also be understood using the notion of emergent anomalies[228], which we briefly discuss in Appendix F.

Another consequence of the equivalence relation Eq. (3.25) is that the magnitude of ν is no longer meaningful. In fact any value of ν can be made arbitrarily close to either 0 or 1 by appropriately multiplying some factor $(2n+1)/(2m+1)$. For rational values of ν, we can uniquely write $\nu = 2^n p/q \sim 2^n$ with p, q odd and $n \in \mathbb{Z}$. Curiously, we can write this relation more compactly as

$$\nu \sim |1/\nu|_2, \quad \text{if} \quad \nu \in \mathbb{Q}, \tag{3.27}$$

where $|...|_p$ denotes the p-adic magnitude.

Finally we notice that the $\mathbb{Z}_2 \times \mathbb{Z}$ anomaly is unambiguously defined only if the $U(1) \times \mathbb{Z}$ filling anomaly is trivial (namely the system has integer charge filling). Otherwise we can make a large $U(1)$ gauge transform $A \to A + 2\pi N c$ ($N \in \mathbb{Z}$) in the filling anomaly Eq. (3.14), which results in a shift of the coefficient of the $\mathbb{Z}_2 \times \mathbb{Z}$ anomaly.

3.3.3 $\mathbb{Z} \times \mathbb{Z}$ anomaly

The final $(1+1)$d example we want to discuss is the most nontrivial and involves four chiral modes, two right-handed and two left-handed, protected only by the translational symmetry. The $U(1)$ and C_2 symmetries can still be there but are not important for the following discussion. This situation will be relevant to the time-reversal invariant Weyl semimetal, which will be discussed in Sec. 3.4.3.

We consider a modified model of the previous (1+1)d spinful fermionic system Eq. (3.20), in which both the C_2 rotation and inversion symmetries are broken, so that only the trans-

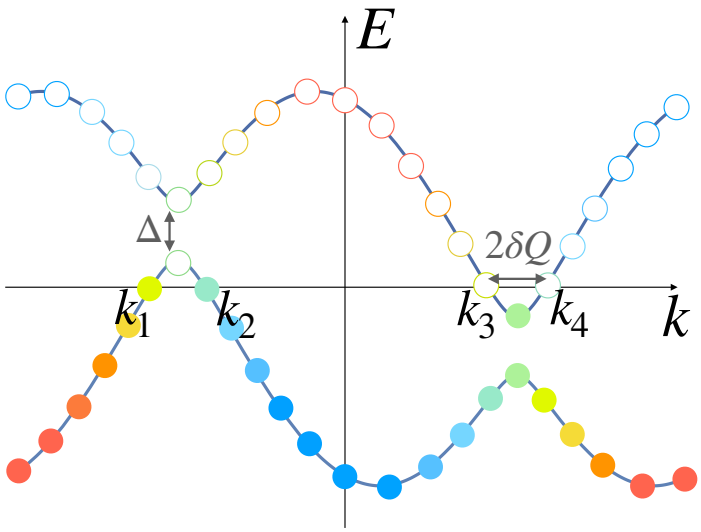

Figure 3.4: (Color online) The blue (red) band in Fig. 3.3 is shifted to the right (left) by δQ. C_2 symmetry is not necessary for the protection of the states anymore as indicated by the colour hybridisation. Instead, the filled states now possess a non-trivial total momentum, leading to a $\mathbb{Z} \times \mathbb{Z}$ chiral anomaly.

lational symmetry remains

$$\begin{aligned} H &= \sum_{\langle i,j \rangle} \Big[\cos \delta Q c_i^\dagger \sigma^z c_j - m\, c_i^\dagger \sigma^z c_i + \Delta c_i^\dagger \sigma^x c_i \\ &- \frac{i}{2} \sin \delta Q (c_i^\dagger c_j - c_j^\dagger c_i) \Big] \\ &= \sum_k c_k^\dagger \left[(\cos \delta Q \cos k - m)\, \sigma^z + \Delta \sigma^x - \sin \delta Q \sin k \right] c_k. \end{aligned} \tag{3.28}$$

We now have have positive chirality gapless nodes at $\pm k_+$ and negative chirality gapless nodes at $\pm k_-$, with $k_\pm = Q \pm \delta Q$ (taking the C_2 symmetry breaking parameter Δ to be negligible for simplicity). This is essentially a shifted version of the two overlaid bands studied in the previous section, shown in Fig. 3.3, where each band is moved by δQ in opposite directions as shown in Fig. 3.4. The low energy modes in this model are solely protected by translational symmetry in the z direction, which suggests the existence of an anomaly relating to the translational gauge field.

A key feature of this shifted dispersion is the existence of total ground state z-component

of the crystal momentum given by

$$P_z = \sum_{k_z=k_-}^{k_+} k_z - \sum_{k_z=-k_+}^{-k_-} k_z = \pi\lambda L_z + O(1) \quad , \tag{3.29}$$

where $\lambda = 2Q\delta Q/\pi^2$ (defined mod 2). This relation is similar to Eq. (3.13) and (3.21), with the symmetry charge being the total momentum. Similar to the previous examples, the $O(1)$ piece in Eq. (3.29) is required for proper momentum quantization: $L_z P_z/2\pi \in \mathbb{Z}$. For $\lambda = 1$ the $O(1)$ piece can simply be $\delta P_z = \pi$. For fractional $\lambda \notin \mathbb{Z}$ one can show that the $O(1)$ piece has to take some nontrivial form, in particular it can not be analytic in $1/L_z$. This means that for $\lambda \in [0, 1)$ some nontrivial IR modes (like gapless fermions) are needed. Equivalently, a short-range entangled ground state must have λ equal to either 0 or 1 – the latter can be realized by a product state with an odd number of fermions in each unit cell.

We comment on a subtlety with the above discussion. One may worry that the coefficient λ in Eq. (3.29) is not well defined since P_z is only defined mod 2π. In particular, we may arbitrarily shift $\lambda \to \lambda + \eta$ by simply adding a factor $2\pi \lfloor \eta L \rfloor$ to the sequence. One way to view this issue is to regard different choices of λ as being different choices of Brillouin zones over which we do our ground state summation in Eq. (3.29). Thus our job is to fix such a summation convention that allows us to uniquely determine λ.

To specify how λ is determined we demand the following condition on the momentum choice:

$$\frac{P(L)}{2\pi} \leq \frac{P(L+1)}{2\pi} \leq \frac{P(L)}{2\pi} + 1\,, \qquad\qquad P(2) = \pi\,, \tag{3.30}$$

which corresponds to determining ground state momentum via purely counting momenta within 0 and 2π. These two demands uniquely determine the sequence of $P_s(L)$ as $L \to \infty$ and thus a unique λ. Using such a sequence of ground state momenta $P_s(L)$, we may then determine λ via the procedure

$$\lambda \equiv \lim_{L\to\infty} \frac{P_s(L)}{\pi L} \quad . \tag{3.31}$$

To further elucidate the process, let us first consider the trivial case of a fully-filled band with one electron per unit cell. If we choose periodic boundary conditions we may obtain an exact expression for the ground state momentum $P(L) = \pi L - \pi$, where $-\pi$ is the $\mathcal{O}(1)$ term in Eq. (3.29). Such a $P(L)$ automatically satisfies conditions in Eq. (3.30), and via

procedure (3.31) yields $\lambda = 1$ as expected. It is important to note that in this case the $\mathcal{O}(1)$ term is of an analytic nature in $1/L$ which expresses the trivial nature of the system and allows for an insulator to reproduce such a behaviour. However for non-trivial systems the $\mathcal{O}(1/L)$ piece comes about due to the difference between a summation of filled state momenta at L, and the momentum integral in the thermodynamic limit. This pattern is highly configuration and length dependent due the difference between the gapless mode momenta defined in the thermodynamic limit and the corresponding well-defined filled momentum at L. This sort of difference behaves non-analytically in $1/L$ and can only be feasibly reproduced by a gapless or long-range entangled state.

To further support the nontriviality of the $\mathbb{Z} \times \mathbb{Z}$ anomaly, in Appendix G we perform an explicit stability analysis using Luttinger liquid theory. Now we continue by discussing the action that expresses the presence of a total gauge-invariant ground state momentum.

Anomaly term

Expressing the $\mathbb{Z} \times \mathbb{Z}$ anomaly as a topological term is a little more subtle than in the previous two examples. If the spacetime forms a simple torus T^2, i.e. simple periodic boundary condition in both time and space, then the following term can reproduce the response in Eq. (3.29):

$$S = \pi\lambda \int z_t z_z \quad , \tag{3.32}$$

where z_t and z_z are the time and space components of the z gauge field, respectively. This action does not appear to be topological, nor does it show any gauge non-invariance since $z \in H^1(\mathcal{M}, \mathbb{Z})$ does not have any large gauge transform. The resolution is to notice that translation symmetry is in fact different from an on-site $\mathbb{Z}$ symmetry in one important aspect: on a finite-size system with length L_z, the many-body total momentum[4] is quantized $P_z \in \frac{2\pi}{L_z}\mathbb{Z}$. Since $L_z = \oint_{\mathcal{C}_z} z_z$, the momentum quantization imposes a somewhat unconventional large gauge symmetry on a spacetime torus T^d:

$$\begin{aligned} z \to & z + \left(\oint_{\mathcal{C}_z} z_z \right) \alpha, \\ \oint_{\mathcal{C}_z} \alpha = 0, \quad & \oint_{\mathcal{C}_{i\neq z}} \alpha \in \mathbb{Z}. \end{aligned} \tag{3.33}$$

[4]This is true when there is no symmetry flux (twisted boundary condition) from other symmetries, which is justified here since we are focusing on just the translation symmetry.

This gauge symmetry can be understood from the definition of the translation gauge field reviewed in Sec. 3.2.2: the "transverse" part of the gauge field $\oint_{\mathcal{C}_{i\neq z}} \alpha$ measures the displacement in $\hat{z}$ direction as one moves around the $\mathcal{C}_i$ cycle, and this displacement is defined only modulo L_z. This large gauge symmetry also allows us to have more nontrivial gauge field configurations (bundles) with nontrivial $\int_{\mathcal{C}_2} dz$ over some 2-cycles $\mathcal{C}_2$. Specifically, we allow $\int_{\mathcal{C}_2} dz \in L_z\mathbb{Z}$ for $\mathcal{C}_2$ not including any $\mathcal{C}_z$ cycle, and $\int_{\mathcal{C}_2} dz = 0$ if $\mathcal{C}_2$ includes a $\mathcal{C}_z$ cycle. This immediately implies that $\int dz = 0$ in $(1+1)d$, which is relevant for our discussion here, and $\int dzdz = 0$ in $(3+1)d$ which will be relevant for our later discussion in Sec. 3.4.3.

We can now see why the response term Eq. (3.32) is not gauge invariant: under $z_t \to L_z\alpha$, the term changes by $\delta S = N\pi\lambda L_z^2$ for some integer N. For $\lambda = 1$ this change can be made trivial by further supplementing a counter term $\pi \int z_t$ which changes by $N\pi L_z$ (recall that $L_z(L_z+1)$ is always even). For fractional λ there is no such counter term, so the gauge non-invariance is intrinsic and nontrivial IR modes are required to cancel this gauge non-invariant.

Similar to the two previous examples, we can also formally write the response Eq. (3.32) as the boundary descendent of a bulk term

$$\pi\lambda \int_{X_3} zdz = \pi\lambda \int_{X_3} z_z(\partial_u z_t - \partial_t z_u) = \pi\lambda \int_{\partial X_3} z_t z_z, \tag{3.34}$$

where u is the direction perpendicular to the boundary. The equality follows from the requirements on $\int_{\mathcal{C}_2} dz$ discussed above. The topological nature of the response is more manifest in this $\int zdz$ form – the price we pay is that it is defined in one higher dimension.

We can further illustrate how the $\int zdz$ term appears through the standard chiral anomaly analysis. A chiral fermion, coupled to a continuous ($U(1)$ or $\mathbb{R}$) gauge field A, can only be defined on the boundary of a bulk with nontrivial Hall conductance:

$$S = \pm\frac{1}{4\pi}\int A \wedge dA \quad , \tag{3.35}$$

where the sign is determined by the chirality of the fermion. In our current example, we should replace $A \to k_z z$, where k_z is the crystal momentum of the chiral fermion. For the theory defined in Eq. (3.28), the full anomaly is

$$\begin{aligned} S &= \frac{1}{4\pi}\int [(k_+ z)\wedge d(k_+ z) + (-k_+ z)\wedge d(-k_+ z) \\ &- (k_- z)\wedge d(k_- z) - (-k_- z)\wedge d(-k_- z)] \\ &= \pi\lambda \int z \wedge dz \quad , \end{aligned} \tag{3.36}$$

where we have used $\pi\lambda \equiv 2Q\delta Q/\pi = (k_+^2 - k_-^2)/2\pi$.

Similar to the $\mathbb{Z}_2 \times \mathbb{Z}$ anomaly, the $\mathbb{Z} \times \mathbb{Z}$ anomaly is unambiguously defined only if the $U(1) \times \mathbb{Z}$ filling anomaly is trivial (i.e. integer charge filling). Otherwise we can make a large $U(1)$ gauge transform $A \to A + 2\pi N z$ ($N \in \mathbb{Z}$) in the filling anomaly Eq. (3.14) to shift the coefficient of the $\mathbb{Z} \times \mathbb{Z}$ anomaly.

3.4 Three-dimensional topological semimetals

We will now apply the results of Section 3.3 to (3+1)d semimetal systems. The connection between $(1+1)$d and $(3+1)$d anomalies is well-known: in an externally applied magnetic field, a $(3+1)$d system, exhibiting a chiral anomaly, possesses special lowest Landau levels (LLL), which has the corresponding $(1+1)$d chiral anomaly. Here it is worth emphasizing again that the following topological semimetals possess "unquantized anomalies", meaning that symmetry preserving perturbations can continuously alter a non-trivial anomaly coefficient to a trivial one, resulting in a gapped insulator state. In this sense the semimetals are not afforded the degree of stability of the usual quantized anomalies, associated with gapless surface states of topological insulators. However, upon manually fixing the non-trivial anomaly coefficient, which is justified since it is always associated with a conserved and (at least in principle) observable quantity, the same constraint on the low-energy theory results as would arise from a quantized anomaly. This is exactly analogous to fixing a noninteger electron filling in a metal.

3.4.1 TR-broken Weyl semimetal

Let us start with the system that may be viewed as the "hydrogen atom" of topological semimetals, namely the simplest magnetic Weyl semimetal with a pair of nodes, located on the z-axis in momentum space at $k_z = \pm Q$. The gaplessness of such a system is protected purely by $U(1)$ charge symmetry and translational symmetry in the z direction, and is well-known for possessing a chiral anomaly of the form [408, 45]

$$\begin{aligned} S &= -\frac{1}{2}\frac{\nu}{2\pi}\int z \wedge A \wedge dA \quad , \\ &= -\frac{1}{2}\frac{\nu}{2\pi}\int dt\, d^3r\, z_\mu \epsilon^{\mu\nu\lambda\eta} A_\nu \partial_\lambda A_\eta \quad , \end{aligned} \tag{3.37}$$

with $\nu = \frac{2Q}{2\pi}$. Eq. 3.37 encodes the standard topological responses, which have been discussed extensively before, i.e. the anomalous Hall conductivity $\sigma_{xy} = \frac{\nu}{2\pi}$, and the chiral

magnetic effect (CME). In addition, it also encodes more subtle responses, which directly probe translational symmetry defects and involve nontrivial charges on magnetic flux loops linked with crystal dislocations. It is this type of phenomena, generalizable to other kinds of topological semimetals, which do not possess any obvious electromagnetic topological responses, that will be the main focus of this paper.

When a Weyl semimetal with a pair of nodes, separated by $2Q$ along the z-axis, is placed in an external magnetic field along the same direction, it develops a pseudospin-polarized LLL, which disperses along the direction of the field and crosses the Fermi energy at the locations of the Weyl points, exactly as shown in Fig. 3.2(a). Thus the LLL of the magnetic Weyl semimetal in an external magnetic field maps directly onto a $(1+1)$d metal with the $U(1) \times \mathbb{Z}$ chiral anomaly, described in Sec. 3.3.1. Taking into account the LLL orbital degeneracy $N_{LLL} = BL_xL_y/2\pi$, where $L_{x,y}$ are the sample sizes in the x and y-directions, the derivative of the Luttinger volume of this $(1+1)$d metal with respect to the magnetic field gives the Hall conductivity of the Weyl semimetal. This is encoded in the topological response action in the (t, z) plane

$$S = \nu N_{LLL} \int z \wedge A \quad , \tag{3.38}$$

which also follows directly from Eq. (3.37). We may also invert this argument and say that Eq. (3.37) follows from Eq. (3.38). This is the logic we will use to find topological response terms for other semimetals, for which no purely electromagnetic responses, like the Hall effect, exist. Namely we will identify topological response terms by mapping the LLL of these semimetals to one of the $(1+1)$d systems, discussed in Section 3.3.

The incompatibility of the anomalous responses, described above, with a trivial gapped insulator may also be seen explicitly if one attempts to construct such an insulator starting from a gapped superconductor and disordering the phase of the superconducting order parameter by proliferating vortices. As discussed in Refs. [349, 335], a gapped superconducting state can only be obtained in this case using FFLO-type pairing (for weak pairing), where electrons on each side of the two Weyl nodes are paired and the pairs thus carry momentum $\pm 2Q$ [222, 69, 19, 187]. This generally breaks crystal translational symmetry, except when $2Q = \pi$, i.e. half a reciprocal lattice vector.

Consider, say, a right-handed Weyl fermion with a singlet superconducting pairing. The pairing Hamiltonian is given by

$$H = \sum_{\mathbf{k}} c^\dagger_{\mathbf{k}} \boldsymbol{\sigma} \cdot \mathbf{k} c_{\mathbf{k}} + \Delta \sum_{\mathbf{k}} (c^\dagger_{\mathbf{k}\uparrow} c^\dagger_{-\mathbf{k}\downarrow} + c_{-\mathbf{k}\downarrow} c_{\mathbf{k}\uparrow}) \quad . \tag{3.39}$$

Here $\boldsymbol{\sigma}$ are Pauli matrices corresponding to the degree of freedom describing the two bands that touch at the Weyl point and the momentum $\mathbf{k}$ is measured from the location of the Weyl point $Q\hat{z}$. We have also set the Fermi velocity of the Weyl fermion to unity. Introducing the Nambu spinor notation $\psi_{\mathbf{k}} = (c_{\mathbf{k}\uparrow}, c_{\mathbf{k}\downarrow}, c^{\dagger}_{-\mathbf{k}\downarrow}, -c^{\dagger}_{-\mathbf{k}\uparrow})$, this may be rewritten as

$$H = \frac{1}{2}\sum_{\mathbf{k}} \psi^{\dagger}_{\mathbf{k}}(\tau^z \boldsymbol{\sigma}\cdot\mathbf{k} + \Delta\tau^x)\psi_{\mathbf{k}} \quad , \tag{3.40}$$

where the Pauli matrices τ^a act on the particle and hole components of the Nambu spinor. Apart from a factor of $1/2$ in front of the sum over momenta, correcting for the doubling of degrees of freedom in the Nambu representation, Eq. (3.40) has the form of the Hamiltonian of a free Dirac fermion of mass Δ.

Now consider a straight-line vortex of positive unit vorticity along the z-axis, i.e. we take the superconducting order parameter to have the following form in cylindrical coordinates $\Delta(\mathbf{r}) = |\Delta(r)|e^{i\theta}$, where $r = \sqrt{x^2+y^2}$ and $\theta = \arctan(y/x)$. The momentum-space Hamiltonian in Eq. (3.40) is replaced by the following Bogoliubov-de Gennes (BdG) Hamiltonian

$$\begin{aligned} \mathcal{H} &= -i\tau^z(\sigma^x\partial_x + \sigma^y\partial_y) + \tau^z\sigma^z k_z \\ &+ |\Delta(r)|(\cos\theta\tau^x - \sin\theta\tau^y) \quad . \end{aligned} \tag{3.41}$$

This is a classic problem first considered in a different context by Callan and Harvey [50, 342]. Taking first $k_z = 0$ and looking for a θ-independent localized solution of the BdG equation

$$\mathcal{H}\Psi = 0 \quad , \tag{3.42}$$

one obtains, ignoring normalization factor

$$\Psi_R(\mathbf{r}) = \begin{pmatrix} 1 \\ 0 \\ 0 \\ -i \end{pmatrix} e^{-\int_0^r dr'|\Delta(r')|} \quad , \tag{3.43}$$

where the subscript R refers to the right-handed Weyl fermion of Eq. (3.39). It is easy to see that $\Psi_R(\mathbf{r})$ is also an eigenstate of the BdG Hamiltonian (3.41) at a nonzero k_z with eigenvalue k_z, i.e. it describes a right-moving mode, localized in the vortex core. Repeating the same calculation for the left-handed Weyl fermion we have

$$\Psi_L(\mathbf{r}) = \begin{pmatrix} 1 \\ 0 \\ 0 \\ i \end{pmatrix} e^{-\int_0^r dr'|\Delta(r')|} \quad , \tag{3.44}$$

which is an eigenstate of the corresponding BdG Hamiltonian with eigenvalue $-k_z$, i.e. it corresponds to a left-moving mode, localized in the vortex core.

These chiral Majorana modes in the vortex cores prevent a gapped insulating state if the superconducting phase coherence is destroyed by phase fluctuations. This conclusion holds for any odd number of pairs of Weyl nodes, i.e. for any magnetic Weyl semimetal. To obtain an insulating state, we need to condense vortices with higher vorticity, the different possible states are discussed in detail in Refs. [349, 335, 301]. The vortex condensation method's inability to obtain a trivial symmetric gapped insulator with non-trivial Hall conductivity perfectly reflects the anomalous nature of the magnetic Weyl semimetal. In the following subsection we will generalize this analysis to other topological semimetals, which do not have any nontrivial electromagnetic responses, and thus the answer to the question of what exactly is topological about them is far less obvious.

3.4.2 Type-I Dirac semimetal

We will now attempt to generalize the analysis in the previous subsection to the case of type-I Dirac semimetals. Type-I Dirac semimetals are TR and parity invariant which guarantees doubly degenerate bands. Their band dispersions feature a pair of Dirac nodes, located at time-reversed momenta on an axis of rotation, where each node consists of a pair of overlapping negative and positive chirality Weyl nodes. Their gaplessness is protected by a combination of rotational, translational, and $U(1)$ charge conservation symmetries. In a close analogy to magnetic Weyl semimetal, one may think of a type-I Dirac semimetal as an intermediate phase between an ordinary insulator and a weak TR-invariant topological insulator, where the direction of the weak index coincides with the rotation axis.

For concreteness we will consider a specific realization of a type-I Dirac semimetal with four-fold rotational symmetry, described by the following Hamiltonian in momentum space [359]

$$\begin{aligned} &\mathcal{H}(\mathbf{k}) = \sin k_x\, \Gamma_1 + \sin k_y\, \Gamma_2 + m(\mathbf{k})\Gamma_3 \\ + \quad &\gamma_1(\cos k_x - \cos k_y) \sin k_z\, \Gamma_4 + \gamma_2 \sin k_x \sin k_y \sin k_z\, \Gamma_5. \end{aligned} \tag{3.45}$$

Here

$$m(\mathbf{k}) = m_0 - b_{xy}(2 - \cos k_x - \cos k_y) - b_z(1 - \cos k_z), \tag{3.46}$$

and the 4×4 matrices Γ_a, satisfying Clifford algebra $\{\Gamma_a, \Gamma_b\} = 2\delta_{ab}$, are defined as

$$\Gamma_1 = \sigma^x s^z,\ \Gamma_2 = -\sigma^y,\ \Gamma_3 = \sigma^z,\ \Gamma_4 = \sigma^x s^x,\ \Gamma_5 = \sigma^x s^y, \tag{3.47}$$

where the 2×2 Pauli matrices $\boldsymbol{\sigma}$ and $\mathbf{s}$ refer to the orbital parity and the spin degrees of freedom respectively. The parameters in the function $m(\mathbf{k})$ are assumed to be chosen in such a way that band inversion occurs at the Γ-point in the BZ, producing two Dirac points along the $k_x = k_y = 0$ axis, whose location is given by

$$k_z = \pm Q = \pm \arccos\left(1 - m_0/b_z\right) \quad . \tag{3.48}$$

As mentioned above, this Dirac semimetal state may be regarded as an intermediate phase between an ordinary insulator when $m_0 < 0$ and a weak topological insulator with the weak indices $(0, 0, 1)$ when $m_0 > 2b_z$ and $b_{xy} > b_z$. The simplest way to understand this statement is to view the Dirac semimetal as a pair of time-reversed Weyl semimetals. Annihilating the Dirac nodes at the edge of the BZ then creates two time-reversed copies of the integer quantum Hall insulator, i.e. a weak quantum spin Hall insulator.

As we have chosen to define Eq. (3.45) on a cubic lattice $\mathcal{H}(\mathbf{k})$ possesses a C_4 rotational symmetry about the z-axis, with the rotation operator given by $R_4 = e^{i\pi/4} e^{-\frac{i\pi}{4}(2-\sigma^z)s^z}$, where the factor $e^{i\pi/4}$ was inserted for later convenience. This rotational symmetry is what protects the Dirac points, since it prohibits mass terms $\sin k_z \Gamma_{4,5}$, which are odd under rotation $R_4^\dagger \Gamma_{4,5} R_4 = -\Gamma_{4,5}$. Additionally z translation symmetry prevents prohibits a charge density wave from opening a gap, and $U(1)$ charge conservation symmetry prevents superconductivity.

Topologically nontrivial properties of type-I Dirac semimetals are related to the presence of gapless chiral fermions at the Dirac nodes, just as in the simpler magnetic Weyl semimetal case discussed above. Analogously to the magnetic Weyl case, it is then useful to place the system in an external magnetic field along the z-direction, which accomplishes an effective dimensional reduction to a $(1+1)$d problem.

Since type-I Dirac semimetals contain two pairs of Weyl nodes at low energies, there is a pair of LLL with the following dispersion (see Appendix H for detailed derivation)

$$E_{LLL}^{\pm}(k_z) = \pm m(0, 0, k_z) \quad , \tag{3.49}$$

with E_{LLL}^{+} having a C_4 charge of 0, and E_{LLL}^{-} having a C_4 charge of π. One can see that the form of the LLLs is identical to the $1D$ band dispersions discussed in Section 3.3.2 (see Fig. 3.3), except that here we consider C_4 symmetry and there exists an additional Landau level degeneracy of $N_{LLL} = BL_xL_y/2\pi$ per band. The logic we used in Section 3.3.2 may then be applied directly, after taking into account the LLL degeneracy. This implies the following $(1+1)$d topological term (with $\nu \equiv 2Q/2\pi$)

$$S = \pi \nu N_{LLL} \int z \wedge c_4 \quad , \tag{3.50}$$

where $c_4 \in H^1(\mathcal{M}, \mathbb{Z}_4)$ is the C_4 gauge field which around a 1-cycle counts number of C_4 disclinations that are traversed – an example of such a disclination is seen in Fig. 3.5.

Extending Eq. (3.50) back to (3+1) dimensions we obtain the generalized chiral anomaly term, which characterizes type-I Dirac semimetals

$$S = \frac{\nu}{2} \int z \wedge c_4 \wedge dA \quad . \tag{3.51}$$

Unlike the chiral anomaly term in magnetic Weyl semimetal, Eq. (3.51) cannot be interpreted as a purely electromagnetic response (like the Hall conductance). In the Landau level interpretation Eq. (3.50), a nontrivial C_4 charge per length in the $\hat{z}$ direction is associated with a magnetic flux in the xy-plane. Alternatively, we can also consider a C_4 disclination (Fig. 3.5(a)) in the $\hat{z}$ direction ($\int_{\mathcal{C}_{xy}} dc_4 = 1$). The action Eq. (3.51) reduces to the $(1+1)d$ filling anomaly Eq. (3.14) with charge density $\nu/2$. This fractional charge density induced in the disclination is also a characterization of the anomaly of the type-I Dirac semimetal. The anomalous nature is manifest if we consider a "trivial" four-fold disclination ($\int_{xy} dc_4 = 4$), which now carries a charge density 2ν and is fractional if ν takes a nontrivial value. The fractional charge associated with disclinations in symmorphic Dirac semimetals may alternatively be approached from the viewpoint of hinge states in the non-interacting limit [24, 369]. The anomalous response in Eq. (3.51) offers a generalisation of this feature to include both translation and rotational charge responses, valid in both the free-fermion and strongly-correlated regimes.

The response Eq. (3.51) is invariant under large gauge transformations $c_4 \to c_4 + 4\alpha$ if $\nu \in \frac{1}{2}\mathbb{Z}$. Similar to the $\mathbb{Z}_2 \times \mathbb{Z}$ anomaly discussed in Sec. 3.3.2, there is a set of equivalence relations $\nu \sim (4n+1)\nu$ for any $n \in \mathbb{Z}$. We therefore conclude that the response is anomalous unless ν belongs to the set of *exceptional values*

$$\nu_{ex} = \frac{n}{2(2m+1)}, \quad n, m \in \mathbb{Z}. \tag{3.52}$$

We note that at the level of free fermion band structure, the theory appears to be nontrivial at these exceptional values, with Dirac nodes at $k_z = \pm\pi\nu_{ex}$. Our analysis indicates that with strong interactions, a type-I Dirac semimetal with ν_{ex} can form a symmetric short-range entangled state. The resulting insulating state has a gauge invariant response Eq. (3.51) with $\nu = \tilde{n}/2$, where $\tilde{n} = (-1)^m n$. For $n \neq 0 \pmod 4$ this is a nontrivial crystalline SPT state, and can be viewed as a stack (in $\hat{z}$ direction) of $(2+1)d$ insulators with charge $\tilde{n}$ sitting at the C_4 rotation centers. The topological response of such $(2+1)d$ insulators has been discussed in Refs. [195, 321].

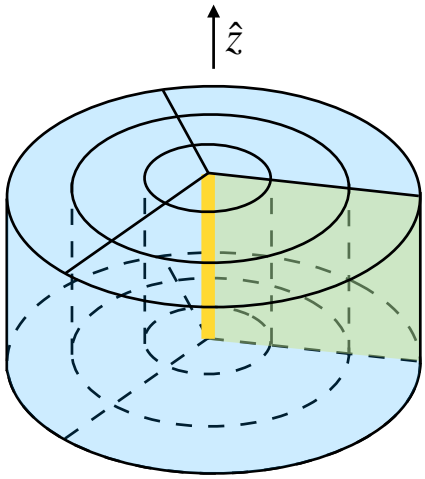

Figure 3.5: (Color online) A C_4 disclination with the Frank vector along $\hat{z}$ is depicted by gluing two lattice faces, rotated by $\pi/2$ with respect to each other, together (shown as yellow surface) to create a defect line shown as a bold yellow line. Close to this defect the lattice appears distorted, however far away the regular square lattice shape is retained.

As in the magnetic Weyl case, it is also useful to see how an attempt to construct a trivial insulator by gapping the Dirac nodes fails, barring the exceptional points Eq. (3.52), explicitly via the vortex condensation method. For this purpose it is convenient to focus on low-energy states and expand Eq. (3.45) to linear order in the transverse momentum components $k_{x,y}$, which gives

$$\mathcal{H}(\mathbf{k}) = k_x \sigma^x s^z - k_y \sigma^y \pm (k_z \pm Q)\sigma^z \quad , \tag{3.53}$$

where we have absorbed the Fermi velocity along the z-direction into the definition of k_z. An ordinary gapped BCS superconducting state is now possible by pairing right- and left-handed fermions separately. For the pair of right-handed fermions we have

$$H = \sum_{\mathbf{k}} c^\dagger_{\mathbf{k}} \boldsymbol{\sigma} \cdot \mathbf{k} c_{\mathbf{k}} + \Delta \sum_{\mathbf{k}} (c^\dagger_{\mathbf{k}1} i\sigma^y c^\dagger_{-\mathbf{k}2} + h.c.) \quad , \tag{3.54}$$

where we have brought the right-handed node Hamiltonian to the form $\boldsymbol{\sigma} \cdot \mathbf{k}$ by a unitary transformation, which also changes the rotation operator to $R_4 = e^{\frac{i\pi}{4}} e^{-\frac{i\pi}{4}(\sigma^z - 2s^z)}$; k_z is measured from the corresponding node location and the $1, 2$ index labels the two eigenvalues of s^z, which distinguish the two right-handed nodes in the pair. Introducing Nambu spinor

$\psi_{\mathbf{k}} = (c_{\mathbf{k}1\uparrow}, c_{\mathbf{k}1\downarrow}, c^\dagger_{-\mathbf{k}2\downarrow}, -c^\dagger_{-\mathbf{k}2\uparrow})$ this becomes

$$H = \sum_{\mathbf{k}} \psi^\dagger_{\mathbf{k}} (s^z \boldsymbol{\sigma} \cdot \mathbf{k} + \Delta s^x) \psi_{\mathbf{k}} \quad , \tag{3.55}$$

which represents two identical copies of Eq. (3.40), describing a single superconducting Weyl fermion. Thus in this case we obtain a pair of Majorana, or a single chiral right-moving Dirac mode in the vortex core. Analogously, the left-handed pair of Weyl nodes produces a single left-moving Dirac mode. From Eqs. (3.43) and (3.44) both of these modes are linear combinations of $c_{\mathbf{k}1\uparrow}$ and $c^\dagger_{-\mathbf{k}2\uparrow}$. This means that they transform under C_4 rotation as

$$R_4 : \psi^{R,L}_{k_z} \to i\psi^{R,L}_{k_z} \quad , \tag{3.56}$$

where $R_4 = e^{\frac{i\pi}{4}(2-\sigma^z+s^z)}$ in the Nambu basis. This means that any pairing of the left- and right-handed modes of the type

$$H = \sum_{k_z} \left[k_z \psi^\dagger_{k_z} \tau^z \psi_{k_z} + \frac{\Delta}{2} \left(\psi^\dagger_{k_z} i\tau^y \psi^\dagger_{-k_z} + h.c. \right) \right] \quad , \tag{3.57}$$

where the eigenvalues of τ^z label the chirality of the 1D Weyl modes, which would gap them out, violates the C_4 symmetry. We then have to consider non-perturbative ways to gap out the fermions. For this it is convenient to first introduce a CDW order

$$m\psi^\dagger_L \psi_R + h.c. \quad , \tag{3.58}$$

which gaps out the fermions by breaking translation symmetry. We then ask if translation symmetry can be restored by condensing defects of m. A calculation similar to that in Sec. 3.3.2 and Appendix F shows that this is possible only if the momenta of the nodes $\pm Q = \pm\pi\nu$ belong to the exceptional values Eq. (3.52).[5] Thus, in a C_4 symmetric state the fermion modes remain gapless and single vortex condensation is impossible unless the Dirac nodes sit at some exceptional momenta defined in Eq. (3.52).

[5]There is an additional subtlety with the exceptional value $\nu = 1/2$. A direct calculation shows that the $\mathbb{Z}_2$ domain wall of the CDW order parameter in the vortex core carries C_4 charge $\pi/4$, which appears to be fractional and therefore disallows vortex condensation. However, notice that a bulk Bogoliubov fermion (not the vortex zero modes) sees the vortex as a π-flux, so if a vortex sits on a C_4 axis the bulk fermion will carry C_4 angular momentum $(2n+1)\pi/4$ ($n \in \mathbb{Z}_4$). So the $\pi/4$ charge associated with the vortex CDW domain wall can be canceled by bring in a bulk fermion into the vortex. The domain wall can then be condensed to give a trivially gapped vortex, which can then be gapped and produce a symmetric insulator.

3.4.3 TR-invariant Weyl semimetal

Finally, let us discuss the most nontrivial case, that of a TR-invariant Weyl semimetal. In a TR-invariant Weyl semimetal the nodes always occur in multiples of four since there are pairs of nodes of equal chirality, related to each other by TR. We will first discuss an example in which all the nodes lie on the z-axis, which is closely related to the $(1+1)$d system, discussed in Section 3.3. We will then generalize to the situation when the nodes are not on the same line.

Nodes separated in the z direction

The simplest model for a TR-invariant Weyl semimetal may be obtained from the model of a type-I Dirac semimetal Eq. (3.45) by adding a C_4 symmetry breaking perturbation $\gamma\sigma^x s^x$ and an inversion-breaking perturbation $g \sin k_z \sigma^z s^z$. The Weyl node locations $k_z = \pm Q \pm \delta Q$ are nontrivial solutions of the equation

$$g^2 \sin^2 k_z = \gamma^2 + m^2(k_z) \quad . \tag{3.59}$$

When a magnetic field is applied along the z-axis, the resulting LLL structure is identical to the $(1+1)$d system, discussed in Section 3.3.3, and shown in Fig. 3.4.

Extending the (1+1)d anomaly action Eq. (3.36) to (3+1) dimensions, we then obtain[6]

$$S = -\frac{\lambda}{2} \int z \wedge dz \wedge A \quad . \tag{3.60}$$

where $\lambda = 2Q\delta Q/\pi^2$. Recall from Sec. 3.3.3 that large gauge transformations in the z_i $(i \neq z)$ components imply that $\int_{C_2} dz$ can be non-zero over some 2-cycle C_2 that does not involve a C_z cycle. This action describes two distinct manifestations of the nontrivial topology of a TR-invariant Weyl semimetal. One is the nontrivial ground state momentum, which appears in the presence of an external magnetic field. This may be obtained by varying the action with respect to the time component of the translation gauge field z_t

$$P_z = \pi \lambda L_z N_{LLL} \quad , \tag{3.61}$$

[6]Under a small gauge transform $A \to A + d\alpha$, the invariance of this action is guaranteed by the relation $\int dzdz = 0$ discussed in Sec. 3.3.3. Physically this requirement implies that no loop linkages between a dislocation line and screw dislocations are inserted over time. Alternatively, if such an object is inserted into the system, the resulting small gauge non-invariance implies that compensating gapless chiral modes must exist along the defect line.

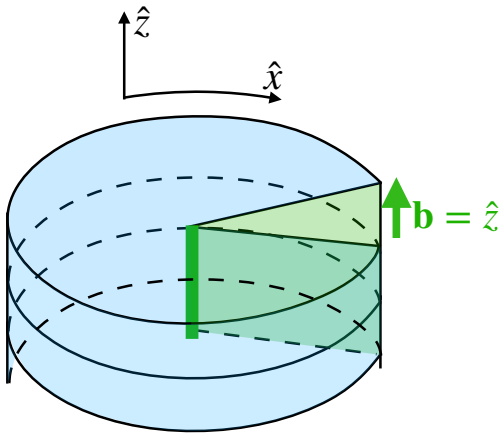

Figure 3.6: (Color online) Cartoon of a screw dislocation, represented by a lattice shear strain along the green surface. The defect line is shown in bold green with a Burgers vector $\mathbf{b} = \hat{z}$.

where $\mathcal{N} = \mathcal{C}_x \times \mathcal{C}_y \times \mathcal{C}_z$ with $\mathcal{C}_\alpha$ being the circumference cycle along the direction $\hat{\alpha}$, $\int_{\mathcal{C}_x \times \mathcal{C}_y} dA/2\pi = BL_xL_y/2\pi = N_{LLL}$, and we have taken $dz = 0$ assuming a perfect crystal without dislocations. We see that the total momentum is exactly the expected momentum output as in Sec. 3.3.3 with N_{LLL} copies from the LLL degeneracy. (ii) The second physical phenomenon can be seen with a screw dislocation where $\int_{\mathcal{C}_{xy}} dz = b$, with the magnitude of Burgers vector $\mathbf{b} = \hat{z}$ (Fig. 3.6). Varying with respect to A_t gives a fractional $1D$ charge density on the screw dislocation

$$\rho = -\frac{\lambda}{2} b \quad . \tag{3.62}$$

We comment on the role of time-reversal symmetry here. The response term Eq. (3.60) does not require time-reversal. But if time-reversal is broken, a Hall conductance term Eq. (3.37) can be induced as the Weyl nodes can shift in asymmetric ways. A large gauge transform $A \to A + 2\pi N z$ ($N \in \mathbb{Z}$) will then shift the coefficient of the term Eq. (3.60). The anomaly is therefore sharply defined only in the absence of Hall conductance.

Analogously to the previous cases, topologically nontrivial nature of the TR-invariant Weyl semimetal also manifests in the impossibility of gapping out the Weyl nodes without either breaking translational symmetry or inducing topological order. The analysis here is essentially identical to the type-I Dirac semimetal case above and we will not show the details for this reason. One starts with a gapped BCS state, obtained by separately pairing right- and left-handed Weyl fermions at time-reversed momenta, described by Eq. (3.54).

A π-flux vortex then binds right- or left-moving 1D Weyl fermion modes, which transform nontrivially under translations, since the modes exist at nonzero momenta, corresponding to the locations of the Weyl nodes. Since the left- and right-handed Weyl nodes are located at different momenta, not related to each other by any symmetry, pairing the corresponding left- and right-moving 1D Weyl fermion modes in the vortex core is impossible without breaking translational symmetry.

Nodes separated in the xz-plane

Weyl nodes in a TR-invariant Weyl semimetal in general are not located on the same line, as in the special example considered above. It is, however, straightforward to extend the above analysis to a more general situation.

For example, consider a system with four Weyl nodes, where the right-handed nodes are at momenta $\mathbf{k} = \pm(\delta Q, 0, Q)$ and the left-handed ones are at $\mathbf{k} = \pm(-\delta Q, 0, Q)$. In such a configuration, an applied magnetic field in the x direction causes the LLL's to carry a total momentum of

$$P_x = \pi \lambda L_z N_{LLL} \quad , \tag{3.63}$$

where $\lambda = 2Q\delta Q/\pi^2$, while a magnetic field in the z direction has LLL's with total momentum

$$P_z = \pi \lambda L_x N_{LLL} \quad . \tag{3.64}$$

Such a response can be described by the action

$$S = -\frac{\lambda}{2} \int (x \wedge dz + z \wedge dx) \wedge A \quad , \tag{3.65}$$

where x is the gauge field corresponding to x translational symmetry. It is important to point out that this term is distinct from the electric polarization action, which has a superficially similar form $P \int x \wedge z \wedge dA$ [322] since the momentum response of the Weyl semimetal is symmetric under $x \leftrightarrow z$, rather than the antisymmetric response from polarization. A polarization response is fully gauge invariant in the bulk and known to be realizable by a short-range entangled insulator and is thus not anomalous. In contrast, the TR-invariant Weyl semimetal has an anomalous response. Similarly to all previous cases of semimetals the anomalous nature is also exhibited by the fractional charge density, carried by a dislocation with Burgers vector $b\hat{z}$ or $b\hat{x}$.

All other cases can be easily generalized from the two presented TR-invariant WSM examples. The most general TR-invariant WSM will have nodes shifted in all three dimensions and be described by a combination of different translational gauge field terms $\sum_{i,j} \int \gamma_{ij} x_i \wedge dx_j \wedge A$, where $(x_1, x_2, x_3) = (x, y, z)$. For a related recent work, discussing topological responses in TR-invariant WSM, see Ref. [75].

3.5 Discussion and conclusion

As we have demonstrated in multiple examples above, the anomalous response of $(3+1)$d symmetry-protected semimetals may be reduced to $(1+1)$d chiral anomalies of their lowest Landau levels in an external magnetic field, involving the relevant protecting symmetries. We have shown that all these $(1+1)$d anomalies in turn stem from an unquantized filling anomaly, which essentially specifies the amount of symmetry charge present in the ground state. The relevant symmetry charges are the $U(1)$ charge, crystalline angular momentum and linear momentum for the cases of magnetic WSM, type-I DSM and TR-invariant WSM, respectively. These charges can be tuned to be trivial while preserving the symmetry of the system, hence leading to tunable quantum anomalies. However if we fix the anomaly prefactor, and thus the total charge, to be non-trivial, while demanding that the relevant symmetries remain unbroken, there must exist compensating IR behaviour such as gapless modes or topological order to maintain gauge invariance. It then becomes natural to view the gaplessness of (3+1)d semimetals as being topologically mandated by a non-trivial prefactor of a tunable anomaly, such as a non-integer (in appropriate units) Hall conductivity for magnetic WSM. In this work, we have extended this concept to cover other topological semimetal systems. The anomalies for the TR-invariant Weyl and type-I Dirac semimetals can also be characterized by fractional $U(1)$ charge densities, induced on crystalline symmetry defects, such as disclinations for type-I DSM and screw dislocations for TR-invariant WSM. To support the non-triviality of these semimetals at a non-perturbative level, we have also shown that a trivial gapped state with a fixed non-trivial anomaly prefactor is not achievable via vortex condensation.

These unquantized, tunable, anomalies naturally generalize the notion of fractional $U(1)$ charge density to other discrete symmetries (like the crystalline symmetries discussed in this work). In realistic systems, the $U(1)$ charge density (filling fraction) is naturally fixed by chemistry, while fixing the coefficients of other tunable anomalies, as one turns on electron-electron interactions, appears to be less natural and necessarily involves some fine-tuning. We can instead take a different viewpoint: given an interacting system in an unknown phase, we can in principle measure the coefficient of the tunable anomalies either

experimentally or numerically, for example by measuring the symmetry charges induced in various defect configurations. We can then constrain the low energy theory (the phase) of this system from such measurement — for example, if the system has a fractional σ_{xy} in appropriate units, then it has to be either a metal, a magnetic Weyl semimetal, or a topologically ordered insulator.

Type-I Dirac semimetals with translational and n-fold rotational symmetry protected gapless states along the rotational axes were found to possess an unquantized $U(1)\times\mathbb{Z}\times\mathbb{Z}_n$ anomaly, except when the momentum separation between the nodes satisfies certain special conditions like Eq. (3.52) for C_4 rotation. Such *exceptional points* form a measure zero but dense subset.

There are many additional questions that can be explored, such as whether there exist gapless $(3+1)$d systems that do not inherently involve $U(1)$ charge symmetry as opposed to the presented semimetal systems — this would be relevant for the study of nodal superconductors. A well known example along this line is the magnetic Weyl semimetal with nodal seperation $2Q \neq N\pi$, which is nontrivial even without $U(1)$ symmetry due to the fractional thermal Hall conductivity. A generalization of these anomalies to systems protected by non-symmorphic symmetries (type-II Dirac semimetals) is also warranted. The fractional charge density, induced on various crystalline defects, predicted in this work can, at least in principle, be tested in experiments.

Chapter 4

Non-zero momentum requires long-range entanglement

In this chapter we will prove a general theorem regarding how non-zero momentum in many-body system requires long-range entanglement. We will explore many consequences of this exciting theorem. The content of this chapter is lifted from published work in Ref. [108][1].

4.1 Introduction

The ubiquitous appearance of translation symmetry in physical systems signals the importance of having a complete picture of the complex role it may play. In particular, although the ground state energy (associated with time-translation symmetry) of a many-body quantum system or a quantum field theory is frequently studied, the ground state *momentum* (associated with space-translation symmetry) is rarely discussed. Rather, in most cases one focuses on the momentum difference between excited states and the ground state. In this work we reveal a connection between the momentum and the entanglement structure of a quantum state, in the context of lattice spin (boson) systems:

Theorem 1. *If a quantum state $|\Psi\rangle$ in a lattice spin (boson) system is an eigenstate of the lattice translation operator $T : |\Psi\rangle \to e^{iP}|\Psi\rangle$ with a non-trivial momentum $e^{iP} \neq 1$, then $|\Psi\rangle$ must be long-range entangled, namely $|\Psi\rangle$ cannot be transformed to an un-entangled*

[1]

product state $|000...\rangle$ *through an adiabatic evolution or a finite-depth quantum circuit (local unitary).*

The intuition behind this statement follows from the sharp difference between translation T and an ordinary onsite symmetry G that is defined as a tensor product of operators acting on each lattice-site (such as the electromagnetic $U(1)$). A product state may recreate any total symmetry charge Q under G by simply assigning individual local Hilbert space states to carry some charge Q_α such that $Q = \sum_\alpha Q_\alpha$. However in the case of non-onsite translation symmetry, all translation-symmetric product states, which take the form $|\alpha\rangle^{\otimes L}$, can only carry trivial charge (lattice momentum). This suggests that non-trivial momentum is an inherently non-local quantity that cannot be reproduced without faraway regions still retaining some entanglement knowledge of each other, i.e. the state must be long-range entangled.

In condensed matter physics, we are often interested in ground states of translational-invariant local Hamiltonians. If the ground state is short-range entangled [61] (SRE) in the sense that it is connected to a product state through a finite-depth (FD) quantum circuit, then we expect the ground state to be unique, with a finite gap separating it from the excited states. In contrast for long-range entangled [61] (LRE) ground states, we expect certain "exotic" features: possible options include spontaneous symmetry-breaking cat states (e.g. GHZ-like states), topological orders (e.g. fractional quantum Hall states), and gapless states (e.g. metallic or quantum critical states). Theorem 1 provides us an opportunity to explore the interplay between translation symmetry and the above modern notions. An immediate corollary is

Corollary 1.1. *If a non-zero momentum state* $|\Psi\rangle$ *is realized as a ground state of a local spin Hamiltonian, then the ground state cannot be simultaneously unique and gapped. Possible options include (1) gapless spectrum, (2) intrinsic topological order and (3) spontaneous translation symmetry breaking.*

In fact, we show in Sec. 4.3.2 that option (2) is a special subset of option (3) through the mechanism of "weak symmetry-breaking" [164].

Our result is reminiscent of the celebrated Lieb-Schultz-Mattis-Oshikawa-Hastings (LSMOH) theorems [189, 263, 132], which state that in systems with charge $U(1)$ and translation symmetries, a ground state with fractional $U(1)$ charge filling (per unit cell) cannot be SRE. In our case the non-trivial lattice momentum $e^{iP} \neq 1$ plays a very similar role as the fractional charge density in LSMOH. In fact, as we discuss in Sec. 4.3.1, our theorem can be viewed as a more basic version of LSMOH that only involves translation symmetry, from which

the standard LSMOH can be easily derived. As a by-product, we also discover a previously unknown version of LSMOH constraint that involves an onsite $\mathbb{Z}_n$ symmetry and lattice translations.

The rest of this paper will be structured as follows: in Sec. 4.2 we provide a proof of Theorem 1 via a quantum circuit approach, and generalize it to fermion systems. Three consequences of Theorem 1 are discussed in Sec. 4.3: in Sec. 4.3.1 we discuss several LSMOH-type theorems; in Sec. 4.3.2 we show that a gapped topological order must *weakly* break translation symmetry if one of its ground states on torus has nonzero momentum – this is a generalization of the Tao-Thouless physics in fractional quantum Hall effect [331, 26]; in Sec. 4.3.3 we discuss the implication of Theorem 1 for the classification of crystalline symmetry-protected topological (SPT) phases. We end with some discussions in Sec. 4.4.

4.2 Proof

In this section we prove that SRE states necessarily possess trivial momentum, conversely implying that all non-trivial momentum ground states must be LRE. The approach that we take utilizes the quantum circuit formalism, which is equivalent to the usual adiabatic Hamiltonian evolution formulation [198, 61] but conceptually cleaner. In particular we will harness the causal structure of quantum circuits, which will allow us to 'cut and paste' existing circuits to create useful new ones.

We shall first prove Theorem 1 in one space dimension, from which the higher-dimensional version follows immediately.

4.2.1 Proof in 1d

First let us specify our setup more carefully. We consider a spin (boson) system with a local tensor product Hilbert space $\mathcal{H} = \otimes_i \mathcal{H}_i$ where $\mathcal{H}_i$ is the local Hilbert space at unit cell i. The system is put on a periodic ring with L unit cells so $i \in \{1, 2...L\}$. In each unit cell the Hilbert space $\mathcal{H}_i$ is q-dimensional (q does not depend on i), with a basis labeled by $\{|a_i\rangle_i\}$ ($a_i \in \{0, 1...q-1\}$). The translation symmetry is implemented by a unitary operator that is uniquely defined through its action on the tensor product basis

$$\begin{aligned} T: \quad & |a_1\rangle_1 \otimes |a_2\rangle_2 \otimes ...|a_{L-1}\rangle_{L-1} \otimes |a_L\rangle_L \\ & \longrightarrow |a_L\rangle_1 \otimes |a_1\rangle_2 \otimes ...|a_{L-2}\rangle_{L-1} \otimes |a_{L-1}\rangle_L. \end{aligned} \tag{4.1}$$

Under this definition of translation symmetry (which is the usual definition), we have[2] $T^L = 1$ and any translational-symmetric product state $|\varphi\rangle^{\otimes L}$ has trivial lattice momentum $e^{iP} = 1$.

Now consider a SRE state $|\Psi_{P(L)}\rangle$ with momentum $P(L)$. By SRE we mean that there is a quantum circuit U with depth $\xi \ll L$ that sends $|\Psi_{P(L)}\rangle$ to the product state $|\mathbf{0}\rangle \equiv |0\rangle^{\otimes L}$ (we do not assume U to commute with translation). The depth ξ will be roughly the correlation length of $|\Psi_{P(L)}\rangle$. Our task is to prove that $P(L) = 0 \mod 2\pi$ as long as $\xi \ll L$. Notice that this statement is in fact stronger than that for FD circuit which requires $\xi \sim O(1)$ as $L \to \infty$. For example, our result holds even if $\xi \sim \text{PolyLog}(L)$, which is relevant if we want the quantum circuit to simulate an adiabatic evolution more accurately [123]. Our result is also applicable if the existence of U requires extra ancilla degrees of freedom (DOF) that enlarges the onsite Hilbert space to $\tilde{\mathcal{H}}_i$ with dimension $\tilde{q} > q$ (for example see Ref. [77]), since ancilla DOFs by definition come in product states and therefore cannot change the momentum.

The proof will be split into two steps where in *Step 1* we first prove that the momentum is trivial for all $L = mn$ where $m, n \in \mathbb{Z}^+$ are mutually coprime satisfying $m, n \gg \xi$. In *Step 2* we use the results of *Step 1* to show that this may be extended to all other lengths.

Step 1: A key ingredient of the proof is to recognize that the entanglement structure of the SRE state $|\Psi_{P(L)}\rangle$ on system size $L = mn$, where $m, n \in \mathbb{Z}^+$ and $n \gg \xi$, is adiabatically connected to that of m identical unentangled length n SRE systems. The existence of such an adiabatic deformation, which is of a similar flavour to those presented in Refs. [320] and [147], is due to the finite correlation length of SRE systems, and will be explained in the following paragraph.

Take the SRE state $|\Psi_{P(L)}\rangle$ placed on a periodic chain of length $L = mn$ with $m, n \in \mathbb{Z}^+$ and $n \gg \xi$. Let us try to decouple this system at some point (say between site i and $i+1$) via an adiabatic evolution, creating an 'open' chain. To show that such a decoupling cut exists, we use the fact that SRE states always have a FD quantum circuit U that sends the ground state to the $|\mathbf{0}\rangle \equiv |0\rangle^{\otimes L}$ product state (see Fig. 4.1(a)). The appropriate cut is then created by modifying this circuit to form a new lightcone-like FD quantum circuit $\tilde{U}$ with all unitaries outside the 'lightcone', i.e. those that do not affect the transformation that sends the two sites i and $i+1$ to $|0\rangle$, set to identity (see Fig. 4.1(b)). Such a modified circuit would span $\sim \xi$ qudits on either side of the cut and by construction takes the two sites on

[2] Importantly, we are not dealing with translation under twisted boundary condition, in which case $T^L = g$ for some global symmetry g. Many of our conclusions in this work need to be rephrased or reexamined for such twisted translations.

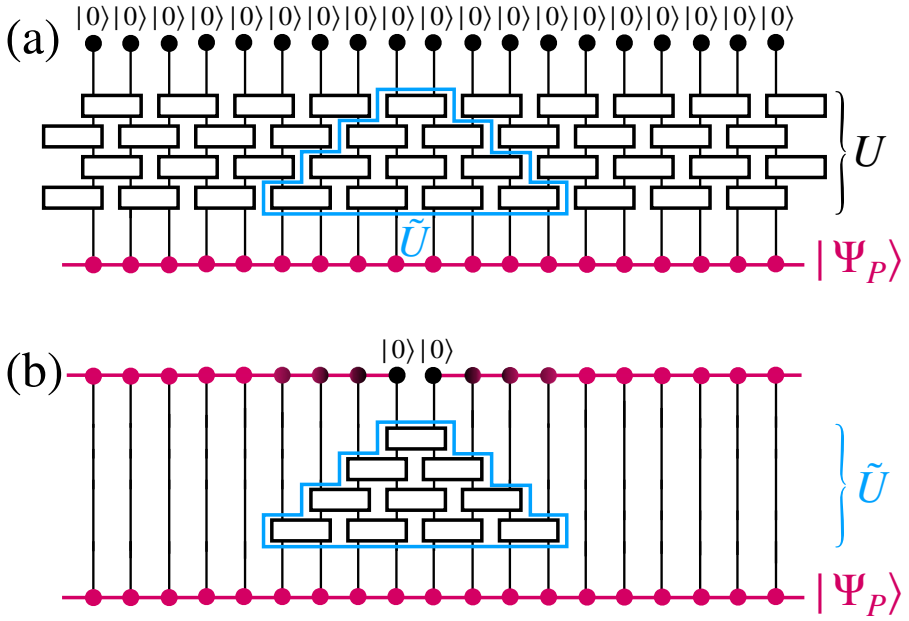

Figure 4.1: (Color online) Depiction of finite-depth quantum circuits applied on $|\Psi_P\rangle$. Here qudits are depicted as solid circles while unitaries are depicted as rectangles. (a) A SRE state $|\Psi_P\rangle$ is always connected to the $|\mathbf{0}\rangle$ trivial state via a FD quantum circuit U. From U a lightcone-like 'adiabatic cut' $\tilde{U}$ can be created (framed in blue). (b) $\tilde{U}$ connects $|\Psi_P\rangle$ to a state that is completely decoupled across the cut.

either side of the cut to $|0\rangle$, thus completely removing any entanglements across the link[3]. Let us concretely take $\tilde{U}^{[0]}$ to denote the appropriate lightcone cut between the last and first qudit (recall that we are on a ring), and define the shifted adiabatic cut between the $x-1$ and xth qudits to be $\tilde{U}^{[x]} \equiv T^x \tilde{U}^{[0]} T^{-x}$. If the ground state is translation-symmetric we have $\tilde{U}^{[x]}|\Psi_{P(L)}\rangle = e^{-ixP(L)} T^x \tilde{U}^{[0]}|\Psi_{P(L)}\rangle$ so we see that $\tilde{U}^{[x]}$ performs the same cut (up to a phase factor) at any link. By construction this means that the local density matrices of a region surrounding the cut obeys $\rho_{lr} = \rho_l \otimes |00\rangle\langle 00| \otimes \rho_r$, where the left (right) region to the cut is denoted l (r), which in turn implies that the operations $\tilde{U}^{[x]}$ disentangles the system along that cut.

The cutting procedure may be simultaneously applied to two separate links, as long as they are separated by a distance much greater than the correlation length. With this in

[3]This can be better understood in reverse: consider the state constructed by $\tilde{U}U^\dagger|\mathbf{0}\rangle$ $(= \tilde{U}|\Psi_{P(L)}\rangle)$ which never directly couples qudits on either side of the cut. Thus $\tilde{U}$ can be understood as completely removing the entanglement across the applied link.

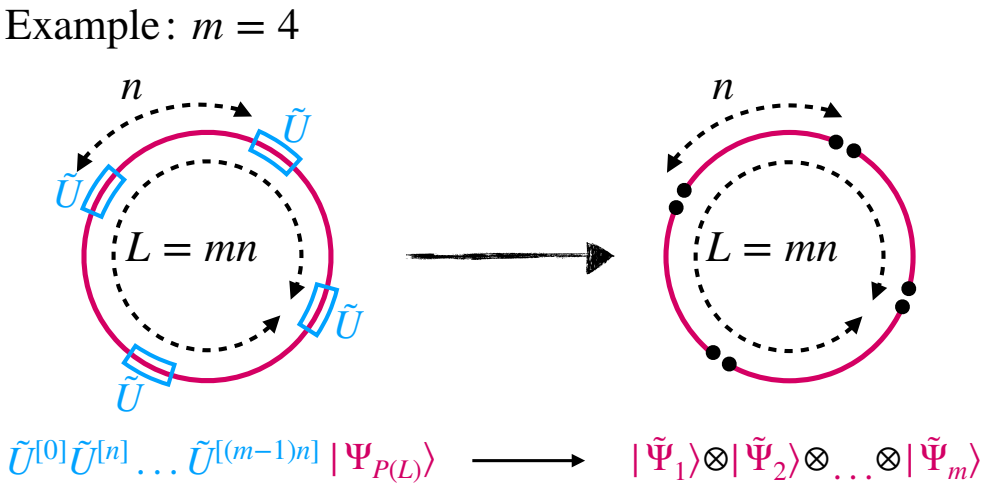

Figure 4.2: (Color online) Illustration of the adiabatic cutting procedure on a periodic length $L = mn$ chain. Here we take $m = 4$ example to demonstrate how four identical cuts, applied by $\tilde{U}$ (blue rectangle) at every nth link, on a length $L = 4n$ state $|\Psi_{P(L)}\rangle$ (purple circle) produces four decoupled length n SRE states.

mind, let us identically apply the cut on an $L = mn$ length system with a cut after every nth qudit, as depicted in Fig. 4.2, via the FD quantum circuit $\tilde{U}^{[0]}\tilde{U}^{[n]}...\tilde{U}^{[(m-1)n]}$. Since the adiabatic deformation fully disentangles the system across the cuts, the resulting state should take the form $|\tilde{\Psi}_1\rangle \otimes |\tilde{\Psi}_2\rangle \otimes ...|\tilde{\Psi}_m\rangle$ where each $|\tilde{\Psi}_i\rangle$ is an n-block SRE state.

Now let us examine the symmetries of this resultant system. The original $\mathbb{Z}_{mn}$ translation symmetry, generated by operator T, of the original system is broken by the adiabatic deformation. However the $\mathbb{Z}_m$ translation symmetry subgroup, generated by operator T^n, is preserved since by construction identical cuts occurs at every nth junction. This immediately implies that all the n-block states are identical $|\tilde{\Psi}_i\rangle = |\tilde{\Psi}\rangle$ and the total state after the cut is simply $|\tilde{\Psi}\rangle^{\otimes m}$. Thus we know that the original $\mathbb{Z}_m$ quantum number is the same as the final one which must be trivial since we are dealing with an n-block product state $|\tilde{\Psi}\rangle^{\otimes m}$. This implies

$$nP(L) = 0 \mod 2\pi \quad , \tag{4.2}$$

$\forall L = mn$ with $m, n \in \mathbb{Z}^+$ and $n \gg \xi$.

Using this relation on a general system length $L = p_1^{q_1} p_2^{q_2} ... p_d^{q_d}$ (here we are using prime

factorisation notation) we arrive at the condition

$$P(L) = 0 \mod \frac{2\pi}{p_1^{r_1} p_2^{r_2} ... p_d^{r_d}} \quad , \tag{4.3}$$

$\forall r_i \in \{1, ..., q_i\}$ such that $p_1^{r_1} p_2^{r_2} ... p_d^{r_d} \gg \xi$. If L factorises into at least two mutually coprime numbers m, n with $m, n \gg \xi$ then these conditions can only be satisfied if

$$P(L) = 0 \mod 2\pi \quad , \tag{4.4}$$

which is satisfied for almost all large enough L.

Step 2: There are a sparse set of cases for which *Step 1* does not enforce trivial momentum, the most notable case being when $\tilde{L} = p^q$ with p prime and $q \in \mathbb{Z}^+$. Factorisations such as $\tilde{L} = p_1^{q_1} p_2$ are also not covered if $p_1^{q_1} \not\gg \xi$.

To show that these cases also possess trivial momentum, once again take a SRE state $|\Psi_{P(L)}\rangle$ on a general length L system with momentum $P(L) \mod 2\pi$. By the definition of a SRE state, there exists a FD quantum circuit V_L such that $|\Psi_{P(L)}\rangle = V_L|\mathbf{0}\rangle$. This circuit obeys $TV_L T^\dagger|\mathbf{0}\rangle = e^{iP(L)} V_L|\mathbf{0}\rangle$, meaning that it boosts the trivial momentum of the $|\mathbf{0}\rangle$ state by $P(L) \mod 2\pi$. Consider the composition of a circuit

$$\left(TV_L^\dagger T^\dagger\right) V_L|\mathbf{0}\rangle = e^{-iP(L)}|\mathbf{0}\rangle \quad . \tag{4.5}$$

As may be understood via the causality structure the phase $e^{-iP(L)}$ will come piecewise from lightcone circuits. Let us understand this in detail: split $\tilde{V}_L \equiv TV_L^\dagger T^\dagger V_L$ into a lightcone circuit $\tilde{V}_{L,1}$ and reverse lightcone circuit $\tilde{V}_{L,2}$ such that $\tilde{V}_L = \tilde{V}_{L,1}\tilde{V}_{L,2}$, as depicted in Fig. 4.3. The causal structure of the light cone guarantees that a gate U_1 in $\tilde{V}_{L,1}$ and a gate U_2 in $\tilde{V}_{L,1}$ must commute if U_2 appears in a layer after U_1, which then allows for the decomposition $\tilde{V}_L = \tilde{V}_{L,1}\tilde{V}_{L,2}$. Although the exact form of this decomposition is quite malleable, for concreteness let us define $\tilde{V}_{L,1}$ to be constructed causally such that the 1st (lowest) layer consists of a single 2-qudit gate (as seen in Fig. 4.3). $\tilde{V}_{L,1}$ will have support over qudits in the range $[L - \eta, L]$, where by the SRE nature $\eta \ll L$. Due to Eq. 4.5 we see that

$$\tilde{V}_{L,2}|\mathbf{0}\rangle = |0...0\rangle^{[1,L-\eta-1]} \otimes |\alpha\rangle^{[L-\eta,L]} \tag{4.6}$$

for some $|\alpha\rangle$. By construction, we have

$$\tilde{V}_{L,1}|\alpha\rangle = e^{-iP(L)}|0...0\rangle^{[L-\eta,L]} \quad , \tag{4.7}$$

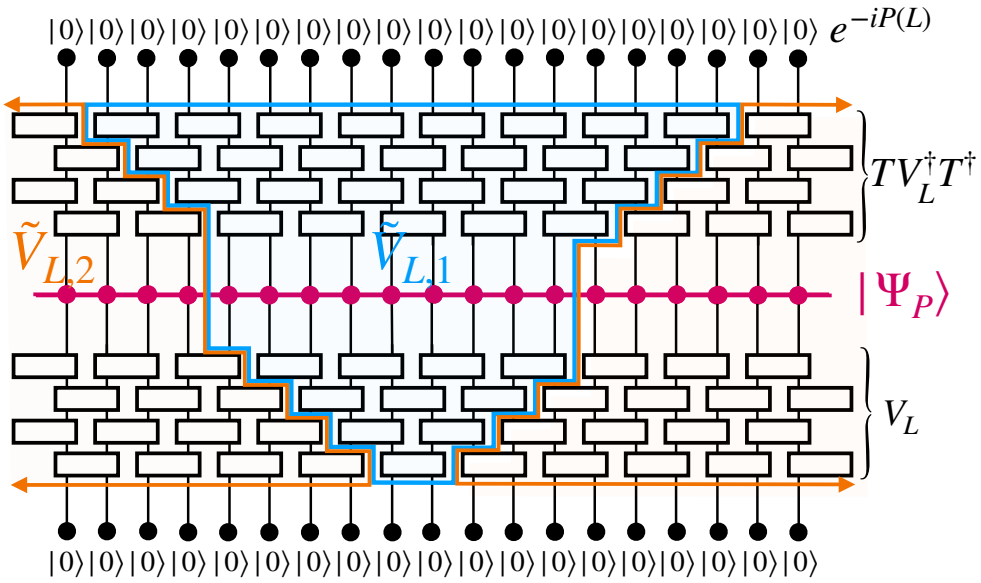

Figure 4.3: (Color online) Illustration of splitting $TV_L^\dagger T^\dagger V_L = \tilde{V}_{L,1}\tilde{V}_{L,2}$ with $\tilde{V}_{L,1}\tilde{V}_{L,2}|\mathbf{0}\rangle = e^{-iP(L)}|\mathbf{0}\rangle$. Here we have taken a snapshot of the circuit to focus on $\tilde{V}_{L,1}$ (framed in blue), however the support of $\tilde{V}_{L,1}$ (in the depicted example 16 qudits) is actually much smaller than the system length. Recall that the circuit is periodic such that the orange arrows, corresponding to components of $\tilde{V}_{L,2}$ (framed in orange), eventually connect on the far side of the ring.

such that we satisfy Eq. 4.5.

Now we will extend the circuit V_L from length L to nL for some $n \in \mathbb{Z}^+$, where n, L are coprime and $\gg \xi$, and denote this extended circuit V_{nL}. To do this we simply unstitch the circuit V_L at some link and reconnect the ends of n consecutive copies of this unstitched V_L circuit to create a FD quantum circuit V_{nL}. Let us see what happens to $\tilde{V}_{nL} \equiv TV_{nL}^\dagger T^\dagger V_{nL}$ by once again splitting the circuit into two $\tilde{V}_{nL} = \tilde{V}_{nL,1}\tilde{V}_{nL,2}$, where $\tilde{V}_{nL,k} = \prod_{j=0}^{n-1} T^{jL}\tilde{V}_{L,k}(T^\dagger)^{jL}$ with $k \in \{1,2\}$. By construction and due to the SRE nature of state construction

$$\tilde{V}_{nL,2}|\mathbf{0}\rangle^{\otimes n} = \left(|0...0\rangle^{[1,L-\eta-1]} \otimes |\alpha\rangle^{[L-\eta,L]}\right)^{\otimes n} \quad . \tag{4.8}$$

However, by Eq. 4.7, we have

$$\tilde{V}_{nL,1}\tilde{V}_{nL,2}|\mathbf{0}\rangle^{\otimes n} = e^{-inP(L)}|\mathbf{0}\rangle^{\otimes n} \quad , \tag{4.9}$$

so this implies

$$TV_{nL}T^\dagger|\mathbf{0}\rangle^{\otimes n} = e^{inP(L)}V_{nL}|\mathbf{0}\rangle^{\otimes n} \quad , \tag{4.10}$$

which means that V_{nL} boosts the momentum of $|\mathbf{0}\rangle$ on a length nL system to a state with momentum $P(nL) = nP(L) \mod 2\pi$. In *Step 1* we showed that $P(nL) = 0 \mod 2\pi$, so this implies $nP(L) = 0 \mod 2\pi$. Since this holds for two mutually coprime values of n, one concludes that 1d SRE translation-symmetric states have $P(L) = 0 \mod 2\pi$ for all $L \gg \xi$.

4.2.2 Higher-dimensional extension

Our result can be extended to higher dimensions. Consider a d-dimensional lattice system and a state $|\Psi\rangle$ that has nontrivial momentum P along, say, $\hat{x}$ direction. We can view the state as a 1d state along the $\hat{x}$ axis, with an enlarged Hilbert space per unit cell (generally exponentially large in $\prod_i L_i$ with i denoting the transverse directions). A finite-depth quantum circuit of the d-dimensional system will also be a finite-depth quantum circuit when viewed as a 1d circuit along the $\hat{x}$-direction (a proof and a somewhat subtle example are presented in Appendix I; the converse is not true but that does not concern us here). This immediately implies that a SRE state on the d-dimensional system must also be SRE when viewed as a 1d state along $\hat{x}$. What we proved in Sec. 4.2.1 thus implies that the nontrivial momentum state $|\Psi\rangle$ must be long-range entangled. In particular, imposing locality in the transverse directions will only further restrict possible FD circuit, and will certainly not lead to possibilities beyond the 1d proof. This completes the proof of Theorem 1. ■

4.2.3 Fermion systems

It is not difficult to generalize our Theorem 1 to fermionic system. The only subtlety is that the usual definition of translation symmetry in fermion systems has an extra $\mathbb{Z}_2$ sign structure compared to the naive implementation in Eq. 4.1. Instead of specifying the sign structure in the tensor product basis as in Eq. 4.1, it is more convenient to define translation operator through $Tc_{i,\alpha}T^{-1} = c_{i+1,\alpha}$ where $c_{i,\alpha}$ is a fermion operator in unit cell i with some internal index α, and $c_{L+1,\alpha} = c_{1,\alpha}$. This operator relation, together with $T|\mathbf{0}\rangle = |\mathbf{0}\rangle$ for the fermion vacuum, uniquely determines the action of T on any state. Now consider a product state $|\varphi\rangle^{\otimes L}$, it is easy to verify that the momentum is $e^{iP} = 1$ for odd L and $e^{iP} = \pm 1$ for even L, where the sign is the fermion parity on each site $\langle\varphi|(-1)^{\sum_\alpha c_\alpha^\dagger c_\alpha}|\varphi\rangle$. We can then go through the proof in Sec. 4.2, but now with fermion parity preserving FD quantum circuits, and conclude the following:

Theorem 2. *Any short-range entangled translation eigenstate $|\Psi\rangle$ in a lattice fermion system must have momentum (say in the x-direction) $e^{iP_x} = 1$ if L_x is odd, and $e^{iP_x} = \pm 1$ if L_x is even. States violating this condition must in turn be long-range entangled.*

The details of the proof are presented in Appendix J.

Using the same proof technique, we can extend the above result further in various directions. We mention two such extensions without going into the details: (1) for L_x even, the option of $e^{iP_x} = -1$ is possible for a SRE state only if V/L_x is odd ($V = L_x L_y ...$ being the volume); (2) if the total fermion parity is odd in a system with even V, then any translation eigenstate must be LRE.

4.3 Consequences

One of the beauties of Theorem 1 lies in the non-trivial consequences that easily follow. For this section, it is useful to introduce an alternative, but equivalent, formulation of Theorem 1

Theorem 1 (Equivalent)**.** *If there exists a finite-depth local unitary that boosts a state's momentum to a different value (mod 2π), then the state is necessarily long-range entangled.*

The equivalence of this new formulation with the one introduced in Sec. 4.1 can be understood as follows: if all translation-symmetric SRE states possess trivial momentum then non-trivial momentum states must be LRE. Thus if there exists a finite-depth local unitary that can boost a state's momentum to a different value then at least one of either the original or final state possesses non-trivial momentum and must be LRE. The other state is connected to the LRE state via a finite-depth local unitary and thus must also be LRE. The converse follows by contradiction: assume there exists a SRE state that has non-trivial momentum. Such a state (by definition of SRE) is connected via a FD local unitary to the translation-symmetric direct-product state $|\alpha\rangle^{\otimes L}$ which in turn has trivial momentum. Since there now exists a FD local unitary that boosts the momentum to a different value, this implies that the original state was LRE which leads to the contradiction.

This equivalent formulation allows for a direct test for long-range entanglement that we will demonstrate on known and previously unknown LSM theories, and topological orders. In the following discussions we will mostly focus on spin (boson) systems for simplicity, but the results can be generalized quite readily to fermion systems as well.

4.3.1 LSMOH constraints

The original Lieb-Schultz-Mattis (LSM) theory [189] along with the extensions by Oshikawa [263] and Hastings [132], collectively referred to as LSMOH, and their descendants are powerful tools for understanding the low-energy nature of lattice systems. In one of its most potent forms the theorem states that systems with $U(1)$ and translational symmetry that have non-commensurate $U(1)$ charge filling must be 'exotic', meaning that they cannot be SRE states. Since the conception of the original LSM theory the field has flourished rapidly with many extensions that impose similar simple constraints based on symmetry [244, 362, 273, 203, 202, 392, 66], and connections to various fields of physics such as symmetry-protected topological (SPT) order and t'Hooft anomaly in quantum field theory [68, 156, 70, 228, 79, 394]. These sort of constraints also have immediate experimental consequences, as they provide general constraints in determining candidate materials of exotic states such as quantum spin liquids [14]. Thus, unsurprisingly, there has been a lot of interest in generating more LSMOH-like theorems that provide simple rules to find exotic states. In the following section we provide simple proofs of some known and previously unknown LSMOH theorems.

The first example we consider is the aforementioned non-commensurate 1d $U(1) \times T$ LSM (T denotes the translation symmetry). In this case there exists a local unitary momentum boost that is the large gauge transformation $U = e^{i\frac{2\pi}{L}\sum x\hat{n}_x}$, where $\hat{n}_x$ is the local number operator at x. Notice that this transformation is an on-site phase transformation and thus a FD quantum circuit of depth 1. The commutation relation with translation is $TUT^\dagger = e^{i2\pi\frac{\hat{N}}{L}}U$ ($\hat{N}$ being the total charge) which means that for non-commensurate filling $\frac{\hat{N}}{L} \notin \mathbb{Z}$, we may always boost the momentum by a non-trivial value $2\pi\frac{\hat{N}}{L}$. Via the equivalent formulation of Theorem 1, this immediately implies that non-commensurate filling leads to a LRE state. This observation may be summarised as

Corollary 2.1. ($U(1) \times T$ LSM) A 1d translation and $U(1)$ symmetric state that possesses non-commensurate $U(1)$ charge filling must be long-range entangled.

The standard LSM theorem follows from this statement since we may now apply it to a *ground* state of a 1d translation and $U(1)$ symmetric local spin Hamiltonian to show that the state must be either gapless or a spontaneously symmetry-broken cat state. Notice that, strictly speaking, the statement we proved differs slightly from the standard LSM theorem, in that we did not directly prove the vanishing of the energy gap. Rather we showed that any simultaneous eigenstate of translation and $\hat{N}$ such that $\langle\hat{N}\rangle/L \notin \mathbb{Z}$ must be LRE. In principle we do not even need to assume the parent Hamiltonian to be translation or $U(1)$ symmetric, just that the state itself be translation and $U(1)$ symmetric. In fact the

statement encompasses all states, not just the ground state, which is perhaps unsurprising since LRE is fundamentally a property of a state and not the Hamiltonian.

The higher-dimensional $U(1) \times T$ LSMOH theorem may be proved following the same logic if $\langle \hat{N} \rangle / L_i \notin \mathbb{Z}$ for some direction i (similar to what was done in Ref. [263]). For generic values of L_i the above condition may not hold, and more elaborate arguments are needed (for example see Ref. [393]) which we will not discuss here.

Our proof of the LSM theorem has an appealing feature compared to the classic proof [189]: we did not need to show that the state $|\Omega'\rangle = U|\Omega\rangle$ had excitation energy $\sim O(1/L)$ (relative to the ground state $|\Omega\rangle$); rather it suffices for us to show that $|\Omega'\rangle$ has a different lattice momentum compared to $|\Omega\rangle$, which is enough to establish the LRE nature of $|\Omega\rangle$. Next we shall use this simplifying feature to generalize the $U(1) \times T$ LSM theorem to a new constraint involving only discrete $\mathbb{Z}_n \times T$ symmetries.

Let us consider a spin chain (1d) with translation symmetry and an onsite $\mathbb{Z}_n$ symmetry generated by $Z \equiv \otimes_i Z_i$ ($Z_i^n = 1$). We consider the case when the system size $L = nM$ for some $M \in \mathbb{N}$, and study simultaneous eigenstates of the translation and $\mathbb{Z}_n$ symmetries. If such a state is an unentangled product state $\otimes_i |\varphi\rangle_i$, then by definition $Z = 1$ when acting on this state, namely the state carries trivial $\mathbb{Z}_n$ charge. This turns out to be true for any symmetric SRE state, which we now prove. Suppose a translation eigenstate $|\Psi\rangle$ has $Z|\Psi_P\rangle = e^{i2\pi Q/n}|\Psi\rangle$ for some $Q \neq 0 \pmod n$. We can construct a local unitary which is an $\mathbb{Z}_n$-analogue of the large gauge transform

$$U = \otimes_i Z_i^i, \tag{4.11}$$

where i is the unit cell index. For system size $L = nM$ one can verify that $TUT^{-1}U^\dagger = Z^\dagger$. This means that the momentum of the twisted state $U|\Psi\rangle$ will differ from that of the untwisted $|\Psi\rangle$ by $\langle\Psi|Z^\dagger|\Psi\rangle = e^{-i2\pi Q/n} \neq 1$. By the equivalent form of Theorem 1 $|\Psi\rangle$ must be LRE. We therefore have

Corollary 2.2. ($\mathbb{Z}_n \times T$ LSM) *A 1d translation and $\mathbb{Z}_n$ symmetric ground state that possesses non-trivial $\mathbb{Z}_n$ charge on system lengths $L = nM$ for some $M \in \mathbb{N}$ cannot be short-range entangled, and thus is either gapless or spontaneously symmetry-broken cat state.*

The above statement also generalizes to higher dimensions if $L_i = nM$ for some direction i. For systems with $U(1)$ symmetry, we can choose to consider a Z_L subgroup of the $U(1)$, and the above $\mathbb{Z}_n \times T$ LSM theorem leads to the familiar $U(1) \times T$ LSMOH theorem.

The two LSM-type theorems discussed so far, together with our Theorem 1, can all be viewed as "filling-type" LSM theorems, in the sense that these theorems constraint a

symmetric many-body state $|\Psi\rangle$ to be LRE when $|\Psi\rangle$ carries certain non-trivial quantum numbers, such as lattice momentum $e^{iP} \neq 1$, total $U(1)$ charge $Q \notin L\mathbb{Z}$ or total $\mathbb{Z}_n$ charge $Q \notin L\mathbb{Z}/n\mathbb{Z}$.

There is another type of LSM theorems that involve projective symmetry representations in the onsite Hilbert space, the most familiar example being the spin-1/2 chain with $SO(3)$ symmetry. Our Theorem 1 can also be used to understand some (but possibly not all) of the projective symmetry types of LSM. Here we discuss one illuminating example with onsite $\mathbb{Z}_2 \times \mathbb{Z}_2$ symmetry in one dimension [62, 259, 258], such that the generators of the two $\mathbb{Z}_2$ group anti-commutes when acting on the local Hilbert space: $X_i Z_i = -Z_i X_i$ (this can simply be represented by the Pauli matrices σ_x, σ_z). Now set the length $L = 2N$ with odd N, and consider the three local unitaries $U_x = (\mathbb{1} \otimes \sigma_x)^{\otimes N}$, $U_z = (\mathbb{1} \otimes \sigma_z)^{\otimes N}$, and $U_{xz} = (\sigma_x \otimes \sigma_z)^{\otimes N}$. One can verify the commutation relations $TU_xT^\dagger = (-1)^{Q_x} U_x$, $TU_zT^\dagger = (-1)^{Q_z} U_z$, and $TU_{xz}T^\dagger = (-1)^{N+Q_x+Q_z} U_{xz}$. These commutation relations imply that the momentum of any symmetric state $|\Psi\rangle$ will be boosted by $\Delta P = \pi$ by at least one of the three unitaries, therefore $|\Psi\rangle$ must be LRE by Theorem 1.

4.3.2 Topological orders: weak CDW

We now consider an intrinsic (bosonic) topological order on a d-dimensional torus. By definition there will be multiple degenerate ground states, separated from the excitation continuum by a finite energy gap. If one of the ground states $|\Psi_a\rangle$ has a non-trivial momentum, say along the $\hat{x}$ direction, then according to Theorem 1 this state should be LRE even when viewed as a one-dimensional system in $\hat{x}$ direction (with the other dimensions $y, z...$ viewed as internal indices). Since there is no intrinsic topological order in one dimension, the only mechanism for the LRE ground state is spontaneous symmetry breaking. The lattice translation symmetry is the only relevant symmetry here – all the other symmetries can be explicitly broken without affecting the LRE nature of $|\Psi_a\rangle$, since the state will still have nontrivial momentum. Therefore $|\Psi_a\rangle$ must be a cat state that spontaneously breaks the $\hat{x}$-translation symmetry [4], also known as a charge density wave (CDW) state [118]. Furthermore, any other ground state $|\Psi_{b\neq a}\rangle$ can be obtained from $|\Psi_a\rangle$ by a unitary operator U_{ba} that is non-local in the directions transverse to $\hat{x}$, but crucially is local in $\hat{x}$ – for example in two dimensions U_{ba} corresponds to moving an anyon around the transverse cycle. By Theorem 1 we then conclude that $|\Psi_b\rangle$ is also a CDW in $\hat{x}$.

[4] Another way to see this is to note that a cat state is composed of individual SRE states. Since we have proven that translation symmetric SRE states possess trivial momentum, it follows that the cat state may only achieve non-trivial momentum when the individual SRE states break translation symmetry, i.e. the cat state must correspond to translation symmetry breaking.

Perhaps the most familiar example of the above statement is the fractional quantum Hall effect. It is known that the $1/k$ Laughlin state on the torus is adiabatically connected to a quasi-one-dimensional CDW state in the Landau gauge, also known as the Tao-Thouless state [331, 26]. For example for $k = 2$ the Tao-Thouless state with momentum $P = \pi n$, in the Landau orbit occupation number basis, reads

$$|101010...\rangle + e^{i\pi n}|010101...\rangle. \tag{4.12}$$

The CDW nature of the ground states is perfectly compatible with the topological order being a symmetric state, since there is no *local* CDW order parameters with nonzero expectation value. The CDW order parameter in this case is non-local in the directions transverse to $\hat{x}$. For example, in two-dimensions the CDW order parameter is defined on a large loop that wraps around the cycle transverse to $\hat{x}$. This phenomenon is dubbed *weak* symmetry breaking in Ref. [164]. The weak spontaneous symmetry breaking requires a certain degeneracy for the ground state. This degeneracy is naturally accommodated by the ground state manifold of the topological order. For example for the above Tao-Thouless state at $k = 2$ the CDW order requires a two-fold ground state degeneracy, which is nothing but the two degenerate Laughlin states on torus.

The above results can be summarized as follows:

Corollary 2.3. *If a ground state of a gapped topological order on a d-dimensional torus ($d > 1$) has a non-trivial momentum in $\hat{x}$, then any ground state of this topological order must weakly break translation symmetry in $\hat{x}$.*

A further example of these results, alongside the effects of anyon condensation, applied upon the $\mathbb{Z}_2$ topologically ordered Toric code is demonstrated in the Appendix K. The above result also implies the following constraint on possible momentum carried by a topologically ordered ground state:

Corollary 2.4. *If a gapped topological order has q degenerate ground states on torus, then the momentum of any ground state in any direction is quantized:*

$$P_i^{(a)} = 2\pi N_i^{(a)}/q, \tag{4.13}$$

where $N_i^{(a)}$ is an integer depending on the ground state (labeled by a) and direction i.

This is simply because for other values of the momentum, the ground state degeneracy required by the spontaneous translation-symmetry-breaking order will be larger than the

ground state degeneracy from the topological order, which results in an inconsistency. An immediate consequence of the above corollary is that invertible topological orders (higher-dimensional states that are LRE by our definition but has only a unique gapped ground state on closed manifolds), such as the chiral E_8 state[164], cannot have nontrivial momentum on a closed manifolds since $q = 1$.

The above statement immediately implies that the momenta of topological ordered ground states are robust under adiabatic deformations, as long as the gap remains open and translation symmetries remain unbroken. For the Tao-Thouless states this conclusion can also be drawn from the LSM theorem if the $U(1)$ symmetry is unbroken. Our result implies that the momenta of Laughlin-Tao-Thouless states are robustly quantized even if the $U(1)$ symmetry is explicitly broken.

4.3.3 Crystalline symmetry-protected topological phases

There has been growing interest and successes in understanding the symmetry-protected topological (SPT) phases associated with crystalline symmetries [320, 336, 147, 310, 323, 78]. When the protecting symmetry involves lattice translation, a crucial "smoothness" assumption [336, 147] is used. Essentially one assumes that for such SPT phases the inter unit-cell entanglement can be adiabatically removed, possibly with the help of additional ancilla degrees of freedom. This allows one to formally "gauge" the translation symmetry [336] and build crystalline topological phases out of lower-dimensional states [147, 323, 78].

Our result, namely Theorem 1, serves as a non-trivial check on the smoothness assumption in the following sense. If there were SRE states with non-trivial lattice momenta, such states would have irremovable inter-unit cell entanglement since unentangled states cannot have non-trivial momentum. Equivalently the correlation length ξ cannot be tuned to be smaller than the unit cell size a. In fact, if such states exist, they would by definition be non-trivial SPT states protected solely by translation symmetry – such SPT states would be beyond all the recent classifications.

We note that our result is a necessary condition, but not a proof, for the smoothness assumption, as there may be other ways to violate the assumption without involving a ground state momentum. It will be interesting to see if the arguments used in this work can be extended to fully justify the smoothness assumption.

4.4 Discussions

In this paper we have shown that a quantum many-body state with non-trivial lattice momentum is necessarily long-range entangled, hence establishing a simple yet intriguing connection between two extremely familiar concepts in physics: translation symmetry and quantum entanglement. Many directions can be further explored, which we briefly comment on in the remainder of this Section.

One important aspect that we have so far skipped over is that LSM theory is in fact intimately connected to quantum anomalies [68, 156, 70, 228, 79, 394]. This is natural since they both provide UV conditions that constraint the low-energy behaviours. For the "projective symmetry" type of LSM theorems, this connection has been precisely established and it is known that such LSM constraints correspond to certain discrete (quantized) t'Hooft anomalies. For the "partial filling" type of LSM such as the familiar $U(1) \times T$ constraint, however, the connection has been discussed [322, 80, 349, 105] but has yet to be fully developed. As we discussed in Sec. 4.3.1, our main result (Theorem 1) can be viewed as a "partial filling" type of LSM that only involves translation symmetry. It is therefore natural to ask whether Theorem 1 can be understood from an anomaly perspective. To achieve this goal, it is clear that the standard quantized t'Hooft anomaly is insufficient (a point which was also emphasized in Ref. [80] for the $U(1) \times T$ LSM) – for example, the toric code discussed in Appendix K has no t'Hooft anomaly since one can condense the e particle to obtain a trivial symmetric state. One would therefore need to expand the notion of anomaly to accommodate the partial-filling type of LSM constraints including the one discussed in this work, possibly along the line of the "unquantized anomaly" discussed in Ref. [105]. We leave this aspect to future work.

Another powerful consequence of the traditional $U(1) \times T$ LSM theorem is on the stability of the LRE ground states (with partial charge filling) under symmetric perturbations: assuming the charge compressibility is finite (could be zero), then a small perturbation will not change the charge filling discontinuously, so the system remains LRE under small symmetric perturbations (unless the perturbation leads to spontaneous symmetry-breaking like the BCS attraction). It is natural to ask whether the other "partial filling" types of LSM theorems can serve similar purposes. In fact Ref. [105] discussed precisely this point under the notion of "unquantized anomaly". The unquantized anomalies are very similar to Theorem 1 and 2 and Corollary 2.2, except that the key quantity is not the discrete charges (lattice momentum or $\mathbb{Z}_n$ charges) on a specific systems size L, but the charge densities (momentum density or $\mathbb{Z}_n$ charge density). Such discrete charge densities can not be defined for a fixed L, but may be defined for a sequence of systems with $L \to \infty$. Ref. [105] argued that, in the context of Weyl and Dirac semimetals, as long as these discrete charge

densities are well behaved in the $L \to \infty$ limit, the unquantized anomalies will protect the LRE nature of the states under symmetric perturbations. Our work here can be viewed as a rigorous justification of the unquantized anomalies in Ref. [105] on fixed system sizes.

Assuming a well-behaving momentum density in the thermodynamic limit, we can also apply our results to a Fermi liquid with a generic Fermi surface shape, such that the ground state from the filled Fermi sea has a non-vanishing momentum density (this requires breaking of time-reversal, inversion and reflection symmetries). This can be viewed as a non-perturbative explanation for the stability of such low-symmetry Fermi surface, even in the absence of the charge $U(1)$ symmetry. (Recall that perturbatively the stability comes from the fact that the Cooper pairing terms no longer connect opposite points on the Fermi surface).

Another question one may ask is whether a broader group of non-onsite symmetries obey similar charge and entanglement restrictions. It is easy to see that exactly the same constraint holds for glide reflections and screw rotations, since when the system is viewed as 1d there is no difference between glide reflection, screw rotation and translation. It is also easy to see that the constraint does *not* hold for point group symmetries (rotations and reflections), because such symmetries will be onsite at some points in space (the fixed points of point groups). It is therefore important that translation symmetry is *everywhere* non-onsite. The question becomes even more intriguing if we consider more general unitary operators (such as quantum cellular automata [117]).

There are many more natural avenues for further exploration. The interplay between the non-local nature of translation symmetry with crystalline symmetry anomalies is not yet well understood and requires more concrete mathematical grounding such as a rigorous proof of when the smoothness condition is valid. Relatedly it remains to be determined whether translation symmetry may be truly treated as an onsite symmetry and gauged, or whether its non-locality and non-trivial momentum may hinder or require modifications to the usual gauging process. Implications of our results on the "emergibility" of phases may also provide fruitful insights to achievable and unachievable states on the lattice [407, 394]. Our work has shown without a doubt that translation symmetry is many-faceted and plays a crucial role in the entanglement properties of crystalline materials.

Chapter 5

Outlook

In experimental condensed matter physics it is often a challenge to realise the same ideal conditions that their theoretical counterparts may work under. One of the most common deviances from ideal conditions occurs during the growing phase of the crystal in which crystalline defects, such as stacking faults and dislocations, are often inadvertently introduced. Therefore, it is integral to understand how such such defects affect the intrinsic material properties, such as the conductivity, of the system, and perhaps with such understanding comes the possibility to even harness the defect physics in order to create novel phases of matter. Some of our current work in progress [216] includes making a connection between the type-I DSM anomaly and the RF term in cSPT systems [217] and the effect of disclinations in both systems. Here we find that we can create an RF-insulator via a charge-density wave in the DSM case, and draw some fun comparisons of the anomaly terms. We are also exploring the topological filling constraints in the context of topological response terms in upcoming work [107]. This applies to classes of gapless materials protected by non-symmorphic symmetries such as type-II DSMs. In future work we also explore possible no-go theorems of Dirac cones in all dimensions via analysis of the quantum anomalies of single Dirac cones [109].

Topological invariants allow us to detect experimentally-measurable features that are stable to local deformations (sometimes, in the context of symmetries). Many famous topological invariants have been explored in the context of gapped systems, such as the Chern number in Chern insulators, or the index in time-reversal protected topological insulators. More recently, the topology of gapless systems, such as semi-metallic systems, has also gained traction with progress on both quantised quantities, e.g. Euler characteristics of Fermi surfaces, and unquantized quantities such as anomalous Hall conductivity in magnetic Weyl semimetals or electron filling in Fermi liquids. As we have seen in previ-

ous chapters, time-reversal invariant Weyl semimetals possess an unquantized topological invariant that is related to the ground state momentum of the lowest Landau level when a magnetic flux is inserted along the separations of the nodes. Such a momentum invariant can also be present in Fermi surfaces where inversion symmetry is broken. Since these invariants are purely associated to translation symmetry, they are likely generalisable to gapless charge symmetry broken systems such as Bogoliubov Fermi surfaces. If so, do these states posses non-trivial responses to dislocations? Does there exist a Luttinger's theorem for momentum filling instead of charge filling? Relatedly, one may ask whether a continuously tunable momentum filling necessitates strong constraints on the low-energy properties of the system.

Regarding momentum, there are many more questions to be asked: how do we even define momentum or momentum density in the thermodynamic limit? What observable features exist in ground states with non-zero momentum? One may also ask, what happens if we add strong interactions to states that have non-trivial ground state momentum? Can we arrive at even more exotic gapped systems that host unusual topological orders? What is the field theory language required to capture such exotic states that involve momentum? Can the momentum LSM type theorem be generalised to quantum cellular automata (QCA)? QCAs are an effective method to model both quantum computations and quantum simulation of physics such as in periodically-driven Floquet systems. QCA are locality-preserving, meaning that local operators are mapped to local operators, which allows the system to emulate relativistic causality. One intuitive example of a QCA is the translation operator, which displaces each qubit to the next qubit along some direction. This concept may be extended to generalized translations, known as shifts, which in lower dimensions may be completely classified by the GNVW indices. The conjecture is that such shifts will obey a similar theorem to the one proved for the simple translation operator: shift-symmetric quantum many-body states with non-trivial eigenvalues must be long-range entangled, which is desirable for topological order and stability. Additionally, such statements may be applicable to Majorana, para-fermionic, and fractonic systems.

Many fun things remain to be explored, which is really what this journey in physics is about, isn't it? I look forward to what the future brings!

References

[1] D. A. Abanin, S. V. Morozov, L. A. Ponomarenko, R. V. Gorbachev, A. S. Mayorov, M. I. Katsnelson, K. Watanabe, T. Taniguchi, K. S. Novoselov, L. S. Levitov, and A. K. Geim. Giant nonlocality near the dirac point in graphene. *Science*, 332(6027):328–330, 2011.

[2] D. A. Abanin, A. V. Shytov, L. S. Levitov, and B. I. Halperin. Nonlocal charge transport mediated by spin diffusion in the spin hall effect regime. *Phys. Rev. B*, 79:035304, Jan 2009.

[3] Stephen L. Adler. Axial-vector vertex in spinor electrodynamics. *Phys. Rev.*, 177:2426–2438, Jan 1969.

[4] Vivek Aji. Adler-bell-jackiw anomaly in weyl semimetals: Application to pyrochlore iridates. *Phys. Rev. B*, 85:241101, Jun 2012.

[5] Anton Yu. Alekseev, Vadim V. Cheianov, and Jürg Fröhlich. Universality of transport properties in equilibrium, the goldstone theorem, and chiral anomaly. *Phys. Rev. Lett.*, 81:3503–3506, Oct 1998.

[6] Alexander Altland and Dmitry Bagrets. Theory of the strongly disordered weyl semimetal. *Phys. Rev. B*, 93:075113, Feb 2016.

[7] Alexander Altland and Ben D. Simons. *Condensed Matter Field Theory*. Cambridge University Press, New York, second edition, 2010.

[8] Philip W Anderson. Absence of diffusion in certain random lattices. *Physical review*, 109(5):1492, 1958.

[9] A.F Andreev and M.Yu Kagan. Hydrodynamcs of a rotating superfluid liquid. *Zh. Eksp. Teor. Fiz.*, 86:546–557, Feb 1984.

[10] Yasufumi Araki and Kentaro Nomura. Spin textures and spin-wave excitations in doped dirac-weyl semimetals. *Phys. Rev. B*, 93:094438, Mar 2016.

[11] P. N. Argyres and E. N. Adams. Longitudinal magnetoresistance in the quantum limit. *Phys. Rev.*, 104:900–908, Nov 1956.

[12] N. P. Armitage, E. J. Mele, and Ashvin Vishwanath. Weyl and dirac semimetals in three-dimensional solids. *Rev. Mod. Phys.*, 90:015001, Jan 2018.

[13] P Baireuther, J A Hutasoit, J Tworzydåo, and C W J Beenakker. Scattering theory of the chiral magnetic effect in a weyl semimetal: interplay of bulk weyl cones and surface fermi arcs. *New Journal of Physics*, 18(4):045009, 2016.

[14] Leon Balents. Spin liquids in frustrated magnets. *Nature*, 464(7286):199–208, 2010.

[15] Leon Balents, Lorenz Bartosch, Anton Burkov, Subir Sachdev, and Krishnendu Sengupta. Putting competing orders in their place near the mott transition. *Phys. Rev. B*, 71:144508, Apr 2005.

[16] Leon Balents, Matthew P. A. Fisher, and Chetan Nayak. Dual order parameter for the nodal liquid. *Phys. Rev. B*, 60:1654–1667, Jul 1999.

[17] Maissam Barkeshli, Parsa Bonderson, Meng Cheng, and Zhenghan Wang. Symmetry fractionalization, defects, and gauging of topological phases. *Physical Review B*, 100(11), sep 2019.

[18] Yuval Baum, Erez Berg, S. A. Parameswaran, and Ady Stern. Current at a distance and resonant transparency in weyl semimetals. *Phys. Rev. X*, 5:041046, Dec 2015.

[19] G. Bednik, A. A. Zyuzin, and A. A. Burkov. Superconductivity in weyl metals. *Phys. Rev. B*, 92:035153, Jul 2015.

[20] G Bednik, A A Zyuzin, and A A Burkov. Anomalous hall effect in weyl superconductors. *New Journal of Physics*, 18(8):085002, 2016.

[21] Jan Behrends, Jun-Won Rhim, Shang Liu, Adolfo G. Grushin, and Jens H. Bardarson. Nodal-line semimetals from weyl superlattices. *Phys. Rev. B*, 96:245101, Dec 2017.

[22] J. S. Bell and R. Jackiw. A pcac puzzle: $\pi^0 \to \gamma\gamma$ in the $\sigma-$model. *Nuovo Cimento A*, 60:4, 1969.

[23] Ilya Belopolski, Kaustuv Manna, Daniel S. Sanchez, Guoqing Chang, Benedikt Ernst, Jiaxin Yin, Songtian S. Zhang, Tyler Cochran, Nana Shumiya, Hao Zheng, Bahadur Singh, Guang Bian, Daniel Multer, Maksim Litskevich, Xiaoting Zhou, Shin-Ming Huang, Baokai Wang, Tay-Rong Chang, Su-Yang Xu, Arun Bansil, Claudia Felser, Hsin Lin, and M. Zahid Hasan. Discovery of topological weyl fermion lines and drumhead surface states in a room temperature magnet. *Science*, 365(6459):1278–1281, 2019.

[24] Wladimir A. Benalcazar, Tianhe Li, and Taylor L. Hughes. Quantization of fractional corner charge in C_n-symmetric higher-order topological crystalline insulators. *Phys. Rev. B*, 99:245151, Jun 2019.

[25] V. Berezinski. Destruction of long-range order in one-dimensional and two-dimensional systems having a continuous symmetry group i. classical systems. *JETP*, 32:493, 1971.

[26] E. J. Bergholtz and A. Karlhede. Quantum hall system in tao-thouless limit. *Phys. Rev. B*, 77:155308, Apr 2008.

[27] B. A. Bernevig and T. L. Hughes. *Topological insulators and topological superconductors*. Princeton University Press, 2013.

[28] B. Andrei Bernevig, Taylor L. Hughes, and Shou-Cheng Zhang. Quantum spin hall effect and topological phase transition in hgte quantum wells. *Science*, 314(5806):1757–1761, 2006.

[29] Guang Bian, Tay-Rong Chang, Hao Zheng, Saavanth Velury, Su-Yang Xu, Titus Neupert, Ching-Kai Chiu, Shin-Ming Huang, Daniel S. Sanchez, Ilya Belopolski, Nasser Alidoust, Peng-Jen Chen, Guoqing Chang, Arun Bansil, Horng-Tay Jeng, Hsin Lin, and M. Zahid Hasan. Drumhead surface states and topological nodal-line fermions in tltase_2. *Phys. Rev. B*, 93:121113, Mar 2016.

[30] Adel Bilal. Lectures on anomalies. *arXiv*, 2008.

[31] Rudro R. Biswas and Shinsei Ryu. Diffusive transport in weyl semimetals. *Phys. Rev. B*, 89:014205, Jan 2014.

[32] Parsa Bonderson, Chetan Nayak, and Xiao-Liang Qi. A time-reversal invariant topological phase at the surface of a 3d topological insulator. *Journal of Statistical Mechanics: Theory and Experiment*, 2013(09):P09016, sep 2013.

[33] Sergey Borisenko, Quinn Gibson, Danil Evtushinsky, Volodymyr Zabolotnyy, Bernd Büchner, and Robert J. Cava. Experimental realization of a three-dimensional dirac semimetal. *Phys. Rev. Lett.*, 113:027603, Jul 2014.

[34] Matthew Brahlek, Namrata Bansal, Nikesh Koirala, Su-Yang Xu, Madhab Neupane, Chang Liu, M. Zahid Hasan, and Seongshik Oh. Topological-metal to band-insulator transition in $(\mathrm{bi}_{1-x}\mathrm{in}_x)_2\mathrm{se}_3$ thin films. *Phys. Rev. Lett.*, 109:186403, Oct 2012.

[35] A. A. Burkov. Anomalous hall effect in weyl metals. *Phys. Rev. Lett.*, 113:187202, Oct 2014.

[36] A. A. Burkov. Chiral anomaly and diffusive magnetotransport in weyl metals. *Phys. Rev. Lett.*, 113:247203, Dec 2014.

[37] A. A. Burkov. Topological response in ferromagnets. *Phys. Rev. B*, 89:155104, Apr 2014.

[38] A. A. Burkov. Chiral anomaly and transport in weyl metals. *Journal of Physics: Condensed Matter*, 27(11):113201, 2015.

[39] A. A. Burkov. Chiral anomaly without relativity. *Science*, 350(6259):378–379, 2015.

[40] A. A. Burkov. Negative longitudinal magnetoresistance in dirac and weyl metals. *Phys. Rev. B*, 91:245157, Jun 2015.

[41] A. A. Burkov. Topological semimetals. *Nature Materials*, 15:1145 EP –, 10 2016.

[42] A. A. Burkov. Giant planar hall effect in topological metals. *Phys. Rev. B*, 96:041110, Jul 2017.

[43] A. A. Burkov. Mirror anomaly in dirac semimetals. *Phys. Rev. Lett.*, 120:016603, Jan 2018.

[44] A. A. Burkov. Quantum anomalies in nodal line semimetals. *Phys. Rev. B*, 97:165104, Apr 2018.

[45] A. A. Burkov. Weyl Metals. *Annual Review of Condensed Matter Physics*, 9:359, 2018.

[46] A. A. Burkov and Leon Balents. Superfluid-insulator transitions on the triangular lattice. *Phys. Rev. B*, 72:134502, Oct 2005.

[47] A. A. Burkov and Leon Balents. Weyl semimetal in a topological insulator multilayer. *Phys. Rev. Lett.*, 107:127205, Sep 2011.

[48] A. A. Burkov, M. D. Hook, and Leon Balents. Topological nodal semimetals. *Phys. Rev. B*, 84:235126, Dec 2011.

[49] Anton A. Burkov and Yong Baek Kim. F_2 and chiral anomalies in topological dirac semimetals. *Phys. Rev. Lett.*, 117:136602, Sep 2016.

[50] C.G. Callan and J.A. Harvey. Anomalies and fermion zero modes on strings and domain walls. *Nuclear Physics B*, 250(1):427 – 436, 1985.

[51] Cui-Zu Chang, Jinsong Zhang, Xiao Feng, Jie Shen, Zuocheng Zhang, Minghua Guo, Kang Li, Yunbo Ou, Pang Wei, Li-Li Wang, Zhong-Qing Ji, Yang Feng, Shuaihua Ji, Xi Chen, Jinfeng Jia, Xi Dai, Zhong Fang, Shou-Cheng Zhang, Ke He, Yayu Wang, Li Lu, Xu-Cun Ma, and Qi-Kun Xue. Experimental observation of the quantum anomalous hall effect in a magnetic topological insulator. *Science*, 340(6129):167–170, 2013.

[52] Guoqing Chang, Su-Yang Xu, Xiaoting Zhou, Shin-Ming Huang, Bahadur Singh, Baokai Wang, Ilya Belopolski, Jiaxin Yin, Songtian Zhang, Arun Bansil, Hsin Lin, and M. Zahid Hasan. Topological hopf and chain link semimetal states and their application to co_2MnGa. *Phys. Rev. Lett.*, 119:156401, Oct 2017.

[53] Ming-Che Chang and Min-Fong Yang. Chiral magnetic effect in a two-band lattice model of weyl semimetal. *Phys. Rev. B*, 91:115203, Mar 2015.

[54] Jing-Yuan Chen, Jun Ho Son, Chao Wang, and S. Raghu. Exact boson-fermion duality on a 3d euclidean lattice. *Phys. Rev. Lett.*, 120:016602, Jan 2018.

[55] Qi Chen and Gregory A. Fiete. Thermoelectric transport in double-weyl semimetals. *Phys. Rev. B*, 93:155125, Apr 2016.

[56] R. Y. Chen, Z. G. Chen, X.-Y. Song, J. A. Schneeloch, G. D. Gu, F. Wang, and N. L. Wang. Magnetoinfrared spectroscopy of landau levels and zeeman splitting of three-dimensional massless dirac fermions in $zrte_5$. *Phys. Rev. Lett.*, 115:176404, Oct 2015.

[57] R. Y. Chen, S. J. Zhang, J. A. Schneeloch, C. Zhang, Q. Li, G. D. Gu, and N. L. Wang. Optical spectroscopy study of three dimensional Dirac semimetal ZrTe$_5$. *ArXiv e-prints*, May 2015.

[58] Xie Chen, Lukasz Fidkowski, and Ashvin Vishwanath. Symmetry enforced non-abelian topological order at the surface of a topological insulator. *Phys. Rev. B*, 89:165132, Apr 2014.

[59] Xie Chen, Zheng-Cheng Gu, Zheng-Xin Liu, and Xiao-Gang Wen. Symmetry-protected topological orders in interacting bosonic systems. *Science*, 338(6114):1604–1606, 2012.

[60] Xie Chen, Zheng-Cheng Gu, Zheng-Xin Liu, and Xiao-Gang Wen. Symmetry protected topological orders and the group cohomology of their symmetry group. *Phys. Rev. B*, 87:155114, Apr 2013.

[61] Xie Chen, Zheng-Cheng Gu, and Xiao-Gang Wen. Local unitary transformation, long-range quantum entanglement, wave function renormalization, and topological order. *Phys. Rev. B*, 82:155138, Oct 2010.

[62] Xie Chen, Zheng-Cheng Gu, and Xiao-Gang Wen. Classification of gapped symmetric phases in one-dimensional spin systems. *Phys. Rev. B*, 83:035107, Jan 2011.

[63] Xie Chen, Zheng-Xin Liu, and Xiao-Gang Wen. Two-dimensional symmetry-protected topological orders and their protected gapless edge excitations. *Phys. Rev. B*, 84:235141, Dec 2011.

[64] Y. Chen, D. L. Bergman, and A. A. Burkov. Weyl fermions and the anomalous hall effect in metallic ferromagnets. *Phys. Rev. B*, 88:125110, Sep 2013.

[65] Y. Chen, Si Wu, and A. A. Burkov. Axion response in weyl semimetals. *Phys. Rev. B*, 88:125105, Sep 2013.

[66] Meng Cheng. Fermionic Lieb-Schultz-Mattis theorems and weak symmetry-protected phases. *Phys. Rev. B*, 99:075143, Feb 2019.

[67] Meng Cheng and Nathan Seiberg. Lieb-schultz-mattis, luttinger, and 't hooft – anomaly matching in lattice systems, 2023.

[68] Meng Cheng, Michael Zaletel, Maissam Barkeshli, Ashvin Vishwanath, and Parsa Bonderson. Translational Symmetry and Microscopic Constraints on Symmetry-Enriched Topological Phases: A View from the Surface. *Physical Review X*, 6(4):041068, December 2016.

[69] Gil Young Cho, Jens H. Bardarson, Yuan-Ming Lu, and Joel E. Moore. Superconductivity of doped weyl semimetals: Finite-momentum pairing and electronic analog of the ^{3}he-a phase. *Phys. Rev. B*, 86:214514, Dec 2012.

[70] Gil Young Cho, Chang-Tse Hsieh, and Shinsei Ryu. Anomaly manifestation of Lieb-Schultz-Mattis theorem and topological phases. *Phys. Rev. B*, 96(19):195105, November 2017.

[71] Suk Bum Chung and Rahul Roy. Hall conductivity in the normal and superconducting phases of the rashba system with zeeman field. *Phys. Rev. B*, 90:224510, Dec 2014.

[72] C. Dasgupta and B. I. Halperin. Phase transition in a lattice model of superconductivity. *Phys. Rev. Lett.*, 47:1556–1560, Nov 1981.

[73] P. G. de Gennes. *Superconductivity of Metals and Alloys*. Perseus Books, 1999.

[74] S Deser, R Jackiw, and S Templeton. Topologically massive gauge theories. *Annals of Physics*, 140(2):372 – 411, 1982.

[75] Oleg Dubinkin, F. J. Burnell, and Taylor L. Hughes. Higher r ank chiral fermions in 3d weyl semimetals, 2021.

[76] I.E. Dzyaloshinskii and G.E. Volovick. Poisson brackets in condensed matter physics. *Annals of Physics*, 125(1):67 – 97, 1980.

[77] Dominic V. Else, Hoi Chun Po, and Haruki Watanabe. Fragile topological phases in interacting systems. *Phys. Rev. B*, 99(12):125122, March 2019.

[78] Dominic V. Else and Ryan Thorngren. Crystalline topological phases as defect networks. *Phys. Rev. B*, 99(11):115116, March 2019.

[79] Dominic V. Else and Ryan Thorngren. Topological theory of lieb-schultz-mattis theorems in quantum spin systems. *Phys. Rev. B*, 101:224437, Jun 2020.

[80] Dominic V. Else, Ryan Thorngren, and T. Senthil. Non-Fermi Liquids as Ersatz Fermi Liquids: General Constraints on Compressible Metals. *Phys. Rev. X*, 11(2):021005, April 2021.

[81] Pavel Etingof, Shlomo Gelaki, Dmitri Nikshych, and Victor Ostrik. *Tensor categories*, volume 205. American Mathematical Soc., 2016.

[82] Chen Fang, Yige Chen, Hae-Young Kee, and Liang Fu. Topological nodal line semimetals with and without spin-orbital coupling. *Phys. Rev. B*, 92:081201, Aug 2015.

[83] Chen Fang, Matthew J. Gilbert, Xi Dai, and B. Andrei Bernevig. Multi-weyl topological semimetals stabilized by point group symmetry. *Phys. Rev. Lett.*, 108:266802, Jun 2012.

[84] Lukasz Fidkowski, Xie Chen, and Ashvin Vishwanath. Non-Abelian Topological Order on the Surface of a 3D Topological Superconductor from an Exactly Solved Model. *Physical Review X*, 3(4):041016, Oct 2013.

[85] Mark H. Fischer, Titus Neupert, Christian Platt, Andreas P. Schnyder, Werner Hanke, Jun Goryo, Ronny Thomale, and Manfred Sigrist. Chiral d-wave superconductivity in srptas. *Phys. Rev. B*, 89:020509, Jan 2014.

[86] Matthew P. A. Fisher. Quantum phase transitions in disordered two-dimensional superconductors. *Phys. Rev. Lett.*, 65:923–926, Aug 1990.

[87] Matthew P. A. Fisher and D. H. Lee. Correspondence between two-dimensional bosons and a bulk superconductor in a magnetic field. *Phys. Rev. B*, 39:2756–2759, Feb 1989.

[88] Serge Florens and Antoine Georges. Slave-rotor mean-field theories of strongly correlated systems and the mott transition in finite dimensions. *Phys. Rev. B*, 70:035114, Jul 2004.

[89] Eduardo Fradkin. *Field theories of condensed matter physics*. Cambridge University Press, 2013.

[90] Jürg Fröhlich and Philipp Werner. Gauge theory of topological phases of matter. *EPL (Europhysics Letters)*, 101(4):47007, 2013.

[91] Liang Fu. Hexagonal warping effects in the surface states of the topological insulator bi_2te_3. *Phys. Rev. Lett.*, 103:266801, Dec 2009.

[92] Liang Fu and Erez Berg. Odd-parity topological superconductors: Theory and application to $cu_xbi_2se_3$. *Phys. Rev. Lett.*, 105:097001, Aug 2010.

[93] Liang Fu and C. L. Kane. Topological insulators with inversion symmetry. *Phys. Rev. B*, 76:045302, Jul 2007.

[94] Liang Fu and C. L. Kane. Superconducting proximity effect and majorana fermions at the surface of a topological insulator. *Phys. Rev. Lett.*, 100:096407, Mar 2008.

[95] Liang Fu, C. L. Kane, and E. J. Mele. Topological insulators in three dimensions. *Phys. Rev. Lett.*, 98:106803, Mar 2007.

[96] K. Fujikawa and H. Suzuki. *Path Integrals and Quantum Anomalies*. International Series of Monographs on Physics. OUP Oxford, 2004.

[97] Kazuo Fujikawa. Path-integral measure for gauge-invariant fermion theories. *Phys. Rev. Lett.*, 42:1195–1198, Apr 1979.

[98] Takahiro Fukui and Takanori Fujiwara. z_2 index theorem for majorana zero modes in a class d topological superconductor. *Phys. Rev. B*, 82:184536, Nov 2010.

[99] Kenji Fukushima, Dmitri E. Kharzeev, and Harmen J. Warringa. Chiral magnetic effect. *Phys. Rev. D*, 78:074033, Oct 2008.

[100] Akira Furusaki, Naoto Nagaosa, Kentaro Nomura, Shinsei Ryu, and Tadashi Takayanagi. Electromagnetic and thermal responses in topological matter: Topological terms, quantum anomalies and d-branes. *Comptes Rendus Physique*, 14(910):871 – 883, 2013.

[101] Shunsuke C. Furuya and Masaki Oshikawa. Symmetry protection of critical phases and a global anomaly in $1 + 1$ dimensions. *Phys. Rev. Lett.*, 118:021601, Jan 2017.

[102] Victor M. Galitski, G. Refael, Matthew P. A. Fisher, and T. Senthil. Vortices and quasiparticles near the superconductor-insulator transition in thin films. *Phys. Rev. Lett.*, 95:077002, Aug 2005.

[103] Scott D. Geraedts, Michael P. Zaletel, Roger S. K. Mong, Max A. Metlitski, Ashvin Vishwanath, and Olexei I. Motrunich. The half-filled landau level: The case for dirac composite fermions. *Science*, 352(6282):197–201, 2016.

[104] L. Gioia, M. G. Christie, U. Zülicke, M. Governale, and A. J. Sneyd. Spherical topological insulator nanoparticles: Quantum size effects and optical transitions. *Phys. Rev. B*, 100:205417, Nov 2019.

[105] L. Gioia, Chong Wang, and A. A. Burkov. Unquantized anomalies in topological semimetals. *Phys. Rev. Research*, 3:043067, Oct 2021.

[106] L. Gioia, U. Zülicke, M. Governale, and R. Winkler. Dirac electrons in quantum rings. *Phys. Rev. B*, 97:205421, May 2018.

[107] Lei Gioia and Sheng-Jie Huang. Topological responses for non-symmorphic crystals and semimetals, In progress.

[108] Lei Gioia and Chong Wang. Nonzero momentum requires long-range entanglement. *Phys. Rev. X*, 12:031007, Jul 2022.

[109] Lei Gioia, Chong Wang, Taylor L. Hughes, and Anton A. Burkov. No-go theorems of dirac nodes, In progress.

[110] Johannes Gooth, Anna C. Niemann, Tobias Meng, Adolfo G. Grushin, Karl Landsteiner, Bernd Gotsmann, Fabian Menges, Marcus Schmidt, Chandra Shekhar, Vicky Süß, Ruben Hühne, Bernd Rellinghaus, Claudia Felser, Binghai Yan, and Kornelius Nielsch. Experimental signatures of the mixed axial–gravitational anomaly in the weyl semimetal nbp. *Nature*, 547:324 EP –, 07 2017.

[111] E. V. Gorbar, V. A. Miransky, I. A. Shovkovy, and P. O. Sukhachov. Quantum oscillations as a probe of interaction effects in weyl semimetals in a magnetic field. *Phys. Rev. B*, 90:115131, Sep 2014.

[112] E. V. Gorbar, V. A. Miransky, I. A. Shovkovy, and P. O. Sukhachov. Dirac semimetals $A_3\mathrm{Bi}$ ($a = \mathrm{Na}, \mathrm{K}, \mathrm{Rb}$) as F_2 weyl semimetals. *Phys. Rev. B*, 91:121101, Mar 2015.

[113] E. V. Gorbar, V. A. Miransky, I. A. Shovkovy, and P. O. Sukhachov. Surface Fermi arcs in Z_2 Weyl semimetals $A_3 Bi$ (A=Na, K, Rb). *ArXiv e-prints*, March 2015.

[114] Jun Goryo. Impurity-induced polar kerr effect in a chiral p-wave superconductor. *Phys. Rev. B*, 78:060501, Aug 2008.

[115] P. Goswami, J. H. Pixley, and S. Das Sarma. Axial anomaly and longitudinal magnetoresistance of a generic three dimensional metal. *ArXiv e-prints*, March 2015.

[116] Pallab Goswami and Sumanta Tewari. Axionic field theory of $(3 + 1)$-dimensional weyl semimetals. *Phys. Rev. B*, 88:245107, Dec 2013.

[117] D. Gross, V. Nesme, H. Vogts, and R. F. Werner. Index theory of one dimensional quantum walks and cellular automata. *Comm. Math. Phys.*, 310(2):419–454, 2012.

[118] G. Grüner. The dynamics of charge-density waves. *Rev. Mod. Phys.*, 60:1129–1181, Oct 1988.

[119] Adolfo G. Grushin. Consequences of a condensed matter realization of lorentz-violating qed in weyl semi-metals. *Phys. Rev. D*, 86:045001, Aug 2012.

[120] Adolfo G. Grushin, Jörn W. F. Venderbos, Ashvin Vishwanath, and Roni Ilan. Inhomogeneous weyl and dirac semimetals: Transport in axial magnetic fields and fermi arc surface states from pseudo-landau levels. *Phys. Rev. X*, 6:041046, Dec 2016.

[121] Zheng-Cheng Gu, Zhenghan Wang, and Xiao-Gang Wen. Classification of two-dimensional fermionic and bosonic topological orders. *Phys. Rev. B*, 91:125149, Mar 2015.

[122] Zheng-Cheng Gu and Xiao-Gang Wen. Symmetry-protected topological orders for interacting fermions: Fermionic topological nonlinear sigma models and a special group supercohomology theory. *Physical Review B*, 90(11), sep 2014.

[123] Jeongwan Haah, Matthew B. Hastings, Robin Kothari, and Guang Hao Low. Quantum algorithm for simulating real time evolution of lattice Hamiltonians. *arXiv e-prints*, January 2018.

[124] Gábor B. Halász and Leon Balents. Time-reversal invariant realization of the weyl semimetal phase. *Phys. Rev. B*, 85:035103, Jan 2012.

[125] F. D. M. Haldane. Model for a quantum hall effect without landau levels: Condensed-matter realization of the "parity anomaly". *Phys. Rev. Lett.*, 61:2015–2018, Oct 1988.

[126] F. D. M. Haldane. Berry curvature on the fermi surface: Anomalous hall effect as a topological fermi-liquid property. *Phys. Rev. Lett.*, 93:206602, Nov 2004.

[127] F. D. M. Haldane. Attachment of Surface "Fermi Arcs" to the Bulk Fermi Surface: "Fermi-Level Plumbing" in Topological Metals. *ArXiv e-prints*, January 2014.

[128] Bertrand I. Halperin. Possible states for a three-dimensional electron gas in a strong magnetic field. *Japanese Journal of Applied Physics*, 26(S3-3):1913, jan 1987.

[129] Lei Hao, Rui Wang, Pavan Hosur, and C. S. Ting. Larkin-ovchinnikov state of superconducting weyl metals: Fundamental differences between restricted and extended pairings in k-space. *Phys. Rev. B*, 96:094530, Sep 2017.

[130] M. Z. Hasan and C. L. Kane. *Colloquium* : Topological insulators. *Rev. Mod. Phys.*, 82:3045–3067, Nov 2010.

[131] M. Zahid Hasan, Su-Yang Xu, Ilya Belopolski, and Shin-Ming Huang. Discovery of weyl fermion semimetals and topological fermi arc states. *Annual Review of Condensed Matter Physics*, 8(1), 2017.

[132] M. B. Hastings. Lieb-schultz-mattis in higher dimensions. *Phys. Rev. B*, 69:104431, Mar 2004.

[133] M. B. Hastings and Xiao-Gang Wen. Quasiadiabatic continuation of quantum states: The stability of topological ground-state degeneracy and emergent gauge invariance. *Physical Review B*, 72(4), jul 2005.

[134] Yasuhiro Hatsugai and Mahito Kohmoto. Exactly solvable model of correlated lattice electrons in any dimensions. *Journal of the Physical Society of Japan*, 61(6):2056–2069, 1992.

[135] Conyers Herring. Accidental degeneracy in the energy bands of crystals. *Phys. Rev.*, 52:365–373, Aug 1937.

[136] Motoaki Hirayama, Ryo Okugawa, Takashi Miyake, and Shuichi Murakami. Topological dirac nodal lines and surface charges in fcc alkaline earth metals. *Nature Communications*, 8:14022, 01 2017.

[137] Max Hirschberger, Satya Kushwaha, Zhijun Wang, Quinn Gibson, Sihang Liang, Carina A. Belvin, B. A. Bernevig, R. J. Cava, and N. P. Ong. The chiral anomaly and thermopower of weyl fermions in the half-heusler gdptbi. *Nat Mater*, 15(11):1161–1165, 11 2016.

[138] Petr Hořava. Stability of fermi surfaces and k theory. *Phys. Rev. Lett.*, 95:016405, Jun 2005.

[139] Kimin Hong and N. Giordano. Approach to mesoscopic magnetic measurements. *Phys. Rev. B*, 51:9855–9862, Apr 1995.

[140] Pavan Hosur, Xi Dai, Zhong Fang, and Xiao-Liang Qi. Time-reversal-invariant topological superconductivity in doped weyl semimetals. *Phys. Rev. B*, 90:045130, Jul 2014.

[141] Pavan Hosur, S. A. Parameswaran, and Ashvin Vishwanath. Charge transport in weyl semimetals. *Phys. Rev. Lett.*, 108:046602, Jan 2012.

[142] Pavan Hosur and Xiaoliang Qi. Recent developments in transport phenomena in weyl semimetals. *Comptes Rendus Physique*, 14(910):857 – 870, 2013. Topological insulators / Isolants topologiques Topological insulators / Isolants topologiques.

[143] Pavan Hosur, Shinsei Ryu, and Ashvin Vishwanath. Chiral topological insulators, superconductors, and other competing orders in three dimensions. *Phys. Rev. B*, 81:045120, Jan 2010.

[144] Timothy H. Hsieh, Gábor B. Halász, and Tarun Grover. All Majorana Models with Translation Symmetry are Supersymmetric. *Physical Review Letters*, 117(16):166802, Oct 2016.

[145] Yichen Hu, Jörn W. F. Venderbos, and C. L. Kane. Fractional excitonic insulator. *Phys. Rev. Lett.*, 121:126601, Sep 2018.

[146] L. Huang, T. M. McCormick, M. Ochi, Z. Zhao, M.-t. Suzuki, R. Arita, Y. Wu, D. Mou, H. Cao, J. Yan, N. Trivedi, and A. Kaminski. Spectroscopic evidence for type II Weyl semimetal state in MoTe2. *ArXiv e-prints*, March 2016.

[147] Sheng-Jie Huang, Hao Song, Yi-Ping Huang, and Michael Hermele. Building crystalline topological phases from lower-dimensional states. *Phys. Rev. B*, 96:205106, Nov 2017.

[148] Shin-Ming Huang, Su-Yang Xu, Ilya Belopolski, Chi-Cheng Lee, Guoqing Chang, Tay-Rong Chang, BaoKai Wang, Nasser Alidoust, Guang Bian, Madhab Neupane, Daniel Sanchez, Hao Zheng, Horng-Tay Jeng, Arun Bansil, Titus Neupert, Hsin Lin, and M. Zahid Hasan. New type of weyl semimetal with quadratic double weyl fermions. *Proceedings of the National Academy of Sciences*, 113(5):1180–1185, 2016.

[149] Shin-Ming Huang, Su-Yang Xu, Ilya Belopolski, Chi-Cheng Lee, Guoqing Chang, BaoKai Wang, Nasser Alidoust, Guang Bian, Madhab Neupane, Chenglong Zhang, Shuang Jia, Arun Bansil, Hsin Lin, and M. Zahid Hasan. A weyl fermion semimetal with surface fermi arcs in the transition metal monopnictide taas class. *Nat Commun*, 6, 06 2015.

[150] Xiaochun Huang, Lingxiao Zhao, Yujia Long, Peipei Wang, Dong Chen, Zhanhai Yang, Hui Liang, Mianqi Xue, Hongming Weng, Zhong Fang, Xi Dai, and Genfu Chen. Observation of the chiral-anomaly-induced negative magnetoresistance in 3d weyl semimetal taas. *Phys. Rev. X*, 5:031023, Aug 2015.

[151] Ze-Min Huang, Longyue Li, Jianhui Zhou, and Hong-Hao Zhang. Torsional response and liouville anomaly in weyl semimetals with dislocations. *Phys. Rev. B*, 99:155152, Apr 2019.

[152] Ze-Min Huang, Jianhui Zhou, and Shun-Qing Shen. Topological responses from chiral anomaly in multi-weyl semimetals. *Physical Review B*, 96(8):085201–, 08 2017.

[153] Zhoushen Huang, Daniel P Arovas, and Alexander V Balatsky. Impurity scattering in weyl semimetals and their stability classification. *New Journal of Physics*, 15(12):123019, 2013.

[154] Jun-ichiro Inoue, Gerrit E. W. Bauer, and Laurens W. Molenkamp. Suppression of the persistent spin hall current by defect scattering. *Phys. Rev. B*, 70:041303, Jul 2004.

[155] Jun-ichiro Inoue, Takashi Kato, Yasuhito Ishikawa, Hiroyoshi Itoh, Gerrit E. W. Bauer, and Laurens W. Molenkamp. Vertex corrections to the anomalous hall effect in spin-polarized two-dimensional electron gases with a rashba spin-orbit interaction. *Phys. Rev. Lett.*, 97:046604, Jul 2006.

[156] Chao-Ming Jian, Zhen Bi, and Cenke Xu. Lieb-Schultz-Mattis theorem and its generalizations from the perspective of the symmetry-protected topological phase. *Phys. Rev. B*, 97(5):054412, February 2018.

[157] C. L. Kane and E. J. Mele. Quantum spin hall effect in graphene. *Phys. Rev. Lett.*, 95:226801, Nov 2005.

[158] C. L. Kane and E. J. Mele. Z_2 topological order and the quantum spin hall effect. *Phys. Rev. Lett.*, 95:146802, Sep 2005.

[159] Anton Kapustin. Symmetry protected topological phases, anomalies, and cobordisms: Beyond group cohomology, 2014.

[160] Anton Kapustin, Ryan Thorngren, Alex Turzillo, and Zitao Wang. Fermionic symmetry protected topological phases and cobordisms. *Journal of High Energy Physics*, 2015(12):1–21, dec 2015.

[161] Andreas Karch and David Tong. Particle-vortex duality from 3d bosonization. *Phys. Rev. X*, 6:031043, Sep 2016.

[162] Udit Khanna, Arijit Kundu, Saurabh Pradhan, and Sumathi Rao. Proximity-induced superconductivity in weyl semimetals. *Phys. Rev. B*, 90:195430, Nov 2014.

[163] Dmitri E. Kharzeev and Ho-Ung Yee. Chiral magnetic wave. *Phys. Rev. D*, 83:085007, Apr 2011.

[164] Alexei Kitaev. Anyons in an exactly solved model and beyond. *Ann. Phys.*, 321(1):2 – 111, 2006.

[165] Alexei Kitaev, Vladimir Lebedev, and Mikhail Feigel'man. Periodic table for topological insulators and superconductors. In *AIP Conference Proceedings*. AIP, 2009.

[166] F. R. Klinkhamer and G. E. Volovik. Emergent cpt violation from the splitting of fermi points. *International Journal of Modern Physics A*, 20(13):2795–2812, 2005.

[167] Shingo Kobayashi and Masatoshi Sato. Topological superconductivity in dirac semimetals. *Phys. Rev. Lett.*, 115:187001, Oct 2015.

[168] Markus Koenig, Steffen Wiedmann, Christoph Bruene, Andreas Roth, Hartmut Buhmann, Laurens W. Molenkamp, Xiao-Liang Qi, and Shou-Cheng Zhang. Quantum spin hall insulator state in hgte quantum wells. *Science*, 318(5851):766–770, 2007.

[169] John B. Kogut. An introduction to lattice gauge theory and spin systems. *Rev. Mod. Phys.*, 51:659–713, Oct 1979.

[170] Mahito Kohmoto, Bertrand I. Halperin, and Yong-Shi Wu. Diophantine equation for the three-dimensional quantum hall effect. *Phys. Rev. B*, 45:13488–13493, Jun 1992.

[171] Liang Kong and Xiao-Gang Wen. Braided fusion categories, gravitational anomalies, and the mathematical framework for topological orders in any dimensions, 2014.

[172] J M Kosterlitz and D J Thouless. Ordering, metastability and phase transitions in two-dimensional systems. *Journal of Physics C: Solid State Physics*, 6(7):1181, 1973.

[173] Alexey A. Kovalev, Jairo Sinova, and Yaroslav Tserkovnyak. Anomalous hall effect in disordered multiband metals. *Phys. Rev. Lett.*, 105:036601, Jul 2010.

[174] N. Kumar, C. Felser, and C. Shekhar. Planar Hall effect in Weyl semimetal GdPtBi. *ArXiv e-prints*, November 2017.

[175] LD Landau. Lifschitz, statistical physics, chap. xiv, 1958.

[176] Sara Laurila and Jaakko Nissinen. Torsional landau levels and geometric anomalies in condensed matter weyl systems. *Phys. Rev. B*, 102:235163, Dec 2020.

[177] Dung-Hai Lee and Matthew P. A. Fisher. Anyon superconductivity and the fractional quantum hall effect. *Phys. Rev. Lett.*, 63:903–906, Aug 1989.

[178] Dung-Hai Lee and Charles L. Kane. Boson-vortex-skyrmion duality, spin-singlet fractional quantum hall effect, and spin-1/2 anyon superconductivity. *Phys. Rev. Lett.*, 64:1313–1317, Mar 1990.

[179] Jong Yeon Lee, Chong Wang, Michael P. Zaletel, Ashvin Vishwanath, and Yin-Chen He. Emergent multi-flavor qed_3 at the plateau transition between fractional chern insulators: Applications to graphene heterostructures. *Phys. Rev. X*, 8:031015, Jul 2018.

[180] Patrick A. Lee and T. V. Ramakrishnan. Disordered electronic systems. *Rev. Mod. Phys.*, 57:287–337, Apr 1985.

[181] Sung-Sik Lee and Patrick A. Lee. U(1) gauge theory of the hubbard model: Spin liquid states and possible application to $\kappa-(\mathrm{BEDT-TTF})_2\mathrm{cu}_2(\mathrm{CN})_3$. *Phys. Rev. Lett.*, 95:036403, Jul 2005.

[182] Michael Levin. Protected edge modes without symmetry. *Phys. Rev. X*, 3:021009, May 2013.

[183] Michael Levin and Ady Stern. Classification and analysis of two-dimensional abelian fractional topological insulators. *Phys. Rev. B*, 86:115131, Sep 2012.

[184] C.-Z. Li, L.-X. Wang, H. Liu, J. Wang, Z.-M. Liao, and D.-P. Yu. Giant negative magnetoresistance induced by the chiral anomaly in individual Cd3As2 nanowires. *ArXiv e-prints*, April 2015.

[185] H. Li, H. Wang, H. He, J. Wang, and S.-Q. Shen. Giant Anisotropic Magnetoresistance and Planar Hall Effect in Dirac Semimetal Cd3As2. *ArXiv e-prints*, November 2017.

[186] Qiang Li, Dmitri E. Kharzeev, Cheng Zhang, Yuan Huang, I. Pletikosic, A. V. Fedorov, R. D. Zhong, J. A. Schneeloch, G. D. Gu, and T. Valla. Chiral magnetic effect in zrte5. *Nat Phys*, 12(6):550–554, 06 2016.

[187] Yi Li and F. D. M. Haldane. Topological nodal cooper pairing in doped weyl metals. *Phys. Rev. Lett.*, 120:067003, Feb 2018.

[188] T. Liang, Q. Gibson, M. Liu, W. Wang, R. J. Cava, and N. P. Ong. Anomalous Hall Effect in ZrTe5. *ArXiv e-prints*, December 2016.

[189] Elliott Lieb, Theodore Schultz, and Daniel Mattis. Two soluble models of an antiferromagnetic chain. *Annals of Physics*, 16(3):407 – 466, 1961.

[190] Chao-Xing Liu, Peng Ye, and Xiao-Liang Qi. Chiral gauge field and axial anomaly in a weyl semimetal. *Phys. Rev. B*, 87:235306, Jun 2013.

[191] Chao-Xing Liu, Shou-Cheng Zhang, and Xiao-Liang Qi. The quantum anomalous hall effect: Theory and experiment. *Annual Review of Condensed Matter Physics*, 7(1):301–321, 2016.

[192] D. F. Liu, A. J. Liang, E. K. Liu, Q. N. Xu, Y. W. Li, C. Chen, D. Pei, W. J. Shi, S. K. Mo, P. Dudin, T. Kim, C. Cacho, G. Li, Y. Sun, L. X. Yang, Z. K. Liu, S. S. P. Parkin, C. Felser, and Y. L. Chen. Magnetic weyl semimetal phase in a kagome crystal. *Science*, 365(6459):1282–1285, 2019.

[193] E. Liu, Y. Sun, L. Müechler, A. Sun, L. Jiao, J. Kroder, V. Süß, H. Borrmann, W. Wang, W. Schnelle, S. Wirth, S. T. B. Goennenwein, and C. Felser. Giant anomalous Hall angle in a half-metallic magnetic Weyl semimetal. *ArXiv e-prints*, December 2017.

[194] Enke Liu, Yan Sun, Nitesh Kumar, Lukas Muechler, Aili Sun, Lin Jiao, Shuo-Ying Yang, Defa Liu, Aiji Liang, Qiunan Xu, Johannes Kroder, Vicky Süß, Horst Borrmann, Chandra Shekhar, Zhaosheng Wang, Chuanying Xi, Wenhong Wang, Walter Schnelle, Steffen Wirth, Yulin Chen, Sebastian T. B. Goennenwein, and Claudia Felser. Giant anomalous hall effect in a ferromagnetic kagome-lattice semimetal. *Nature Physics*, 14(11):1125–1131, 2018.

[195] Shang Liu, Ashvin Vishwanath, and Eslam Khalaf. Shift Insulators: Rotation-Protected Two-Dimensional Topological Crystalline Insulators. *Physical Review X*, 9(3):031003, July 2019.

[196] Xin Liu, Hsiu-Chuan Hsu, and Chao-Xing Liu. In-plane magnetization-induced quantum anomalous hall effect. *Phys. Rev. Lett.*, 111:086802, Aug 2013.

[197] Z. K. Liu, B. Zhou, Y. Zhang, Z. J. Wang, H. M. Weng, D. Prabhakaran, S.-K. Mo, Z. X. Shen, Z. Fang, X. Dai, Z. Hussain, and Y. L. Chen. Discovery of a three-dimensional topological dirac semimetal, na3bi. *Science*, 343(6173):864–867, 2014.

[198] Seth Lloyd. Universal quantum simulators. *Science*, 273(5278):1073–1078, 1996.

[199] Bo Lu, Keiji Yada, Masatoshi Sato, and Yukio Tanaka. Crossed surface flat bands of weyl semimetal superconductors. *Phys. Rev. Lett.*, 114:096804, Mar 2015.

[200] H.-Z. Lu, S.-B. Zhang, and S.-Q. Shen. Quantum Magnetoconductivity of Topological Semimetals in High Magnetic Fields. *ArXiv e-prints*, March 2015.

[201] Ling Lu, Zhiyu Wang, Dexin Ye, Lixin Ran, Liang Fu, John D. Joannopoulos, and Marin Soljačić. Experimental observation of weyl points. *Science*, 349(6248):622–624, 2015.

[202] Yuan-Ming Lu. Lieb-Schultz-Mattis theorems for symmetry protected topological phases. *arXiv e-prints*, 2017.

[203] Yuan-Ming Lu, Ying Ran, and Masaki Oshikawa. Filling-enforced constraint on the quantized hall conductivity on a periodic lattice. *Ann. Phys.*, 413:168060, 2020.

[204] Yuan-Ming Lu and Ashvin Vishwanath. Theory and classification of interacting integer topological phases in two dimensions: A chern-simons approach. *Phys. Rev. B*, 86:125119, Sep 2012.

[205] Andrew Lucas, Richard A. Davison, and Subir Sachdev. Hydrodynamic theory of thermoelectric transport and negative magnetoresistance in weyl semimetals. *Proceedings of the National Academy of Sciences*, 113(34):9463–9468, 2016.

[206] Andreas W. W. Ludwig, Matthew P. A. Fisher, R. Shankar, and G. Grinstein. Integer quantum hall transition: An alternative approach and exact results. *Phys. Rev. B*, 50:7526–7552, Sep 1994.

[207] Rex Lundgren, Pontus Laurell, and Gregory A. Fiete. Thermoelectric properties of weyl and dirac semimetals. *Phys. Rev. B*, 90:165115, Oct 2014.

[208] Roman M. Lutchyn, Pavel Nagornykh, and Victor M. Yakovenko. Gauge-invariant electromagnetic response of a chiral p_x+ip_y superconductor. *Phys. Rev. B*, 77:144516, Apr 2008.

[209] J. M. Luttinger and J. C. Ward. Ground-state energy of a many-fermion system. ii. *Phys. Rev.*, 118:1417–1427, Jun 1960.

[210] B. Q. Lv, H. M. Weng, B. B. Fu, X. P. Wang, H. Miao, J. Ma, P. Richard, X. C. Huang, L. X. Zhao, G. F. Chen, Z. Fang, X. Dai, T. Qian, and H. Ding. Experimental discovery of weyl semimetal taas. *Phys. Rev. X*, 5:031013, Jul 2015.

[211] B. Q. Lv, N. Xu, H. M. Weng, J. Z. Ma, P. Richard, X. C. Huang, L. X. Zhao, G. F. Chen, C. E. Matt, F. Bisti, V. N. Strocov, J. Mesot, Z. Fang, X. Dai, T. Qian, M. Shi, and H. Ding. Observation of weyl nodes in taas. *Nat Phys*, 11(9):724–727, 09 2015.

[212] Joseph Maciejko and Gregory A. Fiete. Fractionalized topological insulators. *Nat Phys*, 11(5):385–388, 05 2015.

[213] Joseph Maciejko and Rahul Nandkishore. Weyl semimetals with short-range interactions. *Phys. Rev. B*, 90:035126, Jul 2014.

[214] Naren Manjunath and Maissam Barkeshli. Crystalline gauge fields and quantized discrete geometric response for abelian topological phases with lattice symmetry. *Phys. Rev. Research*, 3:013040, Jan 2021.

[215] D. J. J. Marchand and M. Franz. Lattice model for the surface states of a topological insulator with applications to magnetic and exciton instabilities. *Phys. Rev. B*, 86:155146, Oct 2012.

[216] Julian May-Mann, Lei Gioia, Mark R. Hirsbrunner, and Taylor L. Hughes. Crystalline responses in dirac semimetal-charge density wave insulators, In progress.

[217] Julian May-Mann, Mark R. Hirsbrunner, Xuchen Cao, and Taylor L. Hughes. Topological field theories of three-dimensional rotation symmetric insulators: Coupling curvature and electromagnetism. *Phys. Rev. B*, 107:205149, May 2023.

[218] Glen Bigan Mbeng, Angelo Russomanno, and Giuseppe E. Santoro. The quantum ising chain for beginners, 2020.

[219] John McGreevy. Quantum phases of matter, Spring 2021.

[220] John McGreevy. Generalized symmetries in condensed matter. *Annual Review of Condensed Matter Physics*, 14(1):57–82, 2023.

[221] T. Meng, A. G. Grushin, K. Shtengel, and J. H. Bardarson. Theory of a 3+1D fractional chiral metal: interacting variant of the Weyl semimetal. *ArXiv e-prints*, February 2016.

[222] Tobias Meng and Leon Balents. Weyl superconductors. *Phys. Rev. B*, 86:054504, Aug 2012.

[223] Tobias Meng and Jan Carl Budich. Unpaired weyl nodes from long-ranged interactions: Fate of quantum anomalies. *Phys. Rev. Lett.*, 122:046402, Feb 2019.

[224] Tobias Meng, Adolfo G. Grushin, Kirill Shtengel, and Jens H. Bardarson. Theory of a 3+1d fractional chiral metal: Interacting variant of the weyl semimetal. *Phys. Rev. B*, 94:155136, Oct 2016.

[225] Andrej Mesaros and Ying Ran. Classification of symmetry enriched topological phases with exactly solvable models. *Phys. Rev. B*, 87:155115, Apr 2013.

[226] Max A. Metlitski, Lukasz Fidkowski, Xie Chen, and Ashvin Vishwanath. Interaction effects on 3D topological superconductors: surface topological order from vortex condensation, the 16 fold way and fermionic Kramers doublets. *arXiv e-prints*, page arXiv:1406.3032, Jun 2014.

[227] Max A. Metlitski, C. L. Kane, and Matthew P. A. Fisher. Symmetry-respecting topologically ordered surface phase of three-dimensional electron topological insulators. *Phys. Rev. B*, 92:125111, Sep 2015.

[228] Max A. Metlitski and Ryan Thorngren. Intrinsic and emergent anomalies at deconfined critical points. *Phys. Rev. B*, 98(8):085140, August 2018.

[229] Max A. Metlitski and Ashvin Vishwanath. Particle-vortex duality of two-dimensional dirac fermion from electric-magnetic duality of three-dimensional topological insulators. *Phys. Rev. B*, 93:245151, Jun 2016.

[230] D. L. Miller and B. Laikhtman. Longitudinal magnetoresistance of superlattices caused by barrier inhomogeneity. *Phys. Rev. B*, 54:10669–10674, Oct 1996.

[231] V. P. Mineev and K. V. Samokhin. Helical phases in superconductors. *JETP*, 78:401, 1994.

[232] V. P. Mineev and K. V. Samokhin. Nonuniform states in noncentrosymmetric superconductors: Derivation of Lifshitz invariants from microscopic theory. *Phys. Rev. B*, 78(14):144503, October 2008.

[233] E. G. Mishchenko, A. V. Shytov, and B. I. Halperin. Spin current and polarization in impure two-dimensional electron systems with spin-orbit coupling. *Phys. Rev. Lett.*, 93:226602, Nov 2004.

[234] Philip J. W. Moll, Nityan L. Nair, Toni Helm, Andrew C. Potter, Itamar Kimchi, Ashvin Vishwanath, and James G. Analytis. Transport evidence for fermi-arc-mediated chirality transfer in the dirac semimetal cd3as2. *Nature*, 535(7611):266–270, 07 2016.

[235] Philip J. W. Moll, Andrew C. Potter, Nityan L. Nair, B. J. Ramshaw, K. A. Modic, Scott Riggs, Bin Zeng, Nirmal J. Ghimire, Eric D. Bauer, Robert Kealhofer, Filip Ronning, and James G. Analytis. Magnetic torque anomaly in the quantum limit of weyl semimetals. *Nature Communications*, 7:12492 EP –, 08 2016.

[236] Eun-Gook Moon, Cenke Xu, Yong Baek Kim, and Leon Balents. Non-fermi-liquid and topological states with strong spin-orbit coupling. *Phys. Rev. Lett.*, 111:206401, Nov 2013.

[237] Gregory Moore and Nicholas Read. Nonabelions in the fractional quantum hall effect. *Nuclear Physics B*, 360(2):362 – 396, 1991.

[238] J. E. Moore and L. Balents. Topological invariants of time-reversal-invariant band structures. *Phys. Rev. B*, 75:121306, Mar 2007.

[239] Takahiro Morimoto and Naoto Nagaosa. Weyl mott insulator. *Scientific Reports*, 6:19853 EP –, 01 2016.

[240] David F. Mross, Jason Alicea, and Olexei I. Motrunich. Explicit derivation of duality between a free dirac cone and quantum electrodynamics in $(2+1)$ dimensions. *Phys. Rev. Lett.*, 117:016802, Jun 2016.

[241] Michael Mulligan and F. J. Burnell. Topological insulators avoid the parity anomaly. *Phys. Rev. B*, 88:085104, Aug 2013.

[242] Shuichi Murakami. Phase transition between the quantum spin hall and insulator phases in 3d: emergence of a topological gapless phase. *New Journal of Physics*, 9(9):356, 2007.

[243] Shuichi Murakami and Naoto Nagaosa. Berry phase in magnetic superconductors. *Phys. Rev. Lett.*, 90:057002, Feb 2003.

[244] Bruno Nachtergaele and Robert Sims. A multi-dimensional lieb-schultz-mattis theorem. *Comm. Math. Phys.*, 276(2):437–472, 2007.

[245] Naoto Nagaosa, Jairo Sinova, Shigeki Onoda, A. H. MacDonald, and N. P. Ong. Anomalous hall effect. *Rev. Mod. Phys.*, 82:1539–1592, May 2010.

[246] Mikio Nakahara. *Geometry, topology and physics*. CRC press, 2003.

[247] S. Nandy, Girish Sharma, A. Taraphder, and Sumanta Tewari. Chiral anomaly as the origin of the planar hall effect in weyl semimetals. *Phys. Rev. Lett.*, 119:176804, Oct 2017.

[248] Madhab Neupane, Ilya Belopolski, M. Mofazzel Hosen, Daniel S. Sanchez, Raman Sankar, Maria Szlawska, Su-Yang Xu, Klauss Dimitri, Nagendra Dhakal, Pablo Maldonado, Peter M. Oppeneer, Dariusz Kaczorowski, Fangcheng Chou, M. Zahid Hasan, and Tomasz Durakiewicz. Observation of topological nodal fermion semimetal phase in zrsis. *Phys. Rev. B*, 93:201104, May 2016.

[249] Madhab Neupane, Su-Yang Xu, Raman Sankar, Nasser Alidoust, Guang Bian, Chang Liu, Ilya Belopolski, Tay-Rong Chang, Horng-Tay Jeng, Hsin Lin, Arun Bansil, Fangcheng Chou, and M. Zahid Hasan. Observation of a three-dimensional topological dirac semimetal phase in high-mobility cd3as2. *Nat. Commun.*, 5, 05 2014.

[250] H.B. Nielsen and M. Ninomiya. The adler-bell-jackiw anomaly and weyl fermions in a crystal. *Physics Letters B*, 130(6):389 – 396, 1983.

[251] A. J. Niemi and G. W. Semenoff. Axial-anomaly-induced fermion fractionization and effective gauge-theory actions in odd-dimensional space-times. *Phys. Rev. Lett.*, 51:2077–2080, Dec 1983.

[252] J. Nissinen, T. T. Heikkilä, and G. E. Volovik. Topological polarization, dual invariants, and surface flat bands in crystalline insulators. *Phys. Rev. B*, 103:245115, Jun 2021.

[253] J. Nissinen and G. E. Volovik. Dimensional crossover of effective orbital dynamics in polar distorted 3He-A: Transitions to anti-spacetime. *ArXiv e-prints*, October 2017.

[254] J. Nissinen and G. E. Volovik. Tetrads in solids: from elasticity theory to topological quantum hall systems and weyl fermions. *Journal of Experimental and Theoretical Physics*, 127:948–957, Nov 2018.

[255] J. Nissinen and G. E. Volovik. Elasticity tetrads, mixed axial-gravitational anomalies, and $(3+1)$-d quantum hall effect. *Phys. Rev. Research*, 1:023007, Sep 2019.

[256] Jaakko Nissinen. Emergent spacetime and gravitational nieh-yan anomaly in chiral $p+ip$ weyl superfluids and superconductors. *Phys. Rev. Lett.*, 124:117002, Mar 2020.

[257] Mario Novak, Satoshi Sasaki, Kouji Segawa, and Yoichi Ando. Large linear magnetoresistance in the dirac semimetal tlbisse. *Phys. Rev. B*, 91:041203, Jan 2015.

[258] Yoshiko Ogata, Yuji Tachikawa, and Hal Tasaki. General Lieb-Schultz-Mattis Type Theorems for Quantum Spin Chains. *Comm. Math. Phys.*, 385(1):79–99, July 2021.

[259] Yoshiko Ogata and Hal Tasaki. Lieb-Schultz-Mattis Type Theorems for Quantum Spin Chains Without Continuous Symmetry. *Comm. Math. Phys.*, 372(3):951–962, December 2019.

[260] Teemu Ojanen and Takuya Kitagawa. Anomalous electromagnetic response of superconducting rashba systems in trivial and topological phases. *Phys. Rev. B*, 87:014512, Jan 2013.

[261] Ryo Okugawa and Shuichi Murakami. Universal phase transition and band structures for spinless nodal-line and weyl semimetals. *Phys. Rev. B*, 96:115201, Sep 2017.

[262] Shigeki Onoda, Naoyuki Sugimoto, and Naoto Nagaosa. Intrinsic versus extrinsic anomalous hall effect in ferromagnets. *Phys. Rev. Lett.*, 97:126602, Sep 2006.

[263] Masaki Oshikawa. Commensurability, Excitation Gap, and Topology in Quantum Many-Particle Systems on a Periodic Lattice. *Physical Review Letters*, 84(7):1535–1538, Feb 2000.

[264] Masaki Oshikawa. Topological approach to luttinger's theorem and the fermi surface of a kondo lattice. *Phys. Rev. Lett.*, 84:3370–3373, Apr 2000.

[265] H. K. Pal and D. L. Maslov. Necessary and sufficient condition for longitudinal magnetoresistance. *Phys. Rev. B*, 81:214438, Jun 2010.

[266] J. P. Pan. *Solid State Physics*, volume 5. Academic, New York, 1957.

[267] I. Panfilov, A. A. Burkov, and D. A. Pesin. Density response in weyl metals. *Phys. Rev. B*, 89:245103, Jun 2014.

[268] S A Parameswaran. Topological 'luttinger' invariants for filling-enforced nonsymmorphic semimetals. *Journal of Physics: Condensed Matter*, 31(10):104001, jan 2019.

[269] S. A. Parameswaran, T. Grover, D. A. Abanin, D. A. Pesin, and A. Vishwanath. Probing the chiral anomaly with nonlocal transport in three-dimensional topological semimetals. *Phys. Rev. X*, 4:031035, Sep 2014.

[270] Siddharth A. Parameswaran, Ari M. Turner, Daniel P. Arovas, and Ashvin Vishwanath. Topological order and absence of band insulators at integer filling in nonsymmorphic crystals. *Nature Physics*, 9(5):299–303, 2013.

[271] Michael E Peskin. Mandelstam-'t hooft duality in abelian lattice models. *Annals of Physics*, 113(1):122 – 152, 1978.

[272] D. I. Pikulin, Anffany Chen, and M. Franz. Chiral anomaly from strain-induced gauge fields in dirac and weyl semimetals. *Phys. Rev. X*, 6:041021, Oct 2016.

[273] Hoi Chun Po, Haruki Watanabe, Chao-Ming Jian, and Michael P. Zaletel. Lattice Homotopy Constraints on Phases of Quantum Magnets. *Physical Review Letters*, 119(12):127202, September 2017.

[274] Daniel Podolsky, Arun Paramekanti, Yong Baek Kim, and T. Senthil. Mott transition between a spin-liquid insulator and a metal in three dimensions. *Phys. Rev. Lett.*, 102:186401, May 2009.

[275] Frank Pollmann, Erez Berg, Ari M. Turner, and Masaki Oshikawa. Symmetry protection of topological phases in one-dimensional quantum spin systems. *Physical Review B*, 85(7), feb 2012.

[276] A.M. Polyakov. Quark confinement and topology of gauge theories. *Nuclear Physics B*, 120(3):429 – 458, 1977.

[277] Andrew C. Potter, Itamar Kimchi, and Ashvin Vishwanath. Quantum oscillations from surface fermi arcs in weyl and dirac semimetals. *Nat Commun*, 5, 10 2014.

[278] Andrew C. Potter, Chong Wang, Max A. Metlitski, and Ashvin Vishwanath. Realizing topological surface states in a lower-dimensional flat band. *Phys. Rev. B*, 96(23):235114, Dec 2017.

[279] Xiao-Liang Qi, Taylor L. Hughes, S. Raghu, and Shou-Cheng Zhang. Time-reversal-invariant topological superconductors and superfluids in two and three dimensions. *Phys. Rev. Lett.*, 102:187001, May 2009.

[280] Xiao-Liang Qi, Taylor L. Hughes, and Shou-Cheng Zhang. Topological field theory of time-reversal invariant insulators. *Phys. Rev. B*, 78:195424, Nov 2008.

[281] Xiao-Liang Qi, Taylor L. Hughes, and Shou-Cheng Zhang. Chiral topological superconductor from the quantum hall state. *Phys. Rev. B*, 82:184516, Nov 2010.

[282] Xiao-Liang Qi and Shou-Cheng Zhang. Topological insulators and superconductors. *Rev. Mod. Phys.*, 83:1057–1110, Oct 2011.

[283] N. Ramakrishnan, M. Milletari, and S. Adam. Magnetoresistance in 3D Weyl Semimetals. *ArXiv e-prints*, January 2015.

[284] Srinidhi T. Ramamurthy and Taylor L. Hughes. Patterns of electromagnetic response in topological semimetals. *Phys. Rev. B*, 92:085105, Aug 2015.

[285] Srinidhi T. Ramamurthy and Taylor L. Hughes. Quasitopological electromagnetic response of line-node semimetals. *Phys. Rev. B*, 95:075138, Feb 2017.

[286] Syed Raza, Alexander Sirota, and Jeffrey C. Y. Teo. From dirac semimetals to topological phases in three dimensions: A coupled-wire construction. *Phys. Rev. X*, 9:011039, Feb 2019.

[287] N. Read and Dmitry Green. Paired states of fermions in two dimensions with breaking of parity and time-reversal symmetries and the fractional quantum hall effect. *Phys. Rev. B*, 61:10267–10297, Apr 2000.

[288] A. N. Redlich. Gauge noninvariance and parity nonconservation of three-dimensional fermions. *Phys. Rev. Lett.*, 52:18–21, Jan 1984.

[289] Bitan Roy and Pallab Goswami. Z_2 index for gapless fermionic modes in the vortex core of three-dimensional paired dirac fermions. *Phys. Rev. B*, 89:144507, Apr 2014.

[290] W. B. Rui, Y. X. Zhao, and A. P. Schnyder. Topological transport in PT invariant Dirac nodal-line semimetals. *ArXiv e-prints*, March 2017.

[291] Shinsei Ryu, Joel E. Moore, and Andreas W. W. Ludwig. Electromagnetic and gravitational responses and anomalies in topological insulators and superconductors. *Phys. Rev. B*, 85:045104, Jan 2012.

[292] Shinsei Ryu, Andreas P Schnyder, Akira Furusaki, and Andreas W W Ludwig. Topological insulators and superconductors: tenfold way and dimensional hierarchy. *New Journal of Physics*, 12(6):065010, jun 2010.

[293] Subir Sachdev. Topological order, emergent gauge fields, and fermi surface reconstruction. *Reports on Progress in Physics*, 82(1):014001, nov 2018.

[294] Subir Sachdev. *Quantum Phases of Matter*. Cambridge University Press, 2023.

[295] Eran Sagi, Ady Stern, and David F. Mross. Composite Weyl semimetal as a parent state for three-dimensional topologically ordered phases. *Phys. Rev. B*, 98(20):201111, Nov 2018.

[296] K. V. Samokhin. Helical states and solitons in noncentrosymmetric superconductors. *Phys. Rev. B*, 89:094503, Mar 2014.

[297] T. Sato, Kouji Segawa, K. Kosaka, S. Souma, K. Nakayama, K. Eto, T. Minami, Yoichi Ando, and T. Takahashi. Unexpected mass acquisition of dirac fermions at the quantum phase transition of a topological insulator. *Nat Phys*, 7(11):840–844, 11 2011.

[298] Andreas P. Schnyder, Shinsei Ryu, Akira Furusaki, and Andreas W. W. Ludwig. Classification of topological insulators and superconductors in three spatial dimensions. *Phys. Rev. B*, 78:195125, Nov 2008.

[299] Leslie M. Schoop, Mazhar N. Ali, Carola Straßer, Andreas Topp, Andrei Varykhalov, Dmitry Marchenko, Viola Duppel, Stuart S. P. Parkin, Bettina V. Lotsch, and Christian R. Ast. Dirac cone protected by non-symmorphic symmetry and three-dimensional dirac line node in zrsis. *Nature Communications*, 7:11696, 05 2016.

[300] Thomas Schuster, Thomas Iadecola, Claudio Chamon, Roman Jackiw, and So-Young Pi. Dissipationless conductance in a topological coaxial cable. *Phys. Rev. B*, 94:115110, Sep 2016.

[301] Dan Sehayek, Manisha Thakurathi, and A. A. Burkov. Charge density waves in weyl semimetals. *Phys. Rev. B*, 102:115159, Sep 2020.

[302] Nathan Seiberg, T. Senthil, Chong Wang, and Edward Witten. A duality web in 2+1 dimensions and condensed matter physics. *Annals of Physics*, 374:395 – 433, 2016.

[303] Nathan Seiberg and Edward Witten. Gapped boundary phases of topological insulators via weak coupling. *Progress of Theoretical and Experimental Physics*, 2016(12):12C101, Dec 2016.

[304] Akihiko Sekine and Kentaro Nomura. Weyl semimetal in the strong coulomb interaction limit. *Journal of the Physical Society of Japan*, 83(9):094710, 2014.

[305] Gordon W. Semenoff. Condensed-matter simulation of a three-dimensional anomaly. *Phys. Rev. Lett.*, 53:2449–2452, Dec 1984.

[306] T. Senthil and Matthew P. A. Fisher. Z_2 gauge theory of electron fractionalization in strongly correlated systems. *Phys. Rev. B*, 62(12):7850–7881, Sep 2000.

[307] T. Senthil and Michael Levin. Integer quantum hall effect for bosons. *Phys. Rev. Lett.*, 110:046801, Jan 2013.

[308] T. Senthil, Ashvin Vishwanath, Leon Balents, Subir Sachdev, and Matthew P. A. Fisher. Deconfined quantum critical points. *Science*, 303(5663):1490–1494, 2004.

[309] C. Shekhar, A. K. Nayak, S. Singh, N. Kumar, S.-C. Wu, Y. Zhang, A. C. Komarek, E. Kampert, Y. Skourski, J. Wosnitza, W. Schnelle, A. McCollam, U. Zeitler, J. Kubler, S. S. P. Parkin, B. Yan, and C. Felser. Observation of chiral magnetotransport in RPtBi topological Heusler compounds. *ArXiv e-prints*, April 2016.

[310] Ken Shiozaki, Charles Zhaoxi Xiong, and Kiyonori Gomi. Generalized homology and Atiyah-Hirzebruch spectral sequence in crystalline symmetry protected topological phenomena. *arXiv e-prints*, October 2018.

[311] Vasudha Shivamoggi and Matthew J. Gilbert. Weyl phases in point-group symmetric superconductors. *Phys. Rev. B*, 88:134504, Oct 2013.

[312] N. A. Sinitsyn, A. H. MacDonald, T. Jungwirth, V. K. Dugaev, and Jairo Sinova. Anomalous hall effect in a two-dimensional dirac band: The link between the kubo-streda formula and the semiclassical boltzmann equation approach. *Phys. Rev. B*, 75:045315, Jan 2007.

[313] Jairo Sinova, Dimitrie Culcer, Q. Niu, N. A. Sinitsyn, T. Jungwirth, and A. H. MacDonald. Universal intrinsic spin hall effect. *Phys. Rev. Lett.*, 92:126603, Mar 2004.

[314] J.-R. Soh, F. de Juan, M. G. Vergniory, N. B. M. Schröter, M. C. Rahn, D. Y. Yan, J. Jiang, M. Bristow, P. Reiss, J. N. Blandy, Y. F. Guo, Y. G. Shi, T. K. Kim, A. McCollam, S. H. Simon, Y. Chen, A. I. Coldea, and A. T. Boothroyd. Ideal weyl semimetal induced by magnetic exchange. *Phys. Rev. B*, 100:201102, Nov 2019.

[315] Alexey A. Soluyanov, Dominik Gresch, Zhijun Wang, QuanSheng Wu, Matthias Troyer, Xi Dai, and B. Andrei Bernevig. Type-ii weyl semimetals. *Nature*, 527(7579):495–498, 11 2015.

[316] D. T. Son and B. Z. Spivak. Chiral anomaly and classical negative magnetoresistance of weyl metals. *Phys. Rev. B*, 88:104412, Sep 2013.

[317] Dam Thanh Son. Is the composite fermion a dirac particle? *Phys. Rev. X*, 5:031027, Sep 2015.

[318] Dam Thanh Son and Naoki Yamamoto. Berry curvature, triangle anomalies, and the chiral magnetic effect in fermi liquids. *Phys. Rev. Lett.*, 109:181602, Nov 2012.

[319] E. H. Sondheimer. The boltzman equation for anisotropic metals. *Proceedings of the Royal Society of London A: Mathematical, Physical and Engineering Sciences*, 268(1332):100–108, 1962.

[320] Hao Song, Sheng-Jie Huang, Liang Fu, and Michael Hermele. Topological phases protected by point group symmetry. *Phys. Rev. X*, 7:011020, Feb 2017.

[321] Xue-Yang Song, Yin-Chen He, Ashvin Vishwanath, and Chong Wang. From spinon band topology to the symmetry quantum numbers of monopoles in dirac spin liquids. *Phys. Rev. X*, 10:011033, Feb 2020.

[322] Xue-Yang Song, Yin-Chen He, Ashvin Vishwanath, and Chong Wang. Electric polarization as a nonquantized topological response and boundary luttinger theorem. *Phys. Rev. Res.*, 3:023011, Apr 2021.

[323] Zhida Song, Chen Fang, and Yang Qi. Real-space recipes for general topological crystalline states. *Nat. Commun.*, 11(1):4197, 2020.

[324] B. Z. Spivak and A. V. Andreev. Magnetotransport phenomena related to the chiral anomaly in weyl semimetals. *Phys. Rev. B*, 93:085107, Feb 2016.

[325] Julia A. Steinberg, Steve M. Young, Saad Zaheer, C. L. Kane, E. J. Mele, and Andrew M. Rappe. Bulk dirac points in distorted spinels. *Phys. Rev. Lett.*, 112:036403, Jan 2014.

[326] P Streda. Theory of quantised hall conductivity in two dimensions. *Journal of Physics C: Solid State Physics*, 15(22):L717, 1982.

[327] D. Stroud and F. P. Pan. Effect of isolated inhomogeneities on the galvanomagnetic properties of solids. *Phys. Rev. B*, 13:1434–1438, Feb 1976.

[328] Hao Su, Benchao Gong, Wujun Shi, Haifeng Yang, Hongyuan Wang, Wei Xia, Zhenhai Yu, Peng-Jie Guo, Jinhua Wang, Linchao Ding, Liangcai Xu, Xiaokang Li, Xia Wang, Zhiqiang Zou, Na Yu, Zengwei Zhu, Yulin Chen, Zhongkai Liu, Kai Liu, Gang Li, and Yanfeng Guo. Magnetic exchange induced Weyl state in a semimetal EuCd2Sb2. *APL Materials*, 8(1):011109, 01 2020.

[329] Fangdong Tang, Yafei Ren, Peipei Wang, Ruidan Zhong, John Schneeloch, Shengyuan A. Yang, Kun Yang, Patrick A. Lee, Genda Gu, Zhenhua Qiao, and Liyuan Zhang. Three-dimensional quantum hall effect and metal–insulator transition in zrte5. *Nature*, 569(7757):537–541, 2019.

[330] H. X. Tang, R. K. Kawakami, D. D. Awschalom, and M. L. Roukes. Giant planar hall effect in epitaxial (ga,mn)as devices. *Phys. Rev. Lett.*, 90:107201, Mar 2003.

[331] R. Tao and D. J. Thouless. Fractional quantization of hall conductance. *Phys. Rev. B*, 28:1142–1144, Jul 1983.

[332] Edward Taylor and Catherine Kallin. Intrinsic hall effect in a multiband chiral superconductor in the absence of an external magnetic field. *Phys. Rev. Lett.*, 108:157001, Apr 2012.

[333] Jeffrey C. Y. Teo, Liang Fu, and C. L. Kane. Surface states and topological invariants in three-dimensional topological insulators: Application to $\mathrm{bi}_{1-x}\mathrm{sb}_x$. *Phys. Rev. B*, 78:045426, Jul 2008.

[334] Jeffrey C. Y. Teo and C. L. Kane. Topological defects and gapless modes in insulators and superconductors. *Physical Review B*, 82(11), sep 2010.

[335] Manisha Thakurathi and A. A. Burkov. Theory of the fractional quantum hall effect in weyl semimetals. *Phys. Rev. B*, 101:235168, Jun 2020.

[336] Ryan Thorngren and Dominic V. Else. Gauging spatial symmetries and the classification of topological crystalline phases. *Phys. Rev. X*, 8:011040, Mar 2018.

[337] Ryan Thorngren, Tibor Rakovszky, Ruben Verresen, and Ashvin Vishwanath. Higgs condensates are symmetry-protected topological phases: Ii. $u(1)$ gauge theory and superconductors, 2023.

[338] M. M. Vazifeh and M. Franz. Electromagnetic response of weyl semimetals. *Phys. Rev. Lett.*, 111:027201, Jul 2013.

[339] J. Villain. Theory of one- and two-dimensional magnets with an easy magnetization plane. ii. the planar, classical, two-dimensional magnet. *J. Phys. France*, 36(6):581–590, 1975.

[340] Ashvin Vishwanath and T. Senthil. Physics of Three-Dimensional Bosonic Topological Insulators: Surface-Deconfined Criticality and Quantized Magnetoelectric Effect. *Physical Review X*, 3(1):011016, Jan 2013.

[341] G. E. Volovik. An analog of the quantum hall effect in a superfluid ^{3}he film. *Sov. Phys. JETP*, 67:1804, Sep 1988.

[342] G. E. Volovik. Fermion zero modes on vortices in chiral superconductors. *Journal of Experimental and Theoretical Physics Letters*, 70(9):609–614, 1999.

[343] G. E. Volovik. Quantum phase transitions from topology in momentum space. In WilliamG. Unruh and Ralf SchÃ¼tzhold, editors, *Quantum Analogues: From Phase Transitions to Black Holes and Cosmology*, volume 718 of *Lecture Notes in Physics*. Springer Berlin Heidelberg, 2007.

[344] G. E. Volovik. Topological lifshitz transitions. *Low Temperature Physics*, 43(1):47–55, jan 2017.

[345] G.E. Volovik. *The Universe in a Helium Droplet*. Oxford: Clarendon, 2003.

[346] J von Neumann and E. P. Wigner. über das verhalten von eigenwerten bei adiabatischen prozessen. *Physikalische Zeitschrift*, 30:467 – 470, 1929.

[347] Xiangang Wan, Ari M. Turner, Ashvin Vishwanath, and Sergey Y. Savrasov. Topological semimetal and fermi-arc surface states in the electronic structure of pyrochlore iridates. *Phys. Rev. B*, 83:205101, May 2011.

[348] Chenjie Wang and Michael Levin. Braiding statistics of loop excitations in three dimensions. *Phys. Rev. Lett.*, 113:080403, Aug 2014.

[349] Chong Wang, L. Gioia, and A. A. Burkov. Fractional quantum hall effect in weyl semimetals. *Phys. Rev. Lett.*, 124:096603, Mar 2020.

[350] Chong Wang, Adam Nahum, Max A. Metlitski, Cenke Xu, and T. Senthil. Deconfined quantum critical points: Symmetries and dualities. *Phys. Rev. X*, 7:031051, Sep 2017.

[351] Chong Wang, Andrew C. Potter, and T. Senthil. Gapped symmetry preserving surface state for the electron topological insulator. *Phys. Rev. B*, 88:115137, Sep 2013.

[352] Chong Wang, Andrew C. Potter, and T. Senthil. Classification of interacting electronic topological insulators in three dimensions. *Science*, 343(6171):629–631, 2014.

[353] Chong Wang and T. Senthil. Interacting fermionic topological insulators/superconductors in three dimensions. *Phys. Rev. B*, 89(19):195124, May 2014.

[354] Chong Wang and T. Senthil. Dual dirac liquid on the surface of the electron topological insulator. *Phys. Rev. X*, 5:041031, Nov 2015.

[355] Jing Wang, Quan Zhou, Biao Lian, and Shou-Cheng Zhang. Chiral topological superconductor and half-integer conductance plateau from quantum anomalous hall plateau transition. *Phys. Rev. B*, 92:064520, Aug 2015.

[356] Qi Wang, Yuanfeng Xu, Rui Lou, Zhonghao Liu, Man Li, Yaobo Huang, Dawei Shen, Hongming Weng, Shancai Wang, and Hechang Lei. Large intrinsic anomalous hall effect in half-metallic ferromagnet co3sn2s2 with magnetic weyl fermions. *Nature Communications*, 9(1):3681, 2018.

[357] Rui Wang, Lei Hao, Baigeng Wang, and C. S. Ting. Quantum anomalies in superconducting weyl metals. *Phys. Rev. B*, 93:184511, May 2016.

[358] Y. J. Wang, J. X. Gong, D. D. Liang, M. Ge, J. R. Wang, W. K. Zhu, and C. J. Zhang. Planar Hall effect in type-II Weyl semimetal WTe2. *ArXiv e-prints*, January 2018.

[359] Zhijun Wang, Yan Sun, Xing-Qiu Chen, Cesare Franchini, Gang Xu, Hongming Weng, Xi Dai, and Zhong Fang. Dirac semimetal and topological phase transitions in A_3bi (a = Na, k, rb). *Phys. Rev. B*, 85:195320, May 2012.

[360] Zhijun Wang, Hongming Weng, Quansheng Wu, Xi Dai, and Zhong Fang. Three-dimensional dirac semimetal and quantum transport in cd_3as_2. *Phys. Rev. B*, 88:125427, Sep 2013.

[361] Zhong Wang and Shou-Cheng Zhang. Chiral anomaly, charge density waves, and axion strings from weyl semimetals. *Phys. Rev. B*, 87:161107, Apr 2013.

[362] Haruki Watanabe, Hoi Chun Po, Ashvin Vishwanath, and Michael Zaletel. Filling constraints for spin-orbit coupled insulators in symmorphic and nonsymmorphic crystals. *Proc. Natl. Acad. Sci.*, 112(47):14551–14556, 2015.

[363] Huazhou Wei, Sung-Po Chao, and Vivek Aji. Odd-parity superconductivity in weyl semimetals. *Phys. Rev. B*, 89:014506, Jan 2014.

[364] Steven Weinberg. *The quantum theory of fields*, volume 2. Cambridge university press, 1995.

[365] Xiao-Gang Wen. Topological orders and edge excitations in fractional quantum hall states. *Advances in Physics*, 44(5):405–473, oct 1995.

[366] Xiao-Gang Wen. *Quantum field theory of many-body systems: from the origin of sound to an origin of light and electrons*. OUP Oxford, 2004.

[367] Xiao-Gang Wen. Classifying gauge anomalies through symmetry-protected trivial orders and classifying gravitational anomalies through topological orders. *Phys. Rev. D*, 88:045013, Aug 2013.

[368] Hongming Weng, Chen Fang, Zhong Fang, B. Andrei Bernevig, and Xi Dai. Weyl semimetal phase in noncentrosymmetric transition-metal monophosphides. *Phys. Rev. X*, 5:011029, Mar 2015.

[369] Benjamin J. Wieder, Zhijun Wang, Jennifer Cano, Xi Dai, Leslie M. Schoop, Barry Bradlyn, and B. Andrei Bernevig. Strong and fragile topological dirac semimetals with higher-order fermi arcs. *Nature Communications*, 11(1), Jan 2020.

[370] J. H. Wilson, A. A. Allocca, and V. M. Galitski. Repulsive Casimir force between Weyl semimetals. *ArXiv e-prints*, January 2015.

[371] William Witczak-Krempa, Gang Chen, Yong Baek Kim, and Leon Balents. Correlated quantum phenomena in the strong spin-orbit regime. *Annual Review of Condensed Matter Physics*, 5(1):57–82, 2014.

[372] William Witczak-Krempa and Yong Baek Kim. Topological and magnetic phases of interacting electrons in the pyrochlore iridates. *Phys. Rev. B*, 85:045124, Jan 2012.

[373] William Witczak-Krempa, Michael Knap, and Dmitry Abanin. Interacting weyl semimetals: Characterization via the topological hamiltonian and its breakdown. *Phys. Rev. Lett.*, 113:136402, Sep 2014.

[374] Edward Witten. Fermion path integrals and topological phases. *Rev. Mod. Phys.*, 88:035001, Jul 2016.

[375] Ying-Hai Wu and Jainendra K. Jain. Quantum Hall effect of two-component bosons at fractional and integral fillings. *Phys. Rev. B*, 87(24):245123, Jun 2013.

[376] Y. Xia, D. Qian, D. Hsieh, L. Wray, A. Pal, H. Lin, A. Bansil, D. Grauer, Y. S. Hor, R. J. Cava, and M. Z. Hasan. Observation of a large-gap topological-insulator class with a single dirac cone on the surface. *Nat Phys*, 5(6):398–402, 06 2009.

[377] Di Xiao, Ming-Che Chang, and Qian Niu. Berry phase effects on electronic properties. *Rev. Mod. Phys.*, 82:1959–2007, Jul 2010.

[378] J. Xiong, S. Kushwaha, J. Krizan, T. Liang, R. J. Cava, and N. P. Ong. Anomalous conductivity tensor in the Dirac semimetal Na_3Bi. *ArXiv e-prints*, February 2015.

[379] J. Xiong, S. K. Kushwaha, T. Liang, J. W. Krizan, W. Wang, R. J. Cava, and N. P. Ong. Signature of the chiral anomaly in a Dirac semimetal: a current plume steered by a magnetic field. *ArXiv e-prints*, March 2015.

[380] Jun Xiong, Satya K. Kushwaha, Tian Liang, Jason W. Krizan, Max Hirschberger, Wudi Wang, R. J. Cava, and N. P. Ong. Evidence for the chiral anomaly in the dirac semimetal na3bi. *Science*, 350(6259):413–416, 2015.

[381] Gang Xu, Hongming Weng, Zhijun Wang, Xi Dai, and Zhong Fang. Chern semimetal and the quantized anomalous hall effect in $hgcr_2se_4$. *Phys. Rev. Lett.*, 107:186806, Oct 2011.

[382] Su-Yang Xu, Nasser Alidoust, Ilya Belopolski, Zhujun Yuan, Guang Bian, Tay-Rong Chang, Hao Zheng, Vladimir N. Strocov, Daniel S. Sanchez, Guoqing Chang, Chenglong Zhang, Daixiang Mou, Yun Wu, Lunan Huang, Chi-Cheng Lee, Shin-Ming Huang, BaoKai Wang, Arun Bansil, Horng-Tay Jeng, Titus Neupert, Adam Kaminski, Hsin Lin, Shuang Jia, and M. Zahid Hasan. Discovery of a weyl fermion state with fermi arcs in niobium arsenide. *Nat Phys*, 11(9):748–754, 09 2015.

[383] Su-Yang Xu, Ilya Belopolski, Nasser Alidoust, Madhab Neupane, Guang Bian, Chenglong Zhang, Raman Sankar, Guoqing Chang, Zhujun Yuan, Chi-Cheng Lee, Shin-Ming Huang, Hao Zheng, Jie Ma, Daniel S. Sanchez, BaoKai Wang, Arun Bansil, Fangcheng Chou, Pavel P. Shibayev, Hsin Lin, Shuang Jia, and M. Zahid Hasan. Discovery of a weyl fermion semimetal and topological fermi arcs. *Science*, 349(6248):613–617, 2015.

[384] Victor M. Yakovenko. Theory of the high-frequency chiral optical response of a $p_x + ip_y$ superconductor. *Phys. Rev. Lett.*, 98:087003, Feb 2007.

[385] Binghai Yan and Claudia Felser. Topological materials: Weyl semimetals. *Annual Review of Condensed Matter Physics*, 8(1), 2017.

[386] Bohm-Jung Yang, Takahiro Morimoto, and Akira Furusaki. Topological charges of three-dimensional dirac semimetals with rotation symmetry. *Phys. Rev. B*, 92:165120, Oct 2015.

[387] Bohm-Jung Yang and Naoto Nagaosa. Classification of stable three-dimensional dirac semimetals with nontrivial topology. *Nat Commun*, 5, 09 2014.

[388] Kai-Yu Yang, Yuan-Ming Lu, and Ying Ran. Quantum hall effects in a weyl semimetal: Possible application in pyrochlore iridates. *Phys. Rev. B*, 84:075129, Aug 2011.

[389] L. X. Yang, Z. K. Liu, Y. Sun, H. Peng, H. F. Yang, T. Zhang, B. Zhou, Y. Zhang, Y. F. Guo, M. Rahn, D. Prabhakaran, Z. Hussain, S. K. Mo, C. Felser, B. Yan, and Y. L. Chen. Weyl semimetal phase in the non-centrosymmetric compound taas. *Nature Physics*, 11(9):728–732, 2015.

[390] Shengyuan A. Yang. Dirac and weyl materials: Fundamental aspects and some spintronics applications. *SPIN*, 06(02):1640003, 2018/04/16 2016.

[391] Shengyuan A. Yang, Hui Pan, Yugui Yao, and Qian Niu. Scattering universality classes of side jump in the anomalous hall effect. *Phys. Rev. B*, 83:125122, Mar 2011.

[392] Xu Yang, Shenghan Jiang, Ashvin Vishwanath, and Ying Ran. Dyonic Lieb-Schultz-Mattis theorem and symmetry protected topological phases in decorated dimer models. *Phys. Rev. B*, 98:125120, Sep 2018.

[393] Yuan Yao and Masaki Oshikawa. Generalized Boundary Condition Applied to Lieb-Schultz-Mattis-Type Ingappabilities and Many-Body Chern Numbers. *Phys. Rev. X*, 10(3):031008, July 2020.

[394] Weicheng Ye, Meng Guo, Yin-Chen He, Chong Wang, and Liujun Zou. Topological characterization of Lieb-Schultz-Mattis constraints and applications to symmetry-enriched quantum criticality. *arXiv e-prints*, November 2021.

[395] Luke Yeo and Philip W. Phillips. Local entropies across the mott transition in an exactly solvable model. *Phys. Rev. D*, 99:094030, May 2019.

[396] Jinmin Yi, Xuzhe Ying, Lei Gioia, and A. A. Burkov. Topological order in interacting semimetals. *Phys. Rev. B*, 107:115147, Mar 2023.

[397] S. M. Young, S. Zaheer, J. C. Y. Teo, C. L. Kane, E. J. Mele, and A. M. Rappe. Dirac semimetal in three dimensions. *Phys. Rev. Lett.*, 108:140405, Apr 2012.

[398] A. Zee. *Quantum field theory in a nutshell*. Princeton University Press, 2003.

[399] Bei Zeng and Xiao-Gang Wen. Gapped quantum liquids and topological order, stochastic local transformations and emergence of unitarity. *Phys. Rev. B*, 91:125121, Mar 2015.

[400] C. Zhang, S.-Y. Xu, I. Belopolski, Z. Yuan, Z. Lin, B. Tong, N. Alidoust, C.-C. Lee, S.-M. Huang, H. Lin, M. Neupane, D. S. Sanchez, H. Zheng, G. Bian, J. Wang, C. Zhang, T. Neupert, M. Zahid Hasan, and S. Jia. Observation of the Adler-Bell-Jackiw chiral anomaly in a Weyl semimetal. *ArXiv e-prints*, March 2015.

[401] C. Zhang, E. Zhang, Y. Liu, Z.-G. Chen, S. Liang, J. Cao, X. Yuan, L. Tang, Q. Li, T. Gu, Y. Wu, J. Zou, and F. Xiu. Detection of chiral anomaly and valley transport in Dirac semimetals. *ArXiv e-prints*, April 2015.

[402] S. C. Zhang, T. H. Hansson, and S. Kivelson. Effective-field-theory model for the fractional quantum hall effect. *Phys. Rev. Lett.*, 62:82–85, Jan 1989.

[403] Shou-Cheng Zhang and Jiangping Hu. A four-dimensional generalization of the quantum hall effect. *Science*, 294(5543):823–828, 2001.

[404] X.-X. Zhang and N. Nagaosa. Tomonaga-Luttinger liquid and localization in Weyl semimetals. *ArXiv e-prints*, December 2016.

[405] Jianhui Zhou, Hao-Ran Chang, and Di Xiao. Plasmon mode as a detection of the chiral anomaly in weyl semimetals. *Phys. Rev. B*, 91:035114, Jan 2015.

[406] Heinrich-Gregor Zirnstein and Bernd Rosenow. Cancellation of quantum anomalies and bosonization of three-dimensional time-reversal symmetric topological insulators. *Phys. Rev. B*, 88:085105, Aug 2013.

[407] Liujun Zou, Yin-Chen He, and Chong Wang. Stiefel liquids: Possible non-lagrangian quantum criticality from intertwined orders. *Phys. Rev. X*, 11:031043, Aug 2021.

[408] A. A. Zyuzin and A. A. Burkov. Topological response in weyl semimetals and the chiral anomaly. *Phys. Rev. B*, 86:115133, Sep 2012.

[409] A. A. Zyuzin, M. D. Hook, and A. A. Burkov. Parallel magnetic field driven quantum phase transition in a thin topological insulator film. *Phys. Rev. B*, 83:245428, Jun 2011.

[410] A. A. Zyuzin, Si Wu, and A. A. Burkov. Weyl semimetal with broken time reversal and inversion symmetries. *Phys. Rev. B*, 85:165110, Apr 2012.

[411] A. A. Zyuzin and V. A. Zyuzin. Chiral Electromagnetic Waves in Weyl Semimetal. *ArXiv e-prints*, October 2014.

APPENDICES

Appendix A

Band inversion mechanism motivated

In this section we motivate how Dirac nodes may arise from the band inversion mechanism (BIM) using a minimalistic four band model. The most general form of a four band Hamiltonian is given by [387]

$$H(\mathbf{k}) = \sum_{i,j=0}^{3} a_{ij}(\mathbf{k})\tau^i\sigma^j \quad , \tag{A.1}$$

where τ and σ refer to the orbital and spin degrees of freedom respectively and $\tau_{0,1,2,3}$ ($\sigma_{0,1,2,3}$) are the usual identity and Pauli matrices. To obtain Dirac nodes via BIM, we require a C_n point group symmetry to be present, which means the Hamiltonian must obey

$$\left[R^i_{2\pi/n}\right] H(\mathbf{k}) \left[R^i_{2\pi/n}\right]^{-1} = H(\mathcal{R}^i_{2\pi/n}\mathbf{k}) \quad . \tag{A.2}$$

Without loss of generality, we choose the rotation axis to be along k_z. This means that $\mathcal{R}^z_{2\pi/n}\mathbf{k} = \mathbf{k}$ when $\mathbf{k}$ is along the k_z axis. From this it follows that along the k_z axis we have

$$[R^z_{2\pi/n}, H(\mathbf{k})] = 0 \quad , \tag{A.3}$$

This condition allows us to find a basis that simultaneously diagonalises $H(k_z) \equiv H(k_x = 0, k_y = 0, k_z)$ and $R^z_{2\pi/n}$. Thus the Hamiltonian in this basis takes the general form

$$H(k_z) = a_0 + a_1\sigma^3 + a_2\tau^3 + a_3\tau^3\sigma^3 \tag{A.4}$$

where $a_{0,1,2,3}$ are real functions that depend on k_z and some system parameters m. Since we require doubly degenerate bands for DSs, this reduces all but one of $a_{1,2,3}$ to zero.

Additionally degenerate bands are also required to be of opposite spin eigenstates which means $a_1 = 0$. This reduces $H(k_z)$ to

$$H(k_z) = a_0 + a(k_z, m)\Gamma \tag{A.5}$$

where Γ is either τ^z or $\tau^z\sigma^z$. The energy gap of this reduced Hamiltonian is given by $2|a(k_z, m)|$. Thus a crossing point, i.e. a Dirac node, may be achieved when the system parameters are tuned such that $a(k_z, m) = 0$. In order to obtain a DS, we may simply determine the value of m for which this is true in the BZ. The crossings may exist for a range of parameter m since $k_z \in (-\pi, \pi)$. In particular, this has been found to occur in the band inverted regimes of Na_3Bi and Cd_3As_2 [359, 360]. These types of crossings are also referred to as *accidental* band crossings [346] since the crossing are not symmetry enforced and only occur due to the tuning of $a(k_z, m)$.

Appendix B

Quantum anomalies in high-energy physics

In this section we present a brief review and example of how quantum anomalies may arise. We will focus our discussion on the chiral anomaly. Consider a massless Dirac Lagrangian in the presence of an electromagnetic field, A_μ, which has a Lagrangian of the form

$$\mathcal{L} = i\bar{\Psi}\gamma^\mu(\partial_\mu + ieA_\mu)\Psi - \frac{1}{4}F_{\mu\nu}F^{\mu\nu} \tag{B.1}$$

where Ψ is the Dirac fermion wavefunction, $\bar{\Psi} = \Psi^\dagger\gamma^0$ and $F_{\mu\nu} = \partial_\mu A_\nu - \partial_\nu A_\mu$ is the electromagnetic field tensor. This Lagrangian is invariant under the chiral transformation

$$\Psi \to e^{i\alpha\gamma^5}\Psi \quad , \qquad\qquad \bar{\Psi} \to \bar{\Psi}e^{i\alpha\gamma^5} \quad , \tag{B.2}$$

where $\gamma^5 = i\gamma^0\gamma^1\gamma^2\gamma^3$ is the chiral operator and α is assumed to be real. Using Noether's theorem, this implies that there exists an associated conserved chiral current, $j_5^\mu = i\bar{\Psi}\gamma^\mu\gamma^5\Psi$, which is expressed by

$$\partial_\mu j_5^\mu = 0 \quad . \tag{B.3}$$

However it turns out that, when the system is quantised, this chiral conservation no longer holds. One way to understand this is to consider the partition function of a massless QED system which is given by

$$\mathcal{Z}[A] = \int D[\bar{\Psi}, \Psi] \, \exp(\frac{i}{\hbar}\int \mathcal{L} \, d^4x) \tag{B.4}$$

where we are integrating over the fermionic degrees of freedom and have ignored the ghost fields (and other complications) for the purpose of a simplified demonstration of the concepts. Under the chiral gauge transformations:

$$\Psi \to e^{i\alpha(x)\gamma^5}\Psi \quad , \qquad\qquad \bar{\Psi} \to \bar{\Psi}e^{i\alpha(x)\gamma^5} \quad , \tag{B.5}$$

the Lagrangian $\mathcal{L}$ varies as

$$\mathcal{L} \to \mathcal{L}' = \mathcal{L} + \alpha(x)\,\partial_\mu j_5^\mu \quad . \tag{B.6}$$

Initially one might assume that the variation of the action $S \equiv \int \mathcal{L}\; d^4x$ is

$$\delta S = \int \alpha(x)\,\partial_\mu j_5^\mu d^4x,$$

which is equal to zero when the fields satisfy the equations of motion and hence $\partial_\mu j_5^\mu = 0$. However, this conclusion neglects the fact that the measure $D[\bar{\Psi}, \Psi]$ also varies. When we consider the contribution of the variation due to the measure using the Fujikawa method [96, 30], we obtain an extra term in the action of the form:

$$S_{\text{extra}} = -\int \frac{1}{16\pi^2}\epsilon^{\mu\nu\rho\sigma}\alpha(x)F_{\mu\nu}(x)F_{\rho\sigma}(x)\,d^4x \quad , \tag{B.7}$$

where $\epsilon^{\mu\nu\rho\sigma}$ is the Levi-Cevita tensor. The variation of the partition function now demands that $\int \alpha(x)\,\partial_\mu j_5^\mu d^4x + S_{\text{extra}} = 0$ since the chiral transformation may be regarded simply as a change of variables. Thus we have a chiral current that takes the form

$$\partial_\mu j_5^\mu = \frac{1}{16\pi^2}\epsilon^{\mu\nu\rho\sigma}\alpha(x)F_{\mu\nu}(x)F_{\rho\sigma}(x) \quad . \tag{B.8}$$

which clearly shows that the chiral current is not generally conserved in the presence of an electromagnetic field. Hence we have shown that the term that arises from the variation of the measure [Eq. (B.7)] gives rise to the anomalous behaviour. This highlights that classical symmetries, such as the chiral symmetry, may be violated in quantum systems.

Appendix C

Another formulation of the chiral anomaly

Consider a (magnetic) Weyl semimetal with two Weyl nodes in the Brillouin zone separated by a momentum $\Delta\mathbf{k} = 2Q\hat{z}$. We assume charge neutrality so there is no Fermi surface. The symmetries involved in the "chiral anomaly" are the $U(1)$ charge conservation and the translation symmetry in $\hat{z}$ (call the group $\mathbb{Z}^z$ and the generator T_z).

To see the anomaly, we consider "gauging" the $U(1) \times \mathbb{Z}^z$ symmetry by introducing probe gauge fields A_μ and $z \in H^1(M, \mathbb{Z})$ (M is the space-time manifold). The integer gauge field z associated with translation symmetry [336] has the following properties: it is locally flat ($dz = 0$), and the Wilson loop $\int_{C_1} z \in \mathbb{Z}$ over a 1-cycle C_1 essentially counts the number of $\hat{z}$-translations around C_1, and a unit defect in z represents a lattice dislocation with Burgers vector $\vec{B} = \hat{z}$. To probe the thermal response, we also couple the system (in the continuum limit) to a metric g. The chiral anomaly can be understood as a $(4+1)d$ "bulk" term:

$$S_{CA} = i2Q \int_{M_5} z \cup \left(\frac{1}{2} \frac{dA}{2\pi} \wedge \frac{dA}{2\pi} + \frac{1}{192\pi^2} R \wedge R \right), \tag{C.1}$$

where R is the Riemann curvature. The expression in the parenthesis takes integer value on a 4-cycle – this is nothing but the well-known statement that the periodicity of Θ-angle for charged fermions in $(3+1)D$ is 2π (more formally A is a spin$_c$ connection instead of an ordinary $U(1)$ gauge field). Therefore the coefficient $2Q$ takes continuous value in $[0, 2\pi)$, which is consistent with the interpretation that $2Q$ is the momentum separation between the two Weyl nodes in the non-interacting limit. Of course even for interacting fermions the expression Eq. (C.1) still makes sense.

The physical interpretation of Eq. (C.1) is actually quite simple: there is a Hall conductance per layer $\sigma_{xy} = \frac{\Delta k}{2\pi}$ and thermal Hall conductance per layer $\kappa_{xy} = \frac{\Delta k}{2\pi}(\pi^2 k_B^2 T/3)$, as already discussed in the main text. For $2Q = 2\pi$, these conditions can be satisfied by a gapped state which is equivalent to a stack (in $\hat{z}$ direction) of $2D$ integer quantum Hall states, which is why the anomaly disappears. Again this phenomena is well known from band theory, and we emphasize that it remains well-defined in interacting systems.

The chiral anomaly Eq. (C.1) has another consequence, namely a $U(1)$ instanton with $\int d^3x dt\, \mathbf{E} \cdot \mathbf{B} = 4\pi^2$ carries a lattice momentum $\mathbf{k}_{ins} = 2Q\hat{z}$. In the non-interacting limit this follows from textbook $U(1) \times U(1)$ chiral anomaly, but the statement also makes sense in interacting systems (where the axial $U(1)$ no longer makes sense but the translation $\mathbb{Z}^z$ does). When charged degrees of freedom are gapless (as in the semimetal phase), the lattice momentum overlaps with physical charge current, which leads to a charge current induced by the instanton – this is the well-known magnetoresistance from Weyl semimetal [269]. If the system becomes gapped but still preserves the chiral anomaly as defined in Eq. (C.1), the instanton will still carry lattice momentum, but may not induce a charge current.

We also comment that the anomaly Eq. (C.1) is different from the ones typically encountered in the physics of symmetry-protected topological phases, in the sense that the coefficient $2Q$ is not quantized, and therefore is not strictly "protected". Physically this is simply because one can always smoothly bring the two Weyl cones to the same momentum point and eliminate the anomaly. In our study we keep $2Q$ fixed based on the intuition that we demand nontrivial interactions to take effect well below the electron band width. In the most general parameter space this corresponds to fine tuning one parameter. This is similar to another much more familiar situation: in an ordinary metal the charge density is fixed by tuning the chemical potential. There is also an "anomaly" associated with non-integer charge density, which is related to the celebrated Lieb-Schultz-Mattis theorem [189, 264, 132]. In this case the anomaly also comes with a non-quantized coefficient (the density), and generically require fine tuning the chemical potential [322].

Appendix D

Fermi arcs in the FFLO Weyl superconductor

In this section we discuss the effects of the intranodal s-wave interaction on the Fermi arcs of a magnetic Weyl semimetal. We demonstrate the existence of the Fermi arc surface states despite the FFLO pairing interactions creating a bulk gap [129].

To study the Fermi arcs, we need to extend the linearized Weyl Hamiltonian, used in the main text, to the whole Brillouin zone. We choose the following regularized Hamiltonian

$$\begin{aligned} H_0 = \sin k_x \sigma^x + \sin k_y \sigma^y - (\cos k_z - \cos Q)\, \sigma^z \\ + m\,(2 - \cos k_x - \cos k_y)\, \sigma^z \quad , \end{aligned} \tag{D.1}$$

where $Q = \pi/2$ and the lattice constant has been set to one.

The superconducting s-wave coupling occurs intranodally, i.e. coupling states with momentum $\mathbf{k}$ to those of momentum $2\mathbf{Q} - \mathbf{k}$, where $\mathbf{Q} = (0, 0, \pi/2)$. This situation requires a Nambu basis $\Phi_{\mathbf{k}}^\dagger = (c_{\mathbf{k}\uparrow}^\dagger, c_{\mathbf{k}\downarrow}^\dagger, c_{2\mathbf{Q}-\mathbf{k}\uparrow}, c_{2\mathbf{Q}-\mathbf{k}\downarrow})$ and the Nambu Hamiltonian then takes the form

$$H_0^{\text{Nambu}} = \frac{1}{2} \sum_{\mathbf{k}} \Phi_{\mathbf{k}}^\dagger \begin{pmatrix} H_0(\mathbf{k}) & 0 \\ 0 & -H_0^{\mathrm{T}}(2\mathbf{Q} - \mathbf{k}) \end{pmatrix} \Phi_{\mathbf{k}} \quad . \tag{D.2}$$

In order to calculate the Fermi arc surface states, we break the translational symmetry along the x-direction, leaving a finite-size sample of N_x atomic layers. This leaves k_y and k_z as good quantum numbers. Fourier transforming k_x to a real-space coordinates n_x, the

Hamiltonian takes the form

$$\begin{aligned} H_0^{\text{Nambu}} &= \frac{1}{2}\sum_{n_x k_y k_z} \Phi^\dagger_{n_x k_y k_z}\left[h(k_y,k_z)\Phi_{n_x k_y k_z}\right. \\ &+ \left. h_+\Phi_{n_x+1 k_y k_z} + h_-\Phi_{n_x-1 k_y k_z}\right] . \end{aligned} \tag{D.3}$$

with

$$h(k_y,k_z) = \begin{pmatrix} h_0(k_y,k_z) & 0 \\ 0 & -h_0^{\mathrm{T}}(-k_y, 2Q-k_z) \end{pmatrix} \quad , \tag{D.4}$$

$$h_+ = -\frac{1}{2}\left(i\sigma^x + m\tau^z\sigma^z\right) = h_-^\dagger \quad , \tag{D.5}$$

where $h_0(k_y,k_z) = \sin k_y\sigma^y + \big[-(\cos k_z - \cos Q) + m(2-\cos k_y)\big]\sigma^z$, and $\boldsymbol{\tau}$ are Pauli matrices in the Nambu pseudospin space. Diagonalizing this Hamiltonian at every k_z for the $k_y = 0$ slice gives eigenenergies as shown in Fig. D.1a. Since the components of the Nambu spinor involve states at momenta $\mathbf{k}$ and $2\mathbf{Q}-\mathbf{k}$, the set of eigenenergies effectively involve states, shifted by $2Q = \pi$ relative to each other. The same principle applies to the Fermi surface states which now span the whole Brillouin zone. Notice that this is purely the result of the doubling of degrees of freedom in the Nambu formalism. Naturally this has no effect on the bulk Weyl nodes at $k_z = \pm Q$.

Now let us observe what happens when we couple the two Nambu copies in Eq. D.2 with the FFLO pairing interaction of the form

$$H_{\text{int}} = \frac{1}{2}\sum_{\mathbf{k}} \Phi^\dagger_{\mathbf{k}}\Delta\tau^y\sigma^y\Phi_{\mathbf{k}} \quad . \tag{D.6}$$

Under a Fourier transform of k_x, we arrive at

$$H_{\text{int}} = \frac{\Delta}{2}\sum_{n_x k_y k_z} \Phi^\dagger_{n_x k_y k_z}\tau^y\sigma^y\Phi_{n_x k_y k_z} \quad , \tag{D.7}$$

such that our full Hamiltonian is now given by

$$H = H_0^{\text{Nambu}} + H_{\text{int}} \quad . \tag{D.8}$$

When this full Hamiltonian is now diagonalised at every k_z for the $k_y = 0$ slice we arrive at Fig. D.1b. While the bulk states are now gapped, the Fermi arc, spanning the whole Brillouin zone, remains unaffected.

D.1 Helical Majorana fermions in a vertical vortex line

Let us consider a straight-line vortex of vorticity n along the z-direction, which we will take to coincide with the direction of the vector $2\mathbf{Q}$, separating the pair of Weyl nodes. The corresponding Bogoliubov-de Gennes (BdG) Hamiltonian is given by

$$\begin{aligned} H &= -iv_F\tau^z(\sigma^x\partial_x + \sigma^y\partial_y) + v_F\tau^z\sigma^z k_z \\ &+ \Delta(r)[\cos(n\theta)\tau^x - \sin(n\theta)\tau^y], \end{aligned} \tag{D.9}$$

where $r = \sqrt{x^2+y^2}$, $\Delta(r)$ is the real magnitude of the superconducting order parameter and θ is the azimuthal angle in the xy-plane. The eigenstates of H may be easily found explicitly if one assumes $\Delta(r) = \Delta = \text{const}$ [300]. In this case one finds exactly n chiral modes, localized in the vortex core, with the following wavefunctions

$$\Psi_{pk_z}(\mathbf{r}) = \frac{(\Delta r/v_F)^{\frac{n}{2}}}{\sqrt{\mathcal{N}_p}} \begin{pmatrix} e^{i\frac{\pi}{4}} e^{i(p-1)\theta} K_{\frac{n}{2}-p+1}\left(\frac{\Delta r}{v_F}\right) \\ 0 \\ 0 \\ e^{-i\frac{\pi}{4}} e^{-i(n-p)\theta} K_{\frac{n}{2}-p}\left(\frac{\Delta r}{v_F}\right) \end{pmatrix}, \tag{D.10}$$

where $\mathcal{N}_p$ is a normalization factor given by

$$\mathcal{N}_p = \frac{\pi^{3/2} v_F^2}{\Delta^2} \frac{\Gamma(1+n/2)\Gamma(n-p+1)\Gamma(p)}{\Gamma(n/2+1/2)}, \tag{D.11}$$

which is finite and positive when $p = 1, \ldots, n$. As mentioned above, these localized modes are chiral with the dispersion $\epsilon_p(k_z) = v_F k_z$. The degeneracy of the chiral modes with respect to the eigenvalue p is not protected and is lifted when perturbations, such as a finite Fermi energy, are introduced. A finite Fermi energy leads to a term $-\epsilon_F\tau^z$ in the BdG Hamiltonian Eq. (D.9). The problem may no longer be solved exactly (except at $k_z = 0$), but may be solved perturbatively. At first order one obtains

$$\epsilon_p(k_z) = \epsilon_F\left(1 - \frac{2p}{n+1}\right) + v_F k_z. \tag{D.12}$$

Thus, even though the degeneracy is lifted, exactly n fermionic modes are still always present at zero energy in the core of an n-fold vortex. This is in contrast to the analogous

problem of vortex bound states in a superconducting 2D Dirac fermion [98], in which case there is always a single zero mode for odd vorticities and no zero modes for even vorticities. The left-handed Weyl node will have an identical set of modes, but with the left-handed dispersion (simply send $v_F \to -v_F$).

The nontrivial helical Majorana modes in a straight, vertical vortex with odd vorticity can also be understood using the argument in the main text. Recall that a Majorana zero mode is induced whenever a odd vortex penetrates the xy-plane. For a straight, vertical vortex the translation T_z is a good symmetry. We can therefore view the vortex line as a 1D translationally-invariant chain with one Majorana zero mode per unit cell. Such a system has a Lieb-Schultz-Mattis type of constraints on the low energy theory, and cannot be gapped without breaking translation symmetry [144].

For even vorticity, taking $\epsilon_F = 0$, pairs of Majorana modes may be combined into chiral 1D Weyl modes. Since the charge conservation is already violated, pairing terms are always present for these Weyl modes, and they are gapped out by the ordinary BCS pairing interaction of the form

$$H = v_F \sum_{k_z} [k_z c^\dagger_{k_z} \tau^z c_{k_z} + \Delta(c^\dagger_{k_z} i\tau^y c^\dagger_{-k_z} + \text{h.c.})/2], \tag{D.13}$$

where the eigenvalues of τ^z label the chirality of the 1D Weyl modes. This state is also stable to small fluctuations in ϵ_F since it is gapped. Thus vortices with even vorticity do not have zero modes in their cores.

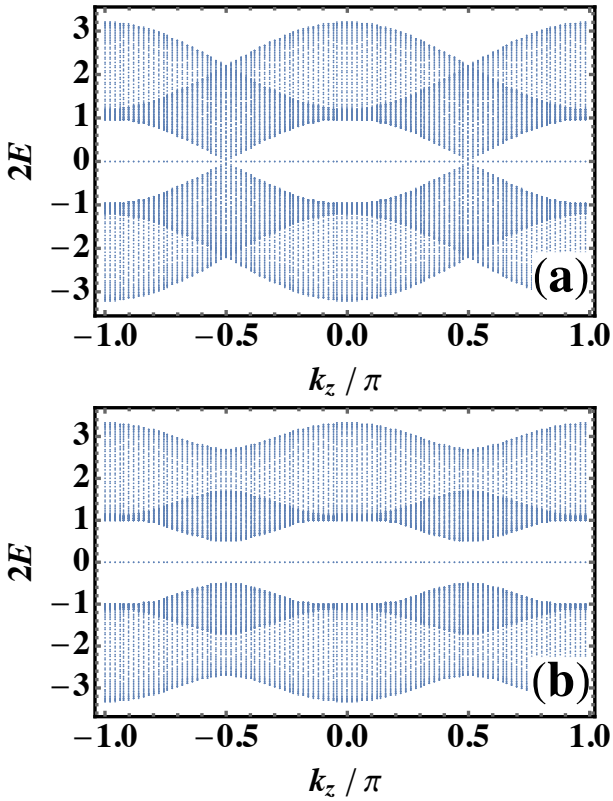

Figure D.1: (Color online) Energy eigenstates for $k_y = 0$ slice along k_z corresponding to Nambu Hamiltonians given by Eq. D.3 (a) and D.8 (b). (a) The zero mode spans the entire Brillouin zone due to doubling of degrees of freedom in the Nambu picture. (b) Intranodal interaction gaps out the bulk Weyl nodes but leaves the surface states unaltered. For both figures $m = 1.1$, $N_x = 50$ and for (b) $\Delta = 0.5$.

Appendix E

Some formal details on vortex condensation in (3+1) dimensions

Here we briefly review some formal aspects of vortex condensation in $(3+1)$ dimensions. The logic is in fact very similar to that used in $(2+1)$ dimensional vortex condensation.

Consider a charged system in $(3+1)$ dimensions (Euclidean for simplicity), with conserved $U(1)$ current satisfying continuity equation $\partial_\mu j_\mu = 0$. This equation can be solved by re-writing

$$j_\mu = \frac{1}{2\pi}\epsilon_{\mu\nu\lambda\rho}\partial_\nu b_{\lambda\rho}, \tag{E.1}$$

where $b_{\lambda\rho}$ is an anti-symmetric two-form gauge field, and the normalization is chosen so that a 2π flux in $\int db$ corresponds to a unit charge of $\int_{space} j^0$ – namely b obeys standard Dirac quantization. For the rest of this section we take unit charge to be $2e$ (Cooper pair), so the coupling to electromagnetism is $2A_\mu j_\mu$.

A free Maxwell-like theory of b, $\mathcal{L} \sim (\partial_{[\nu} b_{\lambda\rho]})^2$ ($[,]$ represents anti-symmetrization) corresponds to a superconductor. This can be most easily seen by integrating out the b fields (which can be done since the theory is Gaussian), and obtain an effective response theory $\sim A^2$. Vorticity in this superconductor is represented as a two-form antisymmetric "current" $J_{\mu\nu}$ that couples to the b field through $J_{\mu\nu}b_{\mu\nu}$. Gauge invariance in b (or simply the fact that vortex lines do not terminate) requires a continuity equation on J which reads $\partial_\mu J_{\mu\nu} = 0$. This can be solved by re-writing

$$J_{\mu\nu} = \frac{1}{2\pi}(\partial_\mu a_\nu - \partial_\nu a_\mu), \tag{E.2}$$

where a_μ is a dynamical $U(1)$ gauge field – the normalization is chosen so that a 2π flux loop in a corresponds to a single vortex.

Now a "vortex condensation" of the simplest kind, where single vortices (together with all higher vortices) have condensed, means that the gauge field a has only a Maxwell action $(\partial_{[\mu} a_{\nu]})^2$. At low energy the Maxwell terms for both a and b becomes irrelevant and we are left with the topological action

$$\mathcal{L} = \frac{1}{2\pi}\epsilon_{\mu\nu\lambda\rho} b_{\mu\nu} \partial_\lambda a_\rho - \frac{2}{2\pi}\epsilon_{\mu\nu\lambda\rho} b_{\mu\nu} \partial_\lambda A_\rho. \tag{E.3}$$

This is also known as a BF theory and describes a gapped phase of matter. With the coefficients in the above equation, this particular BF theory describes a trivial insulator with no intrinsic topological order.

Now consider condensing n-fold vortices ($n > 1$), leaving all the lower vortices uncondensed. This is formally implemented by writing $a = n\tilde{a}$ in Eq. (E.2) where $\tilde{a}$ obeys standard Dirac quantization, and introduce Maxwell term for $\tilde{a}$. The physical meaning is that J can only fluctuate in units of n, which is what we mean by n-fold vortices. Now the resulting BF theory at low energy becomes

$$\mathcal{L} = \frac{n}{2\pi}\epsilon_{\mu\nu\lambda\rho} b_{\mu\nu} \partial_\lambda \tilde{a}_\rho - \frac{2}{2\pi}\epsilon_{\mu\nu\lambda\rho} b_{\mu\nu} \partial_\lambda A_\rho. \tag{E.4}$$

This is known to represent a $\mathbb{Z}_n$ topological order, with particle charges of $\tilde{a}$ being the topological particle excitations, and line charges of b being the topological loop excitations. Charge fractionalization on the particles can also be seen by introducing a $\tilde{j}_\mu \tilde{a}_\mu$ term and taking variation on b, which leads to $\frac{2}{n} A_\mu \tilde{j}_\mu$, meaning that the topological quasi-particle carries electric charge $2/n$. The example considered in this work corresponds to $n = 4$.

Appendix F

The $\mathbb{Z}_2 \times \mathbb{Z}$ anomaly in $(1+1)d$: exceptional points and emergent anomalies

We analyze the low energy theory with four chiral fermions in the bosonized language. The Luttinger liquid consists of four compact bosons $e^{i\phi_I}$ ($I \in \{1,2,3,4\}$), with the Lagrangian

$$\mathcal{L} = -\frac{1}{4\pi}\left[K_{IJ}\partial_t\phi_I\partial_z\phi_J + V_{IJ}\partial_z\phi_I\partial_z\phi_J\right] \quad , \tag{F.1}$$

where

$$K = \begin{pmatrix} 1 & 0 & 0 & 0 \\ 0 & 1 & 0 & 0 \\ 0 & 0 & -1 & 0 \\ 0 & 0 & 0 & -1 \end{pmatrix} \quad , \tag{F.2}$$

and $V = v_F\mathbb{1}$ is the velocity matrix. The fermion creation operators are expressed as $\psi_I^\dagger \sim \kappa^+ e^{i\phi_I}$, where κ^+ are the Klein factors, taking care of the anticommutation relations between different species of fermions. Upon the charge $U(1)$, translational $\mathbb{Z}$ and $\mathbb{Z}_2$ symmetry transformations, the boson phases change as

$$\begin{aligned} U(1): &\quad \phi_I \to \phi_I + \theta \quad , \\ \mathbb{Z}: &\quad \phi_I \to \phi_I + k_I \quad , \\ \mathbb{Z}_2: &\quad \phi_I \to \phi_I + \gamma_I \quad , \end{aligned} \tag{F.3}$$

where $k_I = \pi\nu(1,-1,1,-1)$ and $\gamma_I = \pi(1,0,0,1)$.

We now gap out the fermions by breaking the translation symmetry, keeping $U(1)\times\mathbb{Z}_2$, through a CDW order parameter

$$m[e^{i(\phi_1-\phi_4)} + e^{i(\phi_3-\phi_2)}] + h.c. \quad , \tag{F.4}$$

Under translation $m \to e^{i2\pi\nu}m$. For $\nu \in \mathbb{Q}$, we write $\nu = p/q$ with coprime $p, q \in \mathbb{Z}$. Then m takes value in $\mathbb{Z}_q$. A domain wall of m is defined as a nonlocal operator, such that the CDW operator Eq. (F.4) rotates by a phase $e^{i2\pi/q}$ when commuted with the domain wall. It is not hard to see that the appropriate choice of the domain wall operator is

$$\sigma = \exp\left[i\frac{(\phi_1+\phi_4)-(\phi_2+\phi_3)}{2q}\right] \quad . \tag{F.5}$$

This operator transforms trivially under $U(1)$ (this is expected since the $U(1)\times\mathbb{Z}$ filling anomaly vanishes in this case), but under $\mathbb{Z}_2$ it transforms as

$$\mathbb{Z}_2: \quad \sigma \to e^{i\pi/q}\sigma \quad . \tag{F.6}$$

For even q, the above transformation signals fractional (or projective) $\mathbb{Z}_2$ symmetry charge on σ. For odd q, we can choose a different gauge, for example by demanding that under $\mathbb{Z}_2$: $\phi_{1,4} \to \phi_{1,4} + q\pi$. In this gauge $\mathbb{Z}_2 : \sigma \to -\sigma$, so σ no longer carries fractional charge under $\mathbb{Z}_2$.

We can also consider irrational values of ν (incommensurate CDW). In this case the CDW order parameter m lives on $U(1)$. If we try to disorder m and recover translation symmetry, we should proliferate vortices of m. The vortex operator of m is simply

$$V = \exp\left[i\frac{(\phi_1+\phi_4)-(\phi_2+\phi_3)}{2}\right] \quad , \tag{F.7}$$

which transforms nontrivially under $\mathbb{Z}_2 : V \to -V$. Notice vortices are local operators and we are not free to attach other local operators to it. Therefore the nontrivial action of $\mathbb{Z}_2$ on the vortex operator signals an obstruction to having a symmetric gapped phase.

The above discussions can be rephrased in terms of emergent anomalies[228]. First, as the $U(1)$ gauge field does not explicitly appear in the anomaly Eq. (3.22), we can view the anomaly as coming entirely from the charge neutral sector of the system. But since charge neutral objects are all bosonic in the system, we will only need to consider bosonic anomalies. The t'Hooft anomaly in $(1+1)d$ corresponds to symmetry-protected topological (SPT) phases in $(2+1)d$, which are classified by group cohomology $H^3(G, U(1))$ [59, 60].

For rational $\nu = p/q$, the translation symmetry acts on the low energy theory effectively as a $\mathbb{Z}_q$ symmetry (up to some $U(1)$ gauge transforms). Neglecting $U(1)$ from now on, the effective symmetry group of the low energy theory is $\mathbb{Z}_2 \times \mathbb{Z}_q$. In $(2+1)d$ the mutual anomaly between $\mathbb{Z}_2$ and $\mathbb{Z}_q$ is classified [60] by $\mathbb{Z}_{(2,q)}$ which is $\mathbb{Z}_2$ for even q and trivial for odd q. Therefore for odd q the anomaly of the Luttinger liquid considered above automatically vanishes. For even q, using standard argument (see for example Ref. [204]) the Luttinger liquid described in Eq. (F.1), (F.2) and (F.3) (with $\mathbb{Z}$ replaced by $\mathbb{Z}_q$ in Eq. (F.3)) has a nontrivial $\mathbb{Z}_2$ anomaly. The anomaly can be described by the $(2+1)d$ bulk action $(\pi/q)cda$, where $a \in H^1(\mathcal{M}, \mathbb{Z}_q)$ and $c \in H^1(\mathcal{M}, \mathbb{Z}_2)$. The anomaly vanishes in the bulk once we re-insist that $a = z$ is in fact a $\mathbb{Z}$-valued (instead of $\mathbb{Z}_q$) gauge field and we recover Eq. (3.22) (up to the equivalence relation Eq. (3.25)).

The logic is similar for irrational $\nu = p/q$, except that now $\mathbb{Z}$ acts in the low energy theory effectively as a $U(1)$ symmetry (call it $U(1)_z$ to avoid confusing it with the charge conservation $U(1)$). The Luttinger liquid in Eq. (F.1), (F.2) and (F.3) (with $\mathbb{Z}$ replaced by $U(1)_z$ in Eq. (F.3)) now has a t'Hooft anomaly, described by the $(2+1)d$ bulk action $\pi c dA_z$. Again the anomaly vanishes in the bulk when we insist that $A_z = \nu z$ with z being an integer-valued gauge field.

Appendix G

Stability analysis of the $\mathbb{Z} \times \mathbb{Z}$ anomaly

To further support the nontriviality of the $\mathbb{Z} \times \mathbb{Z}$ anomaly discussed in Sec. 3.3.3, we perform an explicit stability analysis using Luttinger liquid theory. Specifically, we will show that a symmetric gapped state cannot be achieved through symmetric perturbations using the Haldane's Luttinger liquid stability analysis [182, 183].

To address the Luttinger liquid physics, we focus on the four low-energy fermionic modes: two right-movers ψ_1 at $-k_+$, ψ_2 at k_+, and two left-movers ψ_3 at $-k_-$, ψ_4 at k_-. Via the standard bosonization procedure, we may then describe these low-energy modes in terms of bosons $e^{i\phi_I}$ ($I \in \{1,2,3,4\}$), with the Lagrangian

$$\mathcal{L} = -\frac{1}{4\pi}\left[K_{IJ}\partial_t\phi_I\partial_z\phi_J + V_{IJ}\partial_z\phi_I\partial_z\phi_J\right] \quad , \tag{G.1}$$

where

$$K = \begin{pmatrix} 1 & 0 & 0 & 0 \\ 0 & 1 & 0 & 0 \\ 0 & 0 & -1 & 0 \\ 0 & 0 & 0 & -1 \end{pmatrix} \quad ,$$

and $V = v_F\mathbb{1}$ is the velocity matrix. The fermion creation operators are expressed as $\psi_I^\dagger \sim \kappa^+ e^{i\phi_I}$, where κ^+ are the Klein factors, taking care of the anticommutation relations between different species of fermions. Upon the charge $U(1)$ and translational symmetry

transformation, the boson phases change as

$$\begin{aligned} U(1): &\quad \phi_I \to \phi_I + \theta \quad , \\ T_z: &\quad \phi_I \to \phi_I + k_I \quad , \end{aligned}$$

where $k_I = (-k_+, k_+, -k_-, k_-)$.

We now wish to examine whether we can gap these low-energy modes via symmetry-preserving interactions. A general product of creation and annihilation operators in this language will take the form $e^{i\Lambda^T\phi}$, where Λ is a four component integer vector. The particular perturbations we examine are of the form

$$U(\Lambda) = U(z)\cos\left(\Lambda^T\phi - \alpha(z)\right) \quad . \tag{G.2}$$

This term describes the scattering of electrons between the modes of opposite chirality. Since we have two sets of chiral modes, we must add two sets of backscattering terms $\sum_{i=1}^{2} U(\Lambda_i)$ with two linearly independent Λ_1 and Λ_2 terms. As the amplitude of U is increased, we eventually will reach a symmetric gapped state, provided there exists a suitable symmetry-respecting set of $\{\Lambda_i\}$. However we will now show that such a set does not exist.

The Λ_i must satisfy several conditions, including symmetry conditions

$$\sum_I [\Lambda_i]_I = 0 \quad , \tag{G.3}$$

$$\sum_I [\Lambda_i]_I \ \frac{k_I}{2\pi} = n \quad , \tag{G.4}$$

derived from the $U(1)$ charge and translational symmetry respectively, where the conditions must be satisfied for some $n \in \mathbb{Z}$. We will limit out stability analysis to the charge-conserving Luttinger liquids only, keeping in mind application to the $3+1$d topological semimetals in the following section.

Additionally we must impose the Haldane null vector criterion [182]

$$\Lambda_i^T K \Lambda_j = 0 \quad , \tag{G.5}$$

which essentially guarantees that there exists a linear transformation $\phi \to M\phi$ that decouples the Lagrangian into two non-chiral Luttinger liquids, which may be gapped out by the backscattering terms.

We first consider rational values of $k_\pm$. Let $\frac{k_+}{2\pi} = \frac{p}{q}$ and $\frac{k_-}{2\pi} = \frac{l}{m}$, where $p, q, l, m \in \mathbb{Z}$ and p, q and l, m are respective coprimes. The conditions given by Eqs. (G.3), (G.4) and (G.5) yield the general solution

$$\Lambda_i = [\Lambda_i]_1 \begin{pmatrix} 1 \\ 1 \\ -1 \\ -1 \end{pmatrix} + \tilde{n}_\pm \begin{pmatrix} 0 \\ qm \\ -qm \\ 0 \end{pmatrix} \quad , \tag{G.6}$$

where $\tilde{n}_\pm = \frac{n}{pm \pm lq} \in \mathbb{Z}$. Now that the general solution is found, the final step is to find two linearly independent Λ vectors which do not spontaneously break any relevant symmetries when the gap is opened. Specifically we need to check that for all combination a_1 and a_2 with no common factors there does not exist $a_1\Lambda_1 + a_2\Lambda_2 = b\Lambda_3$, where $b \in \mathbb{Z}$, such that Λ_3 is an integer vector that does not obey symmetry constraints given in Eqs. (G.3) and (G.4). This last condition is known as the *primitivity* condition. It is this constraint in combination with the necessity of two linearly independent Λ_1 and Λ_2 terms that causes any solution of the form in Eq. (G.6) to fail: any linearly independent choice of Λ_1 and Λ_2 will always result in $\Lambda_3 = (0, 1, -1, 0)^T$, which breaks the translational symmetry. Thus we cannot open a gap with perturbations of the form $U(\Lambda)$ without spontaneously breaking any symmetries. A similar consideration for irrational values of $k_\pm$ also shows that a gap cannot be opened.

We comment that in principle there is the possibility that a gap can be opened if we include additional "trivial" Luttinger liquids into the theory and couple the additional modes with the original modes. Therefore the analysis here does support, but not prove, the nontriviality of the theory.

Appendix H

Lowest Landau Levels for type-I DSM

The Hamiltonian of a C_4-symmetric type-I Dirac semimetal in an external magnetic field along the z-direction is given by

$$H_{\pm}(\mathbf{k}) = t\pi_x\sigma^x s^z - t\pi_y\sigma^y + m(0,0,k_z)\sigma^z \quad , \tag{H.1}$$

where $\pi_\alpha = -i\partial_\alpha - A_\alpha$, $\nabla \times \mathbf{A} = B_z\hat{z}$, and $[\pi_x, \pi_y] = -ieB_z$, $\alpha \in \{x, y\}$. We may easily solve this by squaring the Hamiltonian to give

$$H_{\pm}(\mathbf{k})^2 = t^2\left(\pi_x^2 + \pi_y^2 - eB_z\sigma^z s^z\right) + m(0,0,k_z)^2, \tag{H.2}$$

which may be written as

$$H_{\pm}(\mathbf{k})^2 = 2eB_z t^2\left(a^\dagger a + \frac{1}{2}(1 - \sigma^z s^z)\right) + m(0,0,k_z)^2, \tag{H.3}$$

using the standard ladder operators

$$a = \frac{1}{\sqrt{2eB_z}}\left(\pi_x - i\pi_y\right), \qquad a^\dagger = \frac{1}{\sqrt{2eB_z}}\left(\pi_x + i\pi_y\right).$$

This gives the LLL dispersions $\pm m(0,0,k_z)$ with the corresponding eigenvectors

$$|\Psi_1\rangle = \begin{pmatrix}1\\0\\0\\0\end{pmatrix}|0\rangle \quad , \qquad |\Psi_2\rangle = \begin{pmatrix}0\\0\\0\\1\end{pmatrix}|0\rangle \quad , \tag{H.4}$$

where $|0\rangle$ is the state with $a^\dagger a|0\rangle = 0$. These are also eigenstates of C_{4z}, with eigenvalues $C_4\Psi_1 = e^{i0}\Psi_1$ and $C_4\Psi_2 = e^{i\pi}\Psi_2$.

Appendix I

Higher dimensional FD quantum circuit

Here we will show that a higher dimensional (d > 1) FD quantum circuit viewed in 1d (say along $\hat{x}$), where each enlarged unit cell Hilbert space is now exponential in the transverse dimension $\prod_i L_i$, is also a FD quantum circuit.

To see this, let us decompose the higher dimensional FD quantum circuit U into two sets of unitaries via 'zig-zag' cuts following lightcone pathways along $\hat{x}$. We depict an example of such a cut applied to a 2d FD quantum circuit U in Fig. I.1. The two sets of unitaries consist of self-commuting 'extended lightcone' unitaries $\{V_i\}$ and a set of self-commuting 'extended reverse lightcone' unitaries $\{W_i\}$, such that $U = \prod_i W_i \prod_j V_j$. Due to the finite correlation length ξ in SRE systems and correlations necessarily arise from the lightcone structure, each unitary component spans $\sim \xi \ll L$ unit cells in $\hat{x}$. This decomposition forms a 1d FD quantum circuit with two layers ($\{V_i\}$ and $\{W_i\}$).

Thus we have shown that higher-dimensional SRE states remain SRE when viewed in 1d.

We now discuss a somewhat subtle example to further illustrate the point[1]. Consider a $(2+1)d$ system of fermions with global symmetry $\mathbb{Z}_2 \times \mathbb{Z}_2^f$ where $\mathbb{Z}_2^f$ is the fermion parity conservation. Essentially we have two flavors of fermions, one that transforms trivially under the global $\mathbb{Z}_2$ and another that transforms with a minus sign. Now put the $\mathbb{Z}_2$-even fermion in a $p+ip$ superconductor and the $\mathbb{Z}_2$-odd fermion in a $p-ip$ superconductor. It seems natural to consider this state SRE since the state can be trivialized by breaking the

[1]We thank an anonymous referee for raising this example.

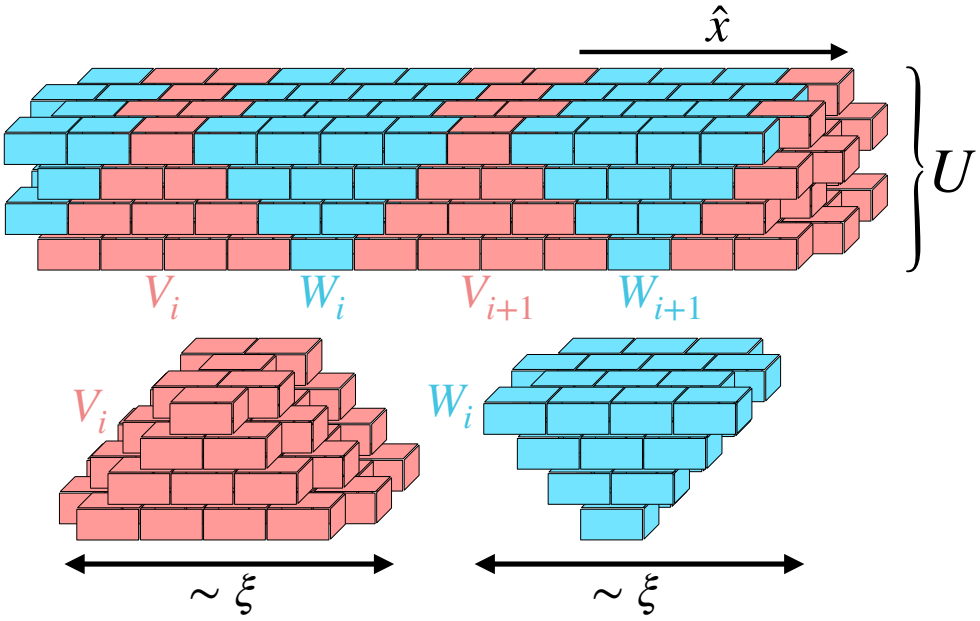

Figure I.1: (Color online) A sample 2d FD quantum circuit U decomposed along $\hat{x}$ into 'extended lightcone' unitaries $\{V_i\}$ (shaded red) and 'extended reverse lightcone' unitaries $\{W_i\}$ (shaded blue). The exact position to begin the lightcone cut is variable, although here we have done so symmetrically.

$\mathbb{Z}_2$ symmetry (which can be seen, for example, by examining the edge states). However, it turns out that when put on torus, the state is strictly SRE only if the two fermions ($\mathbb{Z}_2$ even and odd) have the same boundary conditions in space. If the two fermions have opposite boundary conditions – say one with periodic and the other with anti-periodic boundary conditions in $\hat{y}$, then when viewed as a one-dimensional system along $\hat{x}$, the system forms a Kitaev chain with unpaired Majorana zero modes at the ends. Crucially, a Kitaev chain does not require any global symmetry (besides the $\mathbb{Z}_2^f$ which is anyway un-breakable) and therefore cannot be adiabatically connected to a trivial state. Such "invertible" topological state is considered LRE in the definition adopted in this work. So by simply twisting the boundary condition in $\hat{y}$ direction, we have converted a SRE state to a LRE one!

The above example in fact does not contradict our result in this section. What it really shows is that the $\mathbb{Z}_2$ boundary condition cannot be twisted adiabatically for this state. Namely, there is no adiabatic path (FD quantum circuit) that can change the boundary condition (along a space cycle) from $\mathbb{Z}_2$-periodic to $\mathbb{Z}_2$-anti-periodic. Indeed the most familiar adiabatic operation that could change the boundary condition (say in $\hat{y}$) involves

creating two $\mathbb{Z}_2$ vortices, moving one in $\hat{x}$ across the entires system, and re-annihilate with the other one at the end. This process requires a time scale (or circuit depth) of order $O(L_x)$. One may wonder if a more clever construction can bring the circuit depth down to $O(1)$, but the previous discussion on the SRE vs. LRE nature shows that this is impossible[2].

[2]If the symmetry is not $\mathbb{Z}_2$ but a continuous one such as $U(1)$, the twist can be achieved adiabatically by slowly threading a (continuous) gauge flux. So for continuous symmetries we do not expect the SRE vs. LRE nature to change under twisted boundary conditions – this is indeed compatible with the fact that $p \pm ip$ superconductors are not compatible with $U(1)$ symmetry.

Appendix J

Proof for fermion systems

In this section we will carefully go through the 1d proof for fermionic systems. The key difference between fermionic and bosonic systems, as discussed in Sec. 4.2.3, is that a product state in fermion system has momentum $P = 0 \mod \pi$ instead of mod 2π for bosons. More specifically, for fermion systems with odd system length, all product states have zero momentum, just like the bosonic case. However for even system length, product states may either have zero or π momentum depending on the fermion parity per site being even or odd respectively.[1] Additionally we note that for even system length all translation symmetric product states possess even total fermion parity.

Fermionic local unitaries are defined via fermion parity preserving Hamiltonians [121], and thus can only be represented via parity preserving FD quantum circuits. More specifically, since parity is an on-site symmetry, each unitary that makes up the parity preserving FD quantum circuit must themselves be parity preserving. The proof in Sec. 4.2.1 directly carries over for SRE fermionic systems, but we must now keep in mind the system size and total fermion parity of the system. These initial conditions lead to different possibilities dependent on the achievable translation symmetric fermionic product states, as alluded to above.

The proof for odd length fermionic systems for both even and odd total fermion parity follows step by step with the bosonic proof. For example, in *Step 1* there is no trouble with 'cutting' a system of length $L = mn$ into m segments of length n since the amount of segments (m) will still be odd if L is odd. The resulting odd number of segments implies

[1] Here we demand the translationally-invariant product state to be an eigenstate for the fermion parity in each unit cell. This is because the state must be an eigenstate of the total fermion parity, as required by the fermion parity superselection rule.

trivial momentum when translating by n such that $nP(L) = 0 \mod 2\pi$, just as in the bosonic case. Similarly, in *Step 2*, we may always glue n amounts of length L segments with n being odd; nL will still be odd so that we may then apply *Step* 1 to arrive at the same conclusion that $P(L) = 0 \mod 2\pi$.

The story is slightly more complicated for even length fermionic systems. Let us first consider the even total parity case. Here, in *Step 1* we must be careful when we cut the $L = mn$ length system into m length n segments. If m is even, then we have the condition $nP(L) = 0 \mod \pi$ (note that this is π instead of 2π). If m is odd, then n must be even, and we have the condition $nP(L) = 0 \mod 2\pi$. If L is divisible by two mutually-coprime numbers $p_1 \gg \xi$ and $p_2 \gg \xi$, i.e. $L = p_1 p_2 p_3$ for some $p_3 \in \mathbb{Z}^+$, then we have two scenarios: 1. One is even, say p_1, and one is odd, say p_2, such that we have $p_1 P(L) = 0 \mod \pi$, $p_2 P(L) = 0 \mod 2\pi$ for which we conclude $P(L) = 0 \mod \pi$; 2. Both p_1, p_2 are odd (in this case p_3 will be even such that L is even), then we have $p_1 P(L) = 0 \mod \pi$ and $p_2 P(L) = 0 \mod \pi$ such that $P(L) = 0 \mod \pi$. So the best condition we may arrive at is $P(L) = 0 \mod \pi$, as opposed to $P(L) = 0 \mod 2\pi$ in the bosonic case. For length that *Step 1* does not cover (e.g. $L = 2p$ where p is a prime and $2 \ll \xi$), we again turn to *Step 2*. Here the proof for the bosonic case applies with a minor alteration that in the final step, after the glueing procedure, we can only conclude via *Step 1* that $nP(L) = 0 \mod \pi$. Choosing two mutually-coprime values for n, we may then conclude that $P(L) = 0 \mod \pi$ for all L. Here we may intuitively gain an understanding of the $\mod \pi$ factor from observing the translation symmetric product states with even total fermion parity on even system lengths: the fermion vacuum state $|\mathbf{0}\rangle$ possesses zero momentum and a state with one fermion per site, say $\prod_{i=1}^{L} c_i^\dagger |\mathbf{0}\rangle$ possesses π momentum. The two states can be related to one another via a fermionic FD quantum circuit, e.g. a layer of $|0\rangle_i \otimes |0\rangle_{i+1} \to c_i^\dagger c_{i+1}^\dagger |0\rangle_i \otimes |0\rangle_{i+1}$ operators. This indicates that for SRE states zero and π momentum may be adiabatically connected with each other, thus leading to $\mod \pi$ rather than $\mod 2\pi$.

The story is drastically different for even length systems with odd total fermion parity. Here, the cutting procedure in *Step 1* leads to a contradiction: for $L = mn$ with $m, n \gg \xi$, m and/or n must be even. Let m be even such that we may create a FD quantum circuit that can divide the system into m identical segments of length n. However since m is even and the segments are identical then the total fermion parity must be even. This contradicts our initial assumption, so we must conclude that the initial state cannot be SRE, i.e. a FD quantum circuit that divides the system cannot be created since the FD quantum circuit $U : |\Psi_{P(L)}\rangle \to |\mathbf{0}\rangle$ does not exist. For lengths that *Step 1* does not cover, we may again apply the logic of *Step 2* to arrive at a contradiction: if $|\Psi_{P(L)}\rangle$ is SRE then, via the glueing procedure, we may construct a FD quantum circuit for length nL

with odd n such that the total fermion parity is still odd. n may always be chosen such that $nL = \tilde{n}\tilde{m}$ with $\tilde{m}$ is even and $\tilde{m} \gg \xi$ so we may again create a circuit that divides the system into $\tilde{m}$ identical segments of length $\tilde{n}$, from which we conclude that the total fermion parity is even. By contradiction, this means that all translation symmetric even length fermionic systems with odd total fermion parity must be LRE. Intuitively this may be understood since there exist no even length translation symmetric product states with odd total fermion parity.

Appendix K

Weak CDW example - Toric code

In this section we will demonstrate the effects of weak translation symmetry breaking and anyon condensation on a well-known $\mathbb{Z}_2$ topological order example: the Toric code with a gauge charge at each lattice site.

Take such a modified Toric code on a square lattice $L_x \times L_y$ with even L_x and odd L_y and periodic boundary conditions, with a Hamiltonian given by

$$H = J_e \sum_{+} \prod_{i \in +} \sigma_x - J_m \sum_{\square} \prod_{i \in \square} \sigma_z \quad , \tag{K.1}$$

where $J_e, J_m > 0$. Here we have chosen a positive sign in front of the + term instead of the usual negative sign, which corresponds to a configuration with a gauge charge ("e" anyon) at each lattice site. By construction this system respects translation symmetry in x and y, enacted by operators T_x and T_y.

Let us define large cycle electric and magnetic charge operators $V_x = \prod_{\bar{C}_x} \sigma_x$, $V_y = \prod_{\bar{C}_y} \sigma_x$, $W_x = \prod_{C_x} \sigma_z$, $W_y = \prod_{C_y} \sigma_z$, where $C_{x,y}$ are given by cycles along the lattice links in the x/y directions and $\bar{C}_{x,y}$ are cycles in the x/y direction that are perpendicular to the lattice links. Physically these operators correspond to creating anyon pairs (charge "e" excitations for W operators and flux "m" excitations for V operators), moving one of the anyons along the relevant cycle and then re-annihilating the anyons.

The degenerate ground states of such a system may be derived from the following translation symmetric topological ground state

$$|\mathbf{0}\rangle = (1 + V_x) \prod_{+} (1 - \prod_{i \in +} \sigma_x) |\Uparrow\rangle \quad , \tag{K.2}$$

where $|\Uparrow\rangle$ is the all spin-up state and for simplicity we have ignored normalization. This state is an eigenstate of V_x and W_x with eigenvalue $|v_x, w_x\rangle = |1, 1\rangle$. Due to the relations

$$W_x V_y = -V_y W_x \quad , \qquad W_y V_x = -V_x W_y \quad , \tag{K.3}$$

$$T_x V_y |\mathbf{0}\rangle = -V_y T_x |\mathbf{0}\rangle \quad , \qquad T_x W_y |\mathbf{0}\rangle = W_y T_x |\mathbf{0}\rangle \quad , \tag{K.4}$$

operators V_y and W_y will allow us to generate the remaining ground states $\{|\mathbf{0}\rangle, V_y|\mathbf{0}\rangle = |1, -1\rangle, W_y|\mathbf{0}\rangle = |-1, 1\rangle, V_y W_y|\mathbf{0}\rangle = |-1, -1\rangle\}$ of which $V_y|\mathbf{0}\rangle$ and $V_y W_y|\mathbf{0}\rangle$ have an $\hat{x}$ momentum boost of π compared to the other two ground states. Thus, by Corollary 2.3, all ground states must weakly break translational symmetry. How can we see this more concretely?

The easiest way to see this CDW effect is to take this Toric code system with $L_y = 1$. Since all topological information is contained in a single plaquette, such a system is topologically no different compared to a general odd L_y system. With $L_y = 1$, the system reduces to two spins per unit cell in the $\hat{x}$ direction, which we depict in Fig. K.1.

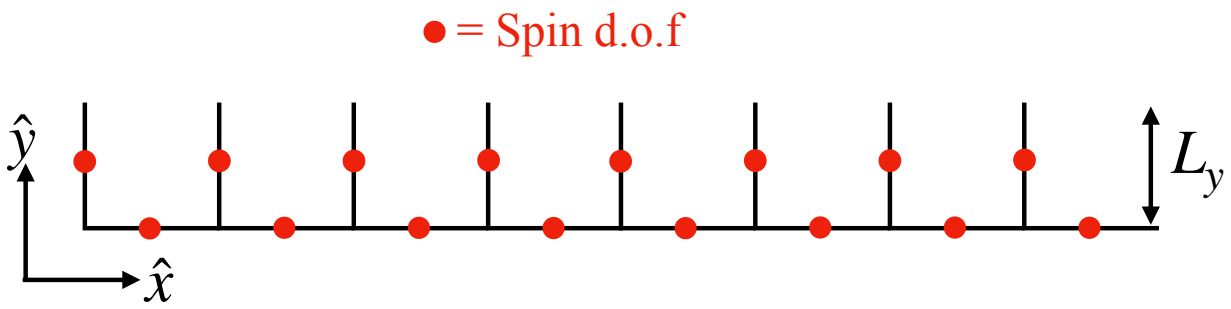

Figure K.1: (Color online) The Toric code system on a periodic lattice with $L_y = 1$. There are two spin degrees of freedom (d.o.f) per unit cell in $\hat{x}$.

Here the Toric code Hamiltonian reduces to

$$H = J_e \sum_{i \in -} \sigma_x^{[i]} \sigma_x^{[i+1]} - J_m \sum_{i \in |} \sigma_z^{[i]} \sigma_z^{[i+1]} \quad , \tag{K.5}$$

where the i sum is over the horizontal lattice sites (denoted $-$) for the first term and over vertical lattice sites (denotes $|$) for the second term. This Hamiltonian simply describes two decoupled Ising chains, where the first term is in an antiferromagnetic state while the second term is in a ferromagnetic state. The ground states for the respective chains are $\{|\Rightarrow\Leftarrow\rangle \equiv |\ \rightarrow\leftarrow\rightarrow\leftarrow\ \ldots\ \rightarrow\leftarrow\rangle, |\Leftarrow\Rightarrow\rangle \equiv |\ \leftarrow\rightarrow\leftarrow\rightarrow\ \ldots\ \leftarrow\rightarrow\rangle\}$ and $\{|\Uparrow\rangle \equiv |\uparrow\uparrow$

$... \uparrow\rangle, |\Downarrow\rangle \equiv |\downarrow\downarrow ... \downarrow\rangle\}$. The four ground states of the total system are thus given by $\{|\Rightarrow\Leftarrow\rangle|\Uparrow\rangle, |\Rightarrow\Leftarrow\rangle|\Downarrow\rangle, |\Leftarrow\Rightarrow\rangle|\Uparrow\rangle, |\Leftarrow\Rightarrow\rangle|\Downarrow\rangle\}$. It is clear that these correspond to CDW states since the antiferromagnetic Ising chain breaks the $\hat{x}$ directional translational $\mathbb{Z}_{L_x}$ symmetry group to $\mathbb{Z}_{L_x/2}$. Relating back to our original ground ("cat") state notation, we have

$$\begin{aligned} |\mathbf{0}\rangle = &|\Rightarrow\Leftarrow\rangle|\Uparrow\rangle + |\Rightarrow\Leftarrow\rangle|\Downarrow\rangle \\ &+ |\Leftarrow\Rightarrow\rangle|\Uparrow\rangle + |\Leftarrow\Rightarrow\rangle|\Downarrow\rangle \quad , \end{aligned} \tag{K.6}$$

$$\begin{aligned} V_y|\mathbf{0}\rangle = &|\Rightarrow\Leftarrow\rangle|\Uparrow\rangle + |\Rightarrow\Leftarrow\rangle|\Downarrow\rangle \\ &- |\Leftarrow\Rightarrow\rangle|\Uparrow\rangle - |\Leftarrow\Rightarrow\rangle|\Downarrow\rangle \quad , \end{aligned} \tag{K.7}$$

$$\begin{aligned} W_y|\mathbf{0}\rangle = &|\Rightarrow\Leftarrow\rangle|\Uparrow\rangle - |\Rightarrow\Leftarrow\rangle|\Downarrow\rangle \\ &+ |\Leftarrow\Rightarrow\rangle|\Uparrow\rangle - |\Leftarrow\Rightarrow\rangle|\Downarrow\rangle \quad , \end{aligned} \tag{K.8}$$

$$\begin{aligned} V_yW_y|\mathbf{0}\rangle = &|\Rightarrow\Leftarrow\rangle|\Uparrow\rangle - |\Rightarrow\Leftarrow\rangle|\Downarrow\rangle \\ &- |\Leftarrow\Rightarrow\rangle|\Uparrow\rangle + |\Leftarrow\Rightarrow\rangle|\Downarrow\rangle \quad , \end{aligned} \tag{K.9}$$

so we see that the toric code ground states indeed corresponds to weak translation symmetry breaking with non-local order parameter $\langle V_y\rangle$, which when viewed in 1d along $\hat{x}$ can be interpreted as a *local* order parameter.

Let us now consider the effects of anyon condensation, and the phases that it may lead to. On general ground we expect that a symmetric, confined state could arise from condensing the e anyon, since the e anyon does not carry any nontrivial projective quantum number in the toric code model. This means that when viewed as a $1d$ system, the e-condensation gives a transition between the CDW phase and a symmetric phase. Since the CDW phase has two-fold symmetry breaking, it is natural to expect that the transition is simply of the Ising type. These phenomena can be easily demonstrated in the $L_y = 1$ limit, as we describe as follows. To drive condensation of the e anyons, we may add a $-h_e \sum_i \sigma_z$ term to Eq. K.1. For the horizontal bonds this simply leads to a transverse-field Ising model. For $h_e < J_e$, we will still be in the topological ordered state, for $h_e = J_e$ we will have the Ising critical point, and for $h_e > J_e$ we are in the disordered (trivial) state. In the $L_y = 1$ example, increasing h_e corresponds to transitioning to the $|\Uparrow\rangle$ phase for the antiferromagnetic Ising chain, which has restored the $\hat{x}$ directional translation symmetry to give the trivial symmetric state.

Similarly we may try to condense the type m anyons by adding a $-h_m \sum_i \sigma_x$ term to Eq. K.1. In this case the anyon behaves non-trivially under either T_x or T_y since they anticommute when acting on m. Condensing the anyon leads to symmetry breaking of either T_x or T_y (dependent on the specific energetics of the system), so we expect to transition to a true 2d cat (i.e. symmetry-broken) state. The effects of this condensation cannot be readily seen on the $L_y = 1$ lattice example since translation in $\hat{y}$ ceases to have meaning. However it is known that such a translation symmetry-breaking transition occurs such that the final state forms a valence bond solid [293].